Expression of S-phase Cyclins affects Sensitivity to DNA Damage Response Modulators

Hyo Yun (Agnes) Jung

Worcester College, University of Oxford

Thesis submitted for the degree of Master of Science by Research
Trinity Term 2018



CRUK/MRC Oxford Institute for Radiation Oncology

Department of Oncology, University of Oxford

CANCER RESEARCH UK | MRC Medical Research Council

OXFORD INSTITUTE FOR RADIATION ONCOLOGY

Expression of S-phase Cyclins affects Sensitivity to DNA Damage Response Modulators

Hyo Yun (Agnes) Jung
Worcester College, University of Oxford
Thesis submitted for the degree of Master of Science by Research
Trinity Term 2018

Abstract

DNA replication stress triggers an intra-S phase checkpoint that is dependent on Ataxia-Telangiectasia and Rad3 related (ATR) kinase signalling. Due to the central role of ATR in the S phase checkpoint, it has been proposed that inhibition of ATR activity could selectively target tumour cells with defects in DNA damage-induced G1 cell cycle checkpoints through accumulation of DNA damage resulting in cell death. However, resistance is a major challenge arising from long-term use of such kinase inhibitors, thus previous work in the laboratory generated independent clonal cell lines (from PC-9 human non-small cell lung cancer cells) that are resistant to AZD6738, a selective ATR inhibitor, which notably expressed lower levels of S phase cyclins.

The aim of this study was to modulate levels of cyclins E1 and A2 to determine their impact on sensitivity to ATR inhibition. Firstly, parental and resistant cells were characterised in response to ATR inhibition. Secondly, cyclins were overexpressed in parental and resistant cells to observe sensitisation of cells to ATR inhibition, and finally, cyclin A2 knockdown was induced in parental cells.

Methods used to investigate response to ATR inhibition included cell proliferation assays, western blot, flow cytometry and live-cell microscopy. Results showed that cyclin modulation had a significant but modest effect on response to ATR inhibition, probably due to strict control of total cellular cyclin levels. Notably, early (post-mitotic) expression of cyclin E1 was detected in ATR inhibitor sensitive PC-9 cells, whereas ATR inhibitor resistant cells exhibited relatively delayed cyclin E1 expression. RNA sequencing and FACS analyses point to the role of the cyclin E-pRb-E2F pathway in inducing premature S phase entry in sensitive cells.

In conclusion from our study, a contributing factor determining sensitivity to ATR inhibition may be the timing of S phase cyclin expression. Specifically, early cyclin E1 expression may indicate the sensitivity of a cell line to ATR inhibition.

Acknowledgements

I would firstly like to thank my supervisor Dr. Anderson Ryan, for providing me with the opportunity to work on a fascinating project and for all the time he spent in giving me invaluable support and feedback throughout writing my thesis. The discussions we had about the project throughout the two years have allowed me to develop an appreciative understanding of science in a way that would not have been at all possible without Andy.

Sincere thanks to all the members of the Ryan lab: Maryam Alkadimi, Fiona Cahill, Süreyya Çorbacioglu, Neele Drobnitzsky, Sophie Ellermann, Marcus Greene, Letitia Harris, Yanyan Jiang, Luiza Madia Lourenço, Jennifer Martin, John Moore, Agata Patel, Yasmin Shanneik and Elysia Traynor, who have all made my time very special, from lab outings to the annual Christmas party. From my first day at the institute, I felt welcome and supported. I will miss you all!

I am furthermore utmost grateful to Michael Lin for his constant moral support and much needed meal deliveries throughout the long hours. Not to mention, his computational advice and willingness to listen to my various lab experiments.

Finally, I give my thanks to my parents and my sister who have provided me unfailing love and continually supported me to pursue this opportunity. Thank you all very much!

Word Count: 27,602

Table of Contents

1 Introduction 13

1.1 The DNA damage response 13

1.2 ATR 14

1.3 Targeting the DDR for cancer therapy 17

1.4 Development of ATR inhibitors in clinic 19

1.5 ATR inhibitor resistant cells 22

1.6 S phase cyclins 24

1.7 Aim of this study 29

2 Materials and Methods 30

2.1 Mammalian Cell Culture 30

2.1.1 Maintenance of cell lines 30

2.1.2 Lentiviral transfection 31

2.1.3 cDNA transfection 34

2.1.5 Cryostorage and thawing of cells 38

2.2 Drug Treatments 38

2.3 Resazurin Cell Viability Assay 39

2.4 PicoGreen Cell Proliferation Assay 39

2.5 ZsGreen Fluorescence Intensity Assay 40

2.5.1 Quantitative fluorescence assay using POLARstar Omega plate reader (BMG Labtech GmbH) 40

2.5.2 Qualitative fluorescence assay using FLoid Cell Imaging Station (Life Technologies) 41

2.6 Protein Detection by Western Blotting 41

2.6.1 Preparation of cell extracts, gel electrophoresis and transfer 41

2.6.2 Immunoblotting and Protein Detection using LI-COR 43

2.7 Synchronisation of Cells *45*

2.8 Live Cell Imaging *46*

2.9 Flow Cytometry: DNA Content Analysis/Cell Cycle Analysis *47*

2.10 DNA Purification from Mammalian Cell Culture (MasterPure kit) *48*

2.11 Data Analysis and Statistics *49*

3 Characterization of Parental and Resistant Cell Lines 50

3.1 Sensitivity of cell lines to DNA damage response modulators *50*

3.2 Growth inhibition in synchronised and unsynchronised parental cells *52*

3.3 Signalling response *54*

3.4 Proliferation of ATR inhibitor resistant clones *57*

3.5 Cell cycle analysis *60*

3.6 Key Findings *61*

4 Overexpression of Cyclins in Parental and Resistant Cell Lines 63

4.1 Growth rate of cDNA-transfected parental cell lines *63*

4.2 Sensitivity of cDNA transfected parental cell lines to ATR inhibitor *64*

4.3 Further cell cycle analysis of cDNA transfected parental cells *67*

4.4 Effect of overexpression of cyclins A2 and E1 in resistant cells *68*

4.5 Sensitivity to ATR inhibitors *71*

4.6 Time-dependent dynamics *73*

5 Knockdown of cyclin A2 in parental cells 77

5.1 Optimisation of knockdown cell lines *77*

5.2 Sensitivity to DNA damage response modulators 81

5.3 Proliferation of knockdown cells in the presence of AZD6738..... 83

6 Discussion 85

7 Conclusion and Hypothesis 91

8 References 93

List of Figures

FIGURE 1.1: ATR is activated when replication stress is induced causing long stretches of ssDNA.....15

FIGURE 1.2: ATR-induced cell cycle arrest is mediated via CHK1 activity.....17

FIGURE 1.3: Key Pathway Analysis showing differential expression of cell cycle proteins in ATR inhibitor-resistant SO25 cells and parental PC-9 cells, using RNA-sequencing data.....24

FIGURE 1.4: Schematic showing different cyclin/CDK partners controlling different phases of the cell cycle.....29

FIGURE 2.1: shERWOOD UltramiR lentiviral inducible shRNA (pZIP-TRE3GS) vector map.....33

FIGURE 2.2: Optimisation of doxycycline concentration in knockdown cells.....34

FIGURE 2.3: Vector map of Vigene ORF of cyclin A2 (CCNA2) or cyclin E1 (CCNE1) in pENTER.....36

FIGURE 2.4: Parameters used in gating populations.....48

FIGURE 3.1: Responses of NSCLC cell lines to different classes of DNA damage response modulators.....51

FIGURE 3.2: Relative cell growth of PC-9 and H1975 cells.....54

FIGURE 3.3: ATR signalling in PC-9 cells.....55

FIGURE 3.4 ATM signalling in PC-9 cells and cyclin levels.....57

FIGURE 3.5: Cell viability of parental and resistant cells.....59

FIGURE 3.6: AZD6738 leads to early S-phase arrest in PC-9 cells.....61

FIGURE 4.1: Cell viability of parental cells and cDNA transfected cells.....64

FIGURE 4.2: Responses of cDNA transfected parental cells to AZD6738.....65

FIGURE 4.3: Cell viability of cDNA transfected parental cells in the presence of AZD6738.....66

FIGURE 4.4: Cell cycle in cDNA transfected PC-9 cells.....68

FIGURE 4.5: Cell viability of cDNA transfected resistant cells.....70

FIGURE 4.6: Responses of cDNA transfected resistant cell lines to ATRi's.....72

FIGURE 4.7: Cell cycle of synchronised cells.....76

FIGURE 5.1: Cyclin levels in knockdown cells lines induced with 2 µg/mL doxycycline reveals 3-fold decrease compared to non-target (NT).....78

FIGURE 5.2: Cyclin levels in knockdown cell lines induced with optimum doxycycline concentration (75 ng/mL) reveals 2-fold decrease.....80

FIGURE 5.3: Response of knockdown cell lines to DNA damage response modulators.....82

FIGURE 5.4: Cell viability of knockdown cells in the presence of AD6738.....84

FIGURE 7: Model of S phase cyclin expression.....92

List of Tables

TABLE 1.1: ATR inhibitors and their chemical structure.....22

TABLE 2.1: Cell lines used in this study.....37

TABLE 2.2: DNA lysis buffer composition.....40

TABLE 2.3: Lysis buffer stock components for western blot cell extract collection.....43

TABLE 2.4: Buffers and solutions used in immunoblotting.....44

TABLE 2.5: Primary antibodies used for immunoblot analysis.....44

TABLE 2.6: Secondary antibodies used for two-colour detection with infrared fluorescence.....45

TABLE 3.1: Sensitivity of various human lung cancer cell lines to AZD6738.....50

TABLE 3.2: Effect of AZD6738 treatment on doubling time of unsynchronised and synchronised PC-9 and H1975 cells.....53

Abbreviations

53BP1	tumour protein p53 binding protein 1
ANOVA	analysis of variance
A-T	Ataxia-telangiectasia
ATCC	American Type Culture Collection
ATM	ataxia-telangiectasia mutated
ATP	adenine triphosphate
ATR	ataxia-telangiectasia and Rad3-related
ATRIP	ATR interacting protein
C	Celsius
CCNA2	cyclin A2
CCNE1	cyclin E1
CDC	cell division cycle
CDK	cyclin dependent kinase
CDT1	chromosome licensing and DNA replication factor 1
CHK1	CHEK1, checkpoint kinase 1
CHK2	CHEK2, checkpoint kinase 2
CLL	chronic lymphocytic leukaemia
CO_2	carbon dioxide
CV	crystal violet
DDR	DNA damage response
dH_2O	distilled water
DMEM	Dulbecco's modified Eagle's medium
DMSO	dimethyl sulfoxide
DNA	deoxyribonucleic acid

DNA-PK	DNA-dependent protein kinase
dNTP	deoxynucleotide triphosphate
DSB	double-strand break
EDTA	ethylenediaminetetraacetic acid
FACS	fluorescence-activated cell sorting
FBS	foetal bovine serum
g	gram(s)
Gln	glutamine
G1 phase	gap phase of cell cycle before DNA replication
G2 phase	gap phase of cell cycle before mitosis
hr	hour(s)
H_2O	water
HCl	hydrochloric acid
HU	hydroxyurea
HUS1	HUS1 checkpoint clamp component
IC_{50}	half-maximal inhibitory concentration
IR	ionizing radiation
KAP1	Krüppel-associated box-associated co-repressor 1
kDa	kilo-Dalton
KPA	key pathway analysis
L	litre
M	molarity
m	metre
min	minute(s)
M phase	mitosis
mAb	monoclonal antibody

mTOR	mechanistic target of rapamycin
Na_3VO_4	sodium orthovanadate
NaCl	sodium chloride
NaF	sodium fluoride
NaOH	sodium hydroxide
NER	nucleotide-excision repair
NSCLC	non-small cell lung cancer
p53 (TP53)	tumour protein 53
pAb	polyclonal antibody
PARP	poly (ADP ribose)-polymerase
pATM	phosphor-ATM
PBS	phosphate buffered saline
PBS-T	phosphate buffered saline with Tween 20
pCHK1	phospho-CHK1
pCHK2	phospho-CHK2
pHH3	phosphor-histone H3
PI	propidium iodide
PI3K	phosphatidylinositol-3-OH kinase
PIKK	phosphatidylinositol 3-kinase-related kinase
pKAP1	phosphor-KAP1
PPIB	peptidyl-prolyl cis-trans isomerase B (Cyclophilin B)
RAD1	radiation sensitivity abnormal 1
RAD17	radiation sensitivity abnormal 17
RAS	rat sarcoma
RFC	replication factor C
RNA	ribonucleic acid

RPA	replication protein A
RT	room temperature
S phase	DNA replication or synthesis phase of the cell cycle
SchB	Schisandrin B
SDS	sodium dodecyl sulphate
sec(s)	second(s)
SEM	standard error of the mean
siRNA	small interfering ribonucleic acid
ssDNA	single-stranded DNA
t	time
TBS	tris-buffered saline
TBS-T	tris-buffered saline with Tween 20
TOPBP1	DNA topoisomerase 2-binding protein 1
UV	ultraviolet
γH2AX	phosphorylated histone H2AX

CHAPTER 1

1 Introduction

1.1 The DNA damage response

The cellular genetic material is continuously subject to damage from endogenous and exogenous sources (Lindahl, 1993; De Bont & van Larebeke, 2004). The resulting DNA lesions must be repaired to prevent senescence, cell death or mutations that may lead to cancer (Hoeijmakers, 2009).

To facilitate the crucial detection and repair of DNA damage, cells have evolved a sophisticated series of interconnected response pathways, collectively termed the DNA damage response (DDR). This complex response pathway involves numerous proteins that sense DNA damage, signal its presence and mediate its repair. The subsequent response will determine a cell's fate: senescence, apoptosis, or transient cell cycle arrest to allow for DNA repair to maintain cell viability and genomic stability (Ciccia & Elledge, 2010). At the centre of this extensive DDR system are the sensory proteins that detect the presence of DNA damage. The apical proteins are part of the phosphatidylinositol-3 kinase-related kinase (PIKK) family of serine/threonine protein kinases that phosphorylate proteins on Ser-Gln and Thr-Gln (SQ/TQ) motifs (Kastan & Bartek, 2004; Cimprich & Cortez, 2008). One member is DNA-dependent protein kinase (DNA-PK), which plays a role in DNA double strand break (DSB) repair (Lovejoy & Cortez, 2009). Two other members, Ataxia Telangiectasia Mutated (ATM) and Ataxia Telangiectasia and Rad3 related (ATR), are involved in the recognition and response to DSBs (ATM) upon exposure to ionising radiation, and stalled replication or resected DSBs (ATR) (Zou & Elledge, 2003). ATR senses replication stress induced by conditions such as UV light, chemotherapeutic agents, radiation and hypoxia, which create long stretches of ssDNA from continued helicase activity despite stalled polymerases (Zou & Elledge, 2003; Cimprich & Cortez, 2008; Dai & Grant, 2010).

1.2 ATR

ATR is an essential gene that encodes a large 301 kDA protein of 2644 amino acids (Bentley et al, 1996). It is essential for cell viability, and loss of function can cause deleterious genomic instability (Brown & Baltimore, 2000; De Klein et al, 2000; Liu et al, 2000; Cortez et al, 2001). Thus, mutations are rare and only hypomorphic or heterozygous mutations have been reported to date (O'Driscoll, 2003). At the whole-organism level, deficiency leads to ageing-related phenotypes, defects in tissue homeostasis, decrease in stem cells and collapse of tissue renewal and homeostatic capability (Ruzankina et al, 2007). The most thoroughly characterised ATR deficiency-related disease is Seckel syndrome, characterized by growth and mental retardation and dwarfism in humans. Mouse models have shown to suffer osteoskeletal abnormalities, accelerated ageing, and at the cellular level, high levels of endogenous replicative stress and DNA damage (Griffith et al, 2008; O'Driscoll, 2009; Murga et al, 2009). Forced expression of ATR induces cell cycle abnormalities, such as the removal of IR-induced G1 arrest (Smith et al, 1998). On the other hand, limited expression or overexpression of kinase-dead forms increases sensitivity to DNA damaging agents and replication inhibitors such as IR or UV radiation, cis-platin and hydroxyurea, due to loss of cell cycle checkpoint control, leading to reduced cell viability (Cliby et al, 1998; Jardim et al, 2009). Notably, ATR is also involved in stabilising fragile sites and ATR loss results in fragile site expression, a form of genomic instability (Casper et al, 2002). In effect of all the above, it is clear that ATR has an indispensable role in maintaining cell viability via its response to abundant sources of replication stress in normal healthy cells as well as in cells exposed to DNA damaging agents.

In order to activate ATR, there is a structural requirement of RPA-coated ssDNA with a 5' double-stranded primer junction and ATR-interacting protein (ATRIP) associated with the ssDNA-bound RPA (see Figure 1.1). ATRIP localises ATR to sites of replication stress by interacting with the N-terminus of ATR. ATRIP may be considered as part of an ATR holoenzyme as loss of either subunits may cause similar phenotypes (Cimprich & Cortez, 2008). RPA also allows the RAD17/RFC2-5 clamp loader complex to bind at the junction of double

stranded and ssDNA. The clamp loader then enables loading of the RAD9-RAD1-HUS1 (9-1-1) heterotrimeric ring clamp onto the DNA. Another component, DNA topoisomerase 2-binding protein 1 (TOPBP1) is recruited onto the DNA by the complex, and it subsequently stimulates the kinase activity of ATR-ATRIP (Kumagai et al, 2006; Delacroix et al, 2007; Mordes et al, 2008). The 9-1-1 complex is known to be recruited to DNA with 5'-recessed ends that exist at damaged replication forks, recombination sites and nucleotide excision repair (NER) sites, and is recruited independently, as is the ATR-ATRIP complex (Ellison & Stillman, 2003; Kondo et al, 2001; Melo et al, 2001). All these taken together suggest regulatory mechanisms in place to ensure the ATR pathway is not activated aberrantly during normal DNA replication.

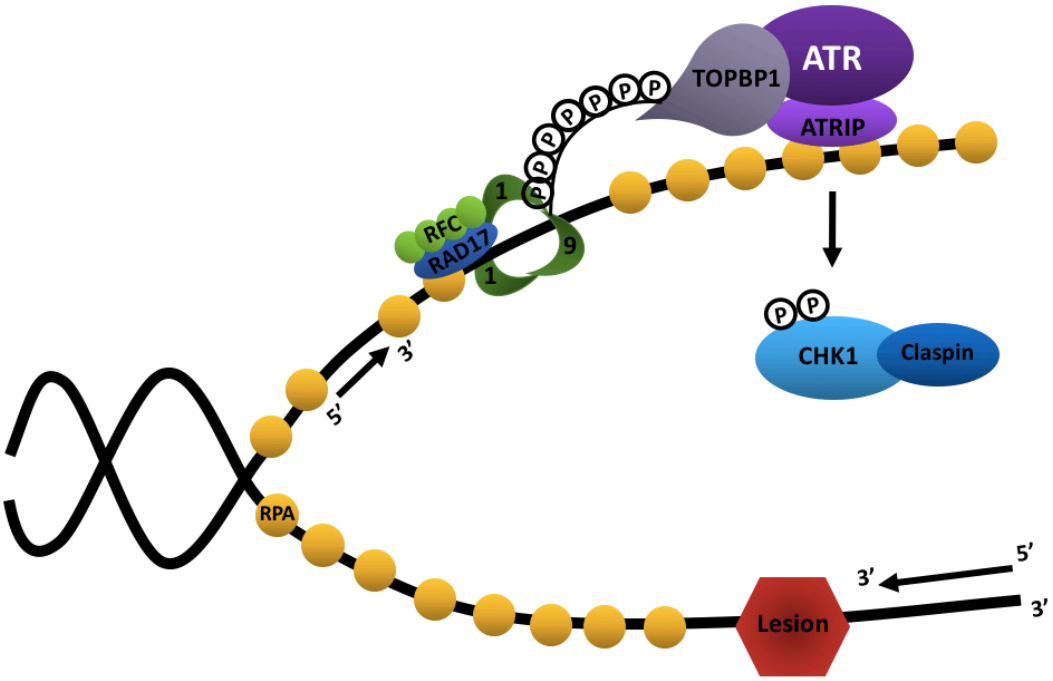


Figure 1.1: ATR is activated when replication stress is induced causing long stretches of ssDNA.

Black lines represent DNA. A DNA lesion (red) leads to helicase continuing to unwind DNA, creating long strands of ssDNA. RPA (yellow) bind these ssDNA regions and allows binding of ATRIP (light purple) that recruits ATR (dark purple) to sites of damage. RPA also recruits the RAD17/RFC2-5 clamp loader complex (blue and light green) that enables loading of the RAD17-RAD1-HUS1 (9-1-1) ring complex (dark green) onto the DNA. This complex subsequently recruits TOPBP1 (grey) that stimulates ATR-ATRIP. Claspin, recruited by RAD17, recruits CHK1, which is phosphorylated by ATR on two serine residues. Once activated, CHK1 dissociated from DNA and induces signals for the appropriate downstream response. Directions of DNA replication are indicated. Modified from Wagner & Kaufmann, 2010.

The key function of ATR within the DDR is to maintain genomic integrity (Cimprich & Cortez, 2008). It does this by signalling to regulate replication origin firing or to repair damaged replication forks, in order to prevent premature mitotic entry of damaged cells with incomplete DNA replication. ATR stabilises stalled replication forks to allow proper completion of replication not only in cells exposed to DNA damaging agents but also if replication stress is present in normal cycling cells. It recognises and phosphorylates a wide range of substrates including DNA damage sensors, mediators, effectors, DNA repair proteins, replisome components and chromatin remodellers (Kim et al, 1999). Thus, ATR's role can be classified into four streams of action: activating the S-phase checkpoint, the G2/M checkpoint, stabilising replication forks, and centrosomal function. The first two functions will be of focus in this study.

Once activated in association with its co-activators (Figure 1.1), ATR phosphorylates substrates to coordinate transient cell cycle arrest and stabilisation of stalled replication forks to promote repair of damaged DNA and subsequent restart of DNA replication (Cimprich & Cortez, 2008; Errico & Constanzo, 2012). A crucial ATR target is claspin for the stabilisation of replication forks. The protein is recruited by RAD17 and once phosphorylated by ATR, claspin recruits CHK1. CHK1 itself is also phosphorylated by ATR at serines 317 and 345 and can be autophosphorylated at serine 296 (Jeong et al, 2003; Kumagai & Dunphy, 2003; Kumagai et al, 2004). Once CHK1 is activated, it dissociates from chromatin to initiate the intra-S phase checkpoint in both DNA damaged cells and normal cycling cells (Sørensen et al, 2003; Xiao et al, 2003; Dai & Grant, 2010). The downstream function of ATR is carried out by CHK1 phosphorylating CDC25A protein phosphatase, which leads to ubiquitin-dependent proteolysis of CDC25A. CDC25A is no longer able to dephosphorylate the inhibitory phosphates located within the CDK2 ATP-binding loop, thus CDK2 remains inactive in its cyclin E/A complex, leading to inhibition or delay of replication origin firing (see Figure 1.2) (Nurse, 1997). Inhibition of origin firing occurs in normal cycling cells which avoids DNA from being re-replicated, and a delay of origin firing allows time for DNA to be repaired in cells with DNA damage (Bartek & Lukas, 2003; Donzelli & Draetta, 2003; Sørensen et al, 2003; Xiao et al, 2003).

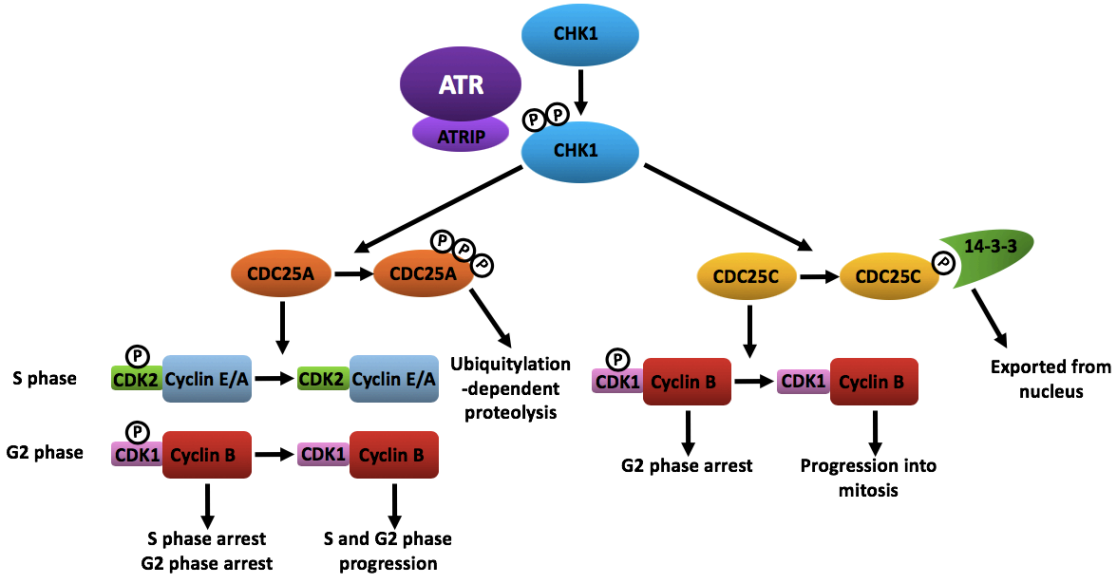


Figure 1.2: ATR-induced cell cycle arrest is mediated via CHK1 activity.
Modified from Wagner & Kaufmann, 2010.

ATR also has a major role in regulating the G2/M checkpoint, a barrier that serves to prevent the cell from entering mitosis with genomic DNA damage or unreplicated DNA. The G2/M checkpoint is accomplished through CHK1 phosphorylation-dependent ubiquitination of CDC25A, thus inhibiting the phosphatase activity of CDC25A, preventing the removal of the inhibitory phosphate on CDK1/cyclin B. Inactive CDK1/cyclin B can no longer phosphorylate and activate its substrates to progress through G2 phase and arrests in G2. CHK1 also phosphorylates CDC25C leading to its export from the nucleus via the 14-3-3 proteins where it is sequestered in the cytoplasm. This relocalisation renders CDC25C unable to dephosphorylate nuclear CDC2, a protein essential for mitosis (Zhao et al, 2002; Xiao et al, 2003; Dai & Grant, 2010; Peng et al, 1997). Another important CHK1 substrate is WEE1, which is stimulated upon ATR activation via CHK1 and inhibits mitotic entry through inhibitory phosphorylation of CDK1 on Tyr15 (Y15).

1.3 Targeting the DDR for cancer therapy

Established DNA-damaging cancer therapies have faced a significant obstacle in its effectiveness due to the emergence of resistance in cancer cells to these therapies. Resistance

can arise as cells modify the regulation of their DDR components to by-pass the effects of DNA damage. However, this resistance can be exploited by the use of DDR-targeting drugs to selectively target tumour cells where resistance is linked with increased DDR signalling, making the DDR an attractive therapeutic target as a radio- or chemo-sensitiser. Furthermore, it is known that many common cancers have mutations in one or more DDR pathways, potentially making them more reliant on the remaining DDR pathways, and more prone to cell death than normal healthy cells when exposed to DDR-targeting inhibitors. (Weber & Ryan, 2015). Thus, DDR modulators represent a novel class of therapeutic agents that are designed to selectively target tumour cells in combination with exogenous DNA damaging agents such as radiation or DNA damaging cytotoxic chemotherapy, or with endogenous or exogenous DNA replication stress such as oncogene activation, BRCA mutations, hydroxyurea or gemcitabine. The modulators can also be used in synthetic lethal approaches to target cancer cells with mutations in DDR genes.

ATR has become an attractive target for therapy as it plays a major role in the regulation of the response to DNA replication stress (López-Contreras & Fernandez-Capetillo, 2010). In addition, ATR can be an effective therapeutic target in cancer cells with genomic defects in components of the DDR. For example, one of the most common mutations in cancer is in the p53 protein, and with its major role in the DDR downstream of ATM in order to arrest cells in G2/M and G1, the functional loss of this protein can lead to high levels of replication stress and sensitisation to ATR inhibition. Toxicity of ATRi in p53-defective tumour cells is increased compared to p53 wild-type cells as the former are more dependent on the ATR pathway for DDR via the S and G2/M checkpoints and consequent cell survival. When ATR is inhibited in p53-defective cells, the major cell cycle checkpoints are lost, leading to accumulation of DNA damage, premature mitotic entry and cell death (Nghiem et al, 2001; Murga et al, 2009; Ruzankina et al, 2009; Kaelin, 2005; Gabrielli et al, 2012). Thus, there is a strong rationale for the development of ATR inhibitors to enhance cytotoxicity of chemotherapeutic agents and also in p53-defective cancer cells, with the potential to use lower doses of chemotherapies that could be less toxic to normal cells.

As discussed previously, ATR is an essential gene along with its downstream substrate CHK1. Its crucial role in regulating DNA replication and maintaining genome integrity puts forward concerns about potential side effects and toxicity to normal proliferating cells with ATR inhibition. This vital function of ATR has most likely led to the restricted development of ATR inhibitors in the clinical setting.

1.4 Development of ATR inhibitors in clinic

Early studies have shown that caffeine can inhibit both ATM and ATR activity and sensitise cells to radiation and DNA damaging agents (Powell et al, 1995; 1996; Blasina et al, 1999; Sarkaria et al, 1999) (see Table 1.1). However, its lack of selectivity and considerably high toxic effects at the effective dose have stalled research into caffeine as a clinical candidate (Newton et al, 1981). The first ATR-selective inhibitor was reported by Nishida el al. in 2009. Schisandrin B, a naturally-occurring dibenzo cyclooctadiene derivative, was found to be able to sensitise human non-small cell lung cancer (NSCLC) cells to UV radiation via the inhibition of CHK1 phosphorylation, thus abolishing the S and G2/M cell cycle checkpoints. Although ATR-selective, it was not found to be a potent inhibitor, and at the effective higher concentrations (30 μM), showed inhibitory activity on ATM.

Subsequently other ATR inhibitors have been reported such as NU6027 and NVP-BEZ235. NU6027 was initially developed as a CDK2 inhibitor but found to have additional ATR inhibitory activity, and able to sensitise breast and ovarian cancer cell lines to various chemotherapeutic agents (Peasland et al, 2011; Sultan et al, 2013). NVP-BEZ235 was primarily developed to inhibit PI3K and mTOR as a dual kinase inhibitor, but was identified as an inhibitor of ATR, ATM and DNA-PKcs., with the ability to radio-sensitise RAS-overexpressing tumours (Maira et al, 2008; Konstantinidou et al, 2009). However, due to the cross-reactivity of these inhibitors to other protein kinases, the search for more potent and selective ATR inhibitors has continued.

The first potent and selective ATR inhibitor was reported by Vertex Pharmaceuticals in a high-throughput screen assay. It competes at the ATP binding site within ATR, and displays ATR

selectivity with low cross-reactivity to other PIKK proteins (Reaper et al, 2011). VE-821 is able to chemo-sensitise cancer cells, with the strongest sensitisation provided when used in combination with cross-linking agents such as cisplatin and carboplatin (Reaper et al, 2011; Jossé et al, 2014). Reaper et al. importantly observed that the combination of VE-821 and cisplatin induced cell death in most cancer cell lines but in non-tumour cell lines, a transient growth arrest occurred. Notably, even when used as a single therapy, the inhibitor is able to induce cell death in hypoxic cells, a common characteristic of cancer cells. In addition, it has been shown that VE-821 can act as a radio-sensitiser in hypoxic cancer cells that have arrested in S phase, which is significant as hypoxic cells are known to be more resistant to radiotherapy (Pires et al, 2012; Prevo et al, 2012; Gray et al, 1953; Wouters & Brown, 1997).

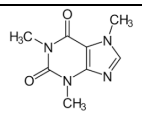
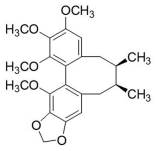
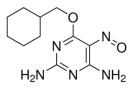
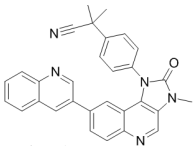
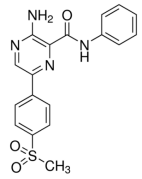
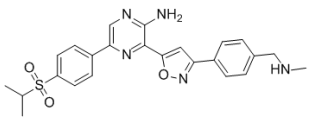
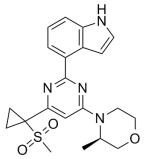
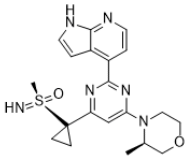
VE822 is an analogue of VE-821 showing improved effectiveness at inhibiting ATR and enhanced bioavailability, solubility and pharmacokinetics (Charrier et al, 2011). In human pancreatic cancer cells, it has demonstrated cytotoxic synergy with ionising radiation and gemcitabine, whilst maintaining low toxicity levels in non-tumour cells (Fokas et al, 2012). In an in vitro model of lung cancer cells, the inhibitor has activity as a chemo-sensitiser to DNA damaging drugs. In vivo data has indicated enhancement of effect of cisplatin when used in combination with VE-822 (Hall et al, 2014). With its increased potency and selectivity, VE-822 has been the first ATR-selective inhibitor to enter clinical trials, in a first-in-human study in combination with cytotoxic chemotherapy (ClinicalTrials.gov: NCT02157792).

The second ATR-selective inhibitor to enter clinical development is AZD6738, a potent and selective ATR inhibitor developed by AstraZeneca. It has been developed from AZ20, an ATR inhibitor shown to have synergistic effects with KU-60019, an ATM inhibitor (Jaq et al, 2012). In vivo data has indicated the potency of AZ20 as a monotherapy in cancer cells deficient in MRE11 DNA repair protein at well-tolerated doses (Foote et al, 2013). AZD6738 was developed to increase bioavailability, solubility, and enhance its pharmacokinetic and biopharmaceutical properties without comprising on potency or selectivity (Jones et al, 2013; Vendetti et al, 2015). The inhibitor acts via the inhibition of ATR substrates such as CHK1, leading to increases in DNA damage and replication stress, and accumulation of cells in S-phase.

It increases ATM-dependent phosphorylation of CHK2 and γH2AX. When used in combination with chemotherapeutic agents such as gemcitabine, or ionising radiation, it significantly increases cytotoxic activity in vivo. Furthermore, anti-tumour activity has been exhibited by AZD6738 in xenograft models of ATM-deficient tumours when used both as a monotherapy and in combination with carboplatin or IR at well-tolerated doses (Guichard et al, 2013; Jones et al, 2013). Guichard et al. importantly noted an increase in γH2AX staining in bone marrow and gut to be transient, implying a good therapeutic index. In NSCLC cell lines it was found that AZD6738 triggered the expected accumulation of cells in G1/S and early S phase, prompting cell death and senescence (Vendetti et al, 2015). In NSCLC cell lines with ATM-deficiency, AZD6738 enhanced the cytotoxic effect of cis-platin, with marked regressions in lung cancer xenografts, and in those with functioning ATM protein, the anti-tumour activities of cisplatin and gemcitabine were elevated. Importantly, AZD6738 was found to be well tolerated in mice for up to 14 days (Vendetti et al, 2015). Currently, a total of 12 clinical trials in phases I and II are underway with the aim of investigating the effects of AZD6738.

A range of DDR modulators targeting ATR (AZD6738, VE822), WEE1 (AZD1775) and CHK1/2 (AZD7762) are of interest for this project.

Table 1.1: ATR inhibitors and their chemical structure.

Compound	Structure
Caffeine	
Schisandrin B	
NU6027	
NVP-BEZ235	
VE-821	
VE-822 (VX-970)	
AZ20	
AZD6738	

1.5 ATR inhibitor resistant cells

Development of resistance has been observed with long-term use of kinase inhibitors. Previously in our laboratory, potential mechanisms of acquired resistance to AZD6738 have been investigated. An in vitro assay system using PC-9 human NSCLC cells generated

independent clonal cells lines (SO25, SO45 and SO46) that were resistant to AZD6738 with increased relative cell viability in presence of AZD6738 compared to parental cells. Western blot analysis showed that S phase cyclins, cyclins A2 and E1, were downregulated in the resistant cell lines, and RNA-sequencing data revealed that resistant cell lines have lower transcript levels of these cyclins (see Figure 1.3). Furthermore, knockdown of cyclin A2 and/or cyclin E1 using siRNA in parental cells increased cell viability in the presence of AZD6738. Together, the data suggested differential cell cycle regulation in resistant clones, with the hypothesis that downregulation of S phase cyclins might confer resistance to ATR inhibitors.

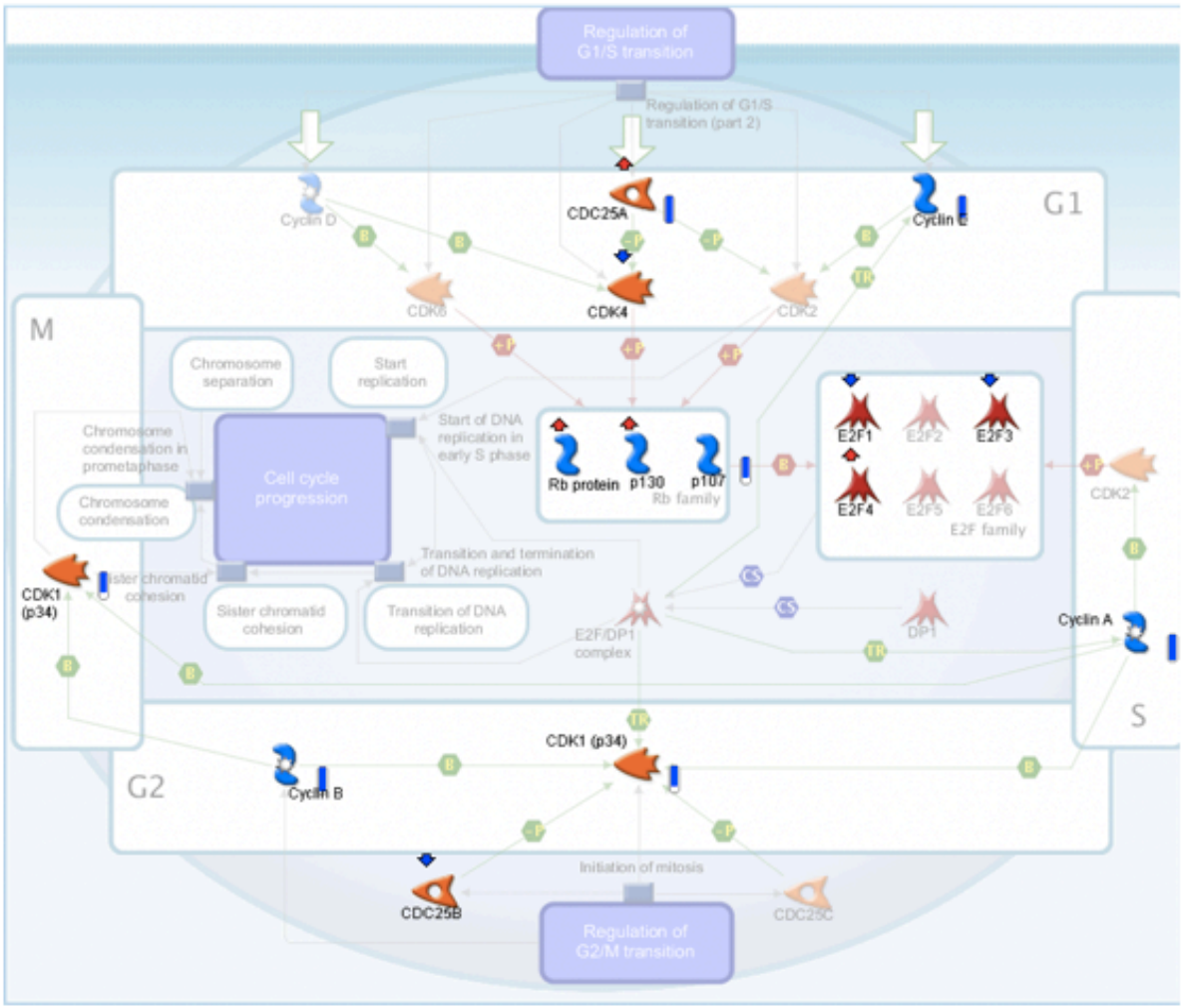


Figure 1.3: Key Pathway Analysis showing differential expression of cell cycle proteins in ATR inhibitor-resistant SO25 cells and parental PC-9 cells, using RNA-sequencing data.

Highlighted proteins are differentially expressed. Blue bars indicate mRNA downregulation in SO25 compared to PC-9 cells. Red arrows indicate pathway activation and blue arrows indicate pathway inhibition. mRNA expression from genes, including cyclins and CDK1, that encode proteins essential for cell cycle progression were found to be prominently downregulated in SO25 cells compared with parental PC-9 cells. RNA-sequencing analysis was carried out using the Illumina HiSeq 2000 platform. The resulting top 1000 genes with the most statistically significant differences in gene expression between PC-9 and SO25 were entered into Metacore Key Pathway Advisor (Thomson Reuters).

1.6 S phase cyclins

Cell-cycle dependent expression of specific cyclins is used by cells to regulate activity of CDKs that are in turn required for orderly progression through the cell cycle (Woo & Poon, 2003). The kinase subunit of the cyclin/CDK holoenzyme is expressed constantly at relatively low levels throughout the cell cycle, whereas their regulatory partner, the cyclins, are synthesised and

degraded in a periodic manner (Dahmann et al, 1995). The S phase cyclins (cyclins E and A) are at the peak of their expression levels during G1-S phase and late S phase respectively. Consistent with the timing of their expression, transition from G1 to S phase and progression through S phase are controlled predominantly by cyclin E/CDK2 and cyclin A/CDK2 respectively (see Figure 1.4). Within this function of cell cycle control, these cyclin/CDK2 complexes are involved in the regulation of S phase entry, progress of replication and prevention of re-replication of DNA.

Cyclin E/CDK2 activity has repeatedly been found to be crucial for DNA replication initiation in many biological systems, such as Drosophila and Xenopus (Jackson et al, 1995; Knoblich et al, 1994; Strausfeld et al, 1994). The complex is implicated in the promotion of S phase in two ways. In its first role, cyclin E/CDK2 induces the release of E2F transcription factor from phosphorylated retinoblastoma protein (pRb), allowing the expression of multiple genes required for S phase, including cyclin A (Schulze et al, 1995). The hyperphosphorylation of pRb by cyclin E/CDK2 allows cells to overcome the pRb-imposed G1 arrest (Zhang et al, 2000). It is not yet clear at which sites cyclin E/CDK2 phosphorylates pRb as the E2F-inhibitory protein has 16 consensus phosphorylation sites that have been shown to be able to be phosphorylated by CDKs partnering with cyclins A, D and E. One model that has been proposed is that each cyclin/CDK complex phosphorylates pRb on different but overlapping sites, thus each playing in part to the inactivation of pRb (Connell-Crowley et al, 1997; Zarkowska & Mittnacht, 1997; Kitagawa et al, 1996). A generally accepted order of pRb phosphorylation is cyclin D/CDK4/6 in early G1 phase, cyclin E/CDK2 in late G1, and cyclin A/CDK2 in S phase. As cyclin A is expressed from S phase, it is not likely to promote G1-S transition via pRb phosphorylation, but it may be key to maintenance of the hyperphosphorylated state of pRb for S phase progression (Knudsen et al, 1998). There have been several reports suggesting that expression of cyclin E alone is sufficient to induce S phase entry from G1, without the need for pRb phosphorylation or the transcription of E2F-activated genes (Lukas et al, 1997; Leng et al, 1997). However, studies by Leone et al, 1999, and DeGregori et al, 1995, have also demonstrated that E2F

overexpression can prompt S phase entry without cyclin E/CDK2 activity. Taken together, this suggests cooperative interaction of E2F and cyclin E/CDK2 for S phase promotion.

In its second role, cyclin E/CDK2 promotes the assembly of prereplication complexes during the G0-G1 transition via the loading of CDC6 to origins of replication and recruitment of MCM2-7 proteins (Su & O'Farrell, 1998; Cook et al, 2002; Coverley et al, 2002). Once licensed to replicate, cyclin E/CDK2 and also CBF4-CDC7 induce initiation of DNA replication by the phosphorylation of the prereplication complex (preRC) components (Kumagai et al, 1999; Jiang et al, 1999; Masai et al, 2000). This allows CDC45, a crucial regulatory component for replication required for loading of RPA and DNA polymerase α onto the origin, to associate with the preRC, finally activating the replication origin (Arata et al, 2000; Zou & Stillman, 2000; Mimura & Takisawa, 1998; Jares & Blow, 2000). Expression levels of cyclin E1 are increased during G1 when mitogen-stimulated activities of CDK4 or CDK6 in association with cyclin D promote transcription of cyclin E1 via the previously-described phosphorylation of pRb. Levels of cyclin E1 decline during the subsequent S phase due to ubiquitination by the SCF^{Cdc4} (Skp1/cullin/Cdc4 F-box protein), leading to degradation by proteasomes (Clurman et al, 1996; Won & Reed, 1996; Strohmaier et al, 2001).

Cyclin A/CDK2 activity allows progress of DNA replication via the phosphorylation of its substrates. It was found that ectopic expression of cyclin A drives cells through S phase and downregulation hinders S phase progression (Yam et al, 2002). In accordance with the timing of the expression of cyclin A, cyclin A/CDK2 complex activates existing preRC. As mentioned previously, CDC45 is an essential component of the preRC, loaded onto replication origins by CDK2 in association with an S phase cyclin, but it is not definitive whether cyclin E or cyclin A, or both are involved (Arata et al, 2000; Zou & Stillman, 2000; Mimura & Takisawa, 1998; Jares & Blow, 2000). Once CDC45 is loaded onto replication origins, ssDNA is stabilised by the binding of RPA, which can be phosphorylated by cyclin A/CDK2 (Walter & Newport, 2000; Tanaka & Nasmyth, 1998; Dutta & Stillman, 1992; Pan et al, 1994). The functional significance of the phosphorylated form of RPA is unclear as both unphosphorylated and phosphorylated forms seem to display similar activity levels in SV40 DNA replication (Hendricksen & Wold,

1994; Pan et al, 1995). Other known substrates of cyclin A/CDK2 include essential parts of the DNA replication machinery such as DNA polyermase α, DNA polyermase δ and PCNA, and as such, cyclin A is found to be co-localised with replication foci in cells (Fotedar & Roberts, 1991; Sobczak-Thepot et al, 1993; Nasheuer et al, 1991; Zeng et al, 1994; Prosperi et al, 1994). Furthermore, it has been found that cyclin A/CDK2 is required to stimulate the elongation activity of DNA polymerase (Bashir et al 2000).

Cyclin A/CDK2 also functions to prevent re-replication of DNA in S-phase and G2 phase via the phosphorylation of CDC6, leading to the subcellular relocalisation of CDC6 from the nucleus, where it is necessary for preRC formation, to the cytoplasm. Unlike in yeast where Cdc6p (CDC6 analogue) levels are tightly regulated throughout the cell cycle, human CDC6 levels do not decrease at the beginning of S phase (Saha et al, 1998; Petersen et al, 1999; Mendez & Stillman, 2000). Rather, CDC6 levels stay relatively constant throughout the different phases of the cell cycle. CDC6 is synthesised during G1 via the transcriptional activity of E2F, during which time it remains in the nucleus, until the onset of S phase, when CDC6 is exported to the cytoplasm via CRM1 (Hateboer et al, 1998; Ohtani et al 1998; Saha et al, 1998; Petersen et al, 1999; Jiang et al, 1999). CDC6 is finally degraded in early G1 in the cytoplasm where it is targeted for proteolysis by APC/C (anaphase promoting complex/cyclosome) with CDH1 targeting subunit (Petersen et al, 2000). Notably, it has been found in mammals that CDK2 is only able to bind and phosphorylate CDC6 when bound to cyclin A, and not when bound to cyclin E (Saha et al, 1998; Petersen et al, 1999; Coverley et al, 2000). This, together with the important function of cyclin E in DNA replication initiation during G0-S phase transition, indicates the order of action by cyclin E/CDK2 and cyclin A/CDK2 to be vital to determine preRC activation and to inhibit repeated initiation (Coverley et al, 2002). It is also noteworthy that the phosphorylation status of CDC6 has been the decisive factor in its localisation, as studies have indicated non-phosphorylatable CDC6 mutant is exclusively nuclear, whilst phosphorylated CDC6 mutant is exclusively cytoplasmic (Jiang et al, 1999; Pelizon et al, 2000). Furthermore, it has been shown that microinjection of non-phosphorylatable mutant CDC6 into human cells prevented DNA replication initiation and hindered S phase progression, signifying

the phosphorylation of CDC6 by cyclin A/CDK2 is critical for a late step in DNA replication initiation (Herbig et al, 2000). Another substrate of cyclin A/CDK2 that acts to prevent re-replication during S phase is MCM4 within the MCM4-MCM6-MCM7 complex, which is associated with DNA helicase activity. This phosphorylation inhibits DNA unwinding by the MCM complex, thereby removing replication competence from already-fired origins (Ishimi et al, 2000). Cyclin A2 levels increase as cyclin E1 levels decrease, and as cells enter mitosis, cyclin A2 associates with and activates CDK1. The cyclin subunit confers different substrate specificity for its kinase partner and differentially interacts and activates CDK1 and CDK2. Cyclin A2 finally becomes targeted for degradation by ubiquitination by APC (Honda et al, 2005).

Notably, both S phase cyclins are transcriptional targets of E2F: cyclin E via the relief of transcriptional repression resulting from the phosphorylation of pRb by cyclin D/CDK4/6, and cyclin A via cyclin E/CDK2's phosphorylation of pRb (Ohtani et al, 1995; Geng et al, 1996; Schulze et al, 1995; Harbour et al, 1999; Zhang et al, 2000). Redundancy has been observed between cyclin E and cyclin A, as it has been demonstrated that substrates of cyclin E/CDK2 can be phosphorylated by cyclin A/CDK2 in vitro. However, studies by Geng et al and Parisi et al in 2003 have shown that in mouse embryo fibroblast cells whilst cyclin E is dispensable for cell cycling, it is indispensable for entry into the cell cycle from quiescent G0 state, due to its role in the assembly of the preRC. Due to the overlapping and sometimes interchangeable functions of cyclin E and cyclin A, both cyclins have been investigated in this study.

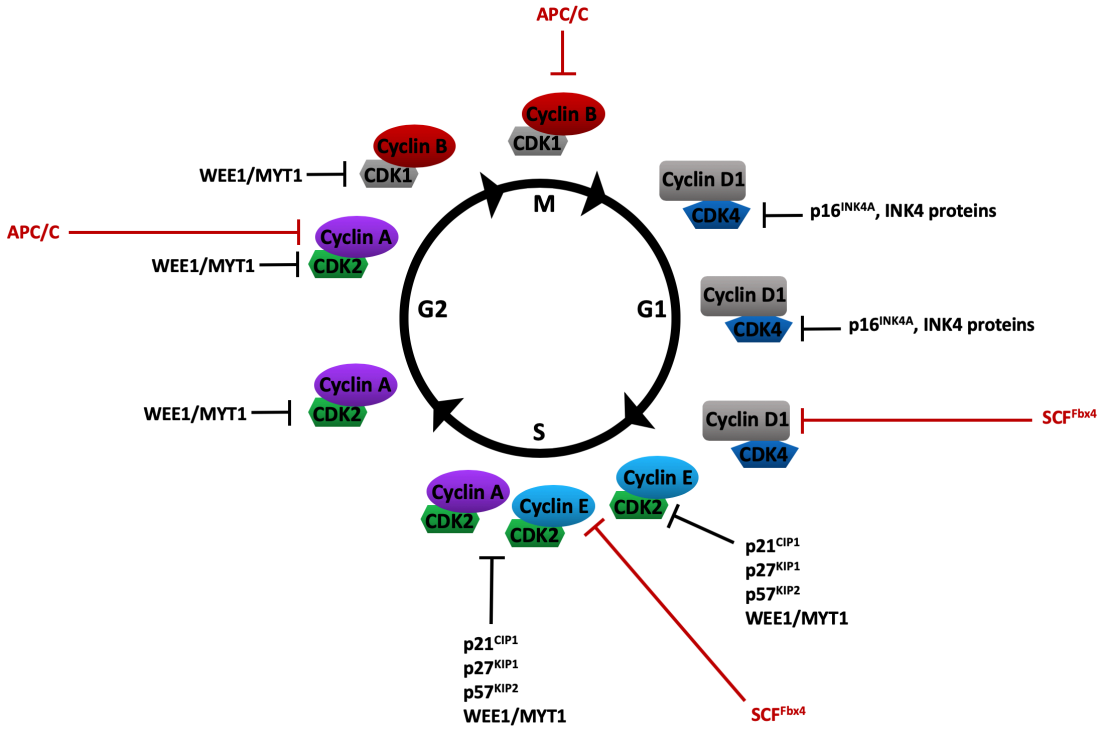


Figure 1.4: Schematic showing different cyclin/CDK partners controlling different phases of the cell cycle.

Adapted from Morgan & Reuter, 2006. Red lines indicate protein degradation pathways of cyclin proteins and black lines indicate inhibitors of CDK activity.

1.7 Aim of this study

The hypothesis is that expression of S phase cyclins may determine sensitivity to ATR inhibitors.

The first aim of this study was to characterise NSCLC lines in response to ATR inhibition, particularly in sensitive (PC-9) and resistant (H1975) cell lines, and also in ATR inhibitor resistant cell lines (SO25, SO45 and SO46). The second aim was to overexpress S phase cyclins in parental (PC-9 and H1975) and ATR inhibitor resistant cells (SO25 and SO45). The third and final aim was to knockdown cyclin A levels in parental cell lines.

CHAPTER 2

2 Materials and Methods

2.1 Mammalian Cell Culture

2.1.1 Maintenance of cell lines

The cell lines used in this study are listed in Table 2.1. Cells were cultured in 25, 75 and 150 cm^2 tissue culture flasks (Corning Incorporated; Corning, NY, USA) and incubated in a standard humidified incubator at 37˚C and 5% CO_2. Cells were cultured in Advanced Dulbecco's Modified Eagle Medium (DMEM)/F12 (Life Technologies, Carlsbad, CA, USA) supplemented with 5% foetal bovine serum (FBS; Sigma-Aldrich; St. Louis, MO, USA), 2mM GlutaMAX™ (Life Technologies), and 50 U penicillin / 50 µg/mL streptomycin (Life Technologies). Derivatives of the parental PC9, H1975, SO25 and SO45 cell lines were cultured in the previously described advanced culture medium that was supplemented with 5% Tet-free FBS[1] (PAN Biotech, Germany). SO25 and SO46 cell lines were cultured in 1 µM AZD6738 (AstraZeneca; Macclesfield, UK), and SO46 in 2 µM AZD6738. shRNA and cDNA-transfected cells were cultured in 0.25 µg/mL puromycin (Calbiochem, San Diego, CA, USA). The cells were passaged at 70-80% confluency, the culture medium was changed every two to five days, and cells were not passaged more than 25 passages. Passages involved aspiration of medium, washing with PBS, and trypsinisation with Trypsin/EDTA (Life Technologies) for five to ten minutes. Growth medium was then added to inactivate the trypsin activity and cells were split between 1:4 and 1:20.

Authenticated cell lines obtained from the ATCC were cultured continuously for no more than 4 months or 25 passages. All cell lines were additionally identified by sequencing highly polymorphic loci in mitochondrial DNA as described by Hutter et al, 2004.

[1] Lot A PO40214TC

2.1.2 Lentiviral transfection

Four derivatives of the parental PC9 and H1975 cell lines were generated by the introduction of the inducible ZIP lentiviral vector pZIP-TRE3GS, which confers puromycin resistance. The vector (Figure 1) contains a synthetic promoter which is activated upon addition of doxycycline to the medium. The Tet-on 3G transactivator protein is synthesised constitutively under the control of human phosphoglycerate kinase (hPGH) promoter. Upon addition of doxycycline, the Tet-on 3G protein undergoes a conformational change allowing it to bind and activate the TRE3GS promoter. The TRE3GS promoter is located upstream of the ZsGreen fluorescent marker gene and shRNA sequence. Two PC9 and two H1975-derived cell lines; pZIP shRNA CCNA2 and pZIP control for each cell line, were generated by lentivirus transduction using this vector. pZIP shRNA CCNA2 cells harbour the shRNA targeting CCNA2 mRNA and a clone with confirmed knockdown of cyclin A2 protein levels has been used in this study. pZIP control cells express a non-targeted (NT) shRNA and a mixed population was used in this study.

shERWOOD-UltramiR Lentiviral Inducible pZIP target gene set for human CCNA2 [2] (Transomic Technologies, Huntsville, AL, USA) was used. ULTRA non-targeting pool shRNA[3] (Transomic) served as a control. The transfer plasmid (shERWOOD-UltramiR CCNA2), packaging plasmid (psPAX2)[4] and envelope plasmid (pMD2.G)[5] (Addgene, Cambridge, MA, USA) were purified by QIAprep Spin Miniprep Kit (Qiagen, Germantown, MD, USA) and propagated in culture for storage in glycerol at -80 ˚C (500 µL). One day before transfection, HEK-293T cells were seeded in complete culture medium in four T75 flasks for 70-95% confluency the following day. After incubating overnight at 37 ˚C to allow for re-attachment, each flask of cells were transfected with 6 µg of transfer vector, 6 µg of packaging plasmid, 3 µg of envelope plasmid and 8 µg of DGCR8 siRNA (targets nuclease Pasha).

First, four separate mixtures, each consisting of 45 µL FuGENE® HD Transfection Reagent (Promega Corporation, Madison, WI, USA) and 870 µL serum-free Opti-MEM® (Life

[2] ULTRA-3409670-pZIP(TRE3G), ULTRA-3409672-pZIP(TRE3G), ULTRA-3409673-pZIP(TRE3G)
[3] TLNSU4300-ULTRA-NT#4-pZIP(TRE3G)
[4] #12260
[5] #12259

Technologies) was prepared for four flasks and incubated for 5 mins at RT. Another four separate transfection tubes were prepared, containing the transfer, packaging and envelope plasmids and DGCR8 siRNA. These were incubated for 15 mins at RT and added drop-wise to cells along with the FuGENE® and Opti-MEM® mixture and mixed. Flasks were incubated at 37 ˚C for 16 h, after which media was replaced with Tet-free FBS media (PAN Biotech), to allow low basal levels of target gene expression.

The following day, virions were collected from HEK-293T cells to be used to transduce target cell lines (PC-9 and H1975). Firstly, 10 mL supernatant was collected from the control transfer vector-transfected flask of transfected cells and loaded onto a syringe and filtered using a 0.45 μm filter into a new 15 mL falcon tube. The flask was replenished with 8 mL Tet-free culture medium to incubate overnight to freeze down the viral supernatant the following day. Each 10 mL supernatant from the other three transfer vector-transfected flasks were collected in a 50 mL falcon and mixed. 10 mL of this mixed supernatant was loaded onto a syringe and filtered into a new 15 mL falcon as done for the control transfer vector. The flasks were replenished with 8 mL Tet-free culture medium and incubated overnight to freeze down the next day. 5 mL of appropriate filtered viral supernatant was added to the appropriate target cell flask and transduced flasks were incubated at 37 ˚C for 24 h. The following day, transduced H1975 cells were washed five times with PBS and replaced with 5 mL Tet-free culture medium. Transduced PC-9 cells were washed ten times with PBS and trypsinised and split 1:10. 48 h post-transduction, the selective marker (puromycin), was added to the transduced cells at a final concentration of 5 μg/mL. Transduced cells were cultured for approximately ten days at this puromycin concentration, and for maintenance, cells were cultured in a decreased puromycin concentration of 0.25 μg/mL.

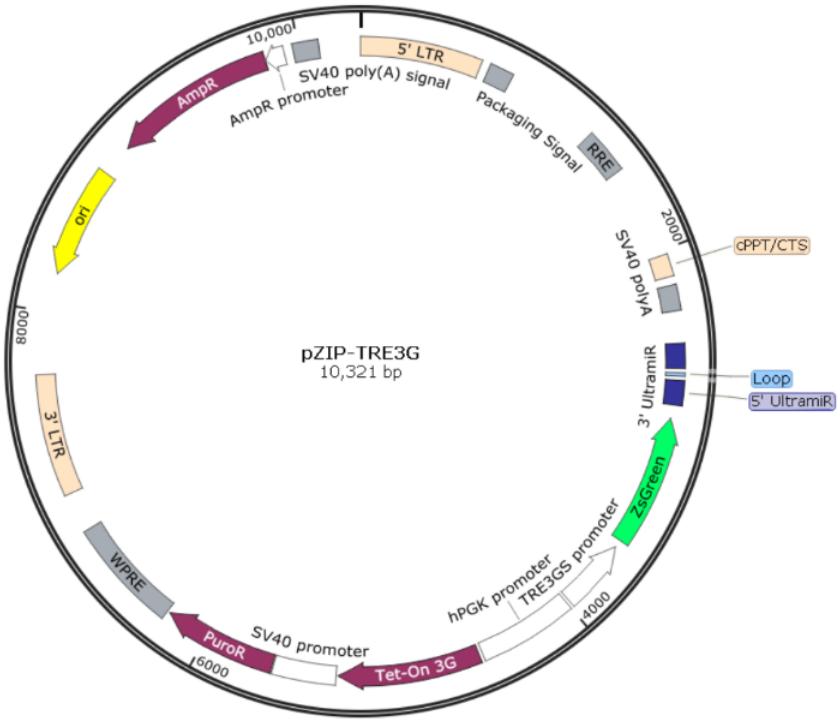


Figure 2.1: shERWOOD UltramiR lentiviral inducible shRNA (pZIP-TRE3GS) vector map.

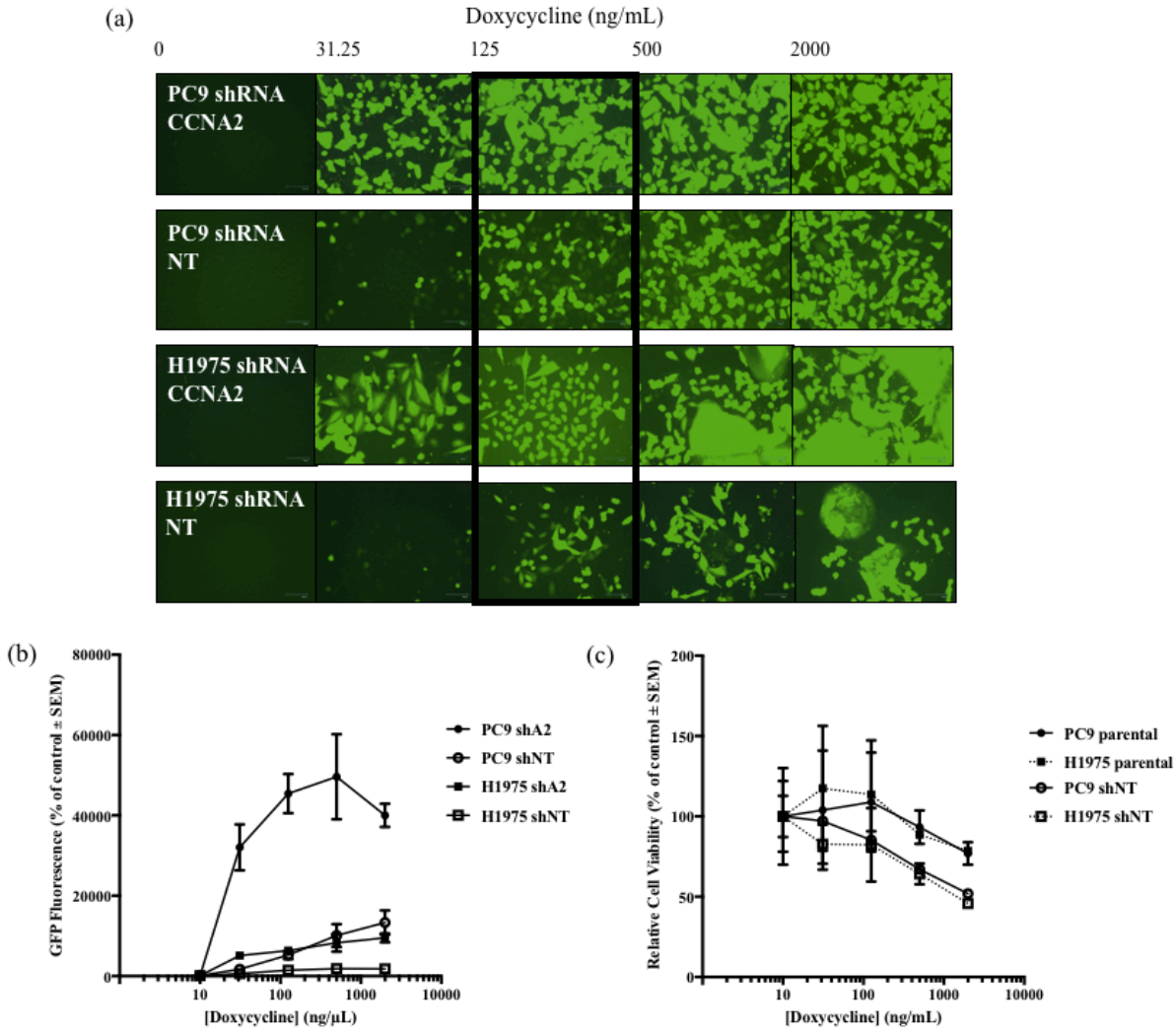


Figure 2.2: Optimisation of doxycycline concentration in knockdown cells.

(a) Knockdown cell lines and their respective non-target (NT) cell lines were transfected with doxycycline and 3 days post-induction, green fluorescence images were taken using FLoid Cell Imaging Station (Life Technologies). (b) The level of GFP fluorescence was recorded using a POLARstar Omega plate reader (BMG Labtech GmbH) 3 days post-induction. (c) Relative cell viability was assessed using the resazurin proliferation assay and normalized to DMSO treated controls. Each point represents the mean of three independent experiments, each performed in triplicate with error bars = SEM. No statistically significant difference was found in relative cell viability between parental and shNT (control) cell lines at the doxycycline concentration chosen for the study (75 ng/mL).

2.1.3 cDNA transfection

Two further cell lines were derived from each parental cell line containing ORF of cyclin A2 or cyclin E1 in pENTER. The cDNA sequence of cyclin A2 or cyclin E1 with a C-terminal Flag and His-tag is positioned downstream of the human cytomegalovirus (CMV) promoter and thus cyclin A2 or cyclin E1 protein is expressed constitutively. Following transfection, a clonal cell

line was used in this study. Six SO25 and SO45-derived cDNA cell lines were also produced, including double cDNA ORF cell lines for each of these parental cell lines. Table 2.1 shows an overview of the cell lines used in this study.

ORF of cyclin A2[6] and cyclin E1[7] in pEnter (Vigene, Biosciences Inc., Rockville, MD, USA) were used. Ice bits from each glycerol bacterial stock were streaked on agar plates with kanamycin (30 μg/mL) and incubated overnight. Individual colonies were picked from each plate, grown up in 2 mL LB broth with kanamycin (30 μg/mL) overnight at 37 ˚C in an incubator shaking at 225 rpm. The next day, 500 μL of each overnight grown culture was kept for bacterial glycerol stocks and the rest was purified using the QIAprep Spin Miniprep Kit (Qiagen). One day before transfection, PC-9 cells were seeded in complete culture medium in a 6-well plate at a density of 125,000 cells/well and H1975 cells were seeded at a density of 200,000 cells/well (1 well per cell line and plasmid). After incubating overnight at 37 ˚C to allow for re-attachment, cells were transfected with 1 μg DNA using 1:2.5 of DNA:Lipofectamine™ 2000 Transfection Reagent (Thermo Scientific; Waltham, MA, USA).

First, separate mixtures of Lipofectamine™ 2000 Transfection Reagent with Opti-MEM®, and the plasmid DNA with Opti-MEM® were prepared and incubated for 5 mins at RT. The two solutions were then combined, mixed and incubated for 20 mins at RT. The mixture was then added to the 6-well plates and incubated overnight at 37 ˚C. Treatments were made with CCNA2 cDNA and CCNE1 cDNA, while there were also wells treated only with transfection reagent and DNase/RNase-free water (Zymo Research; Irvine, CA, USA) and wells left untreated. In order to reduce cytotoxicity to the cells, media from cells were aspirated the next day and once cells were washed with PBS, cells were replenished with fresh complete culture medium containing puromycin. During the selection period, medium was changed every 2-4 days and positive single clones were selected at least 14 days post-transfection. For selection of vector-

[6] #CH818002
[7] #CH847165

containing cells, complete culture medium with 0.5 µg/mL puromycin was used, and for maintenance, cells were cultured in 0.25 µg/mL puromycin.

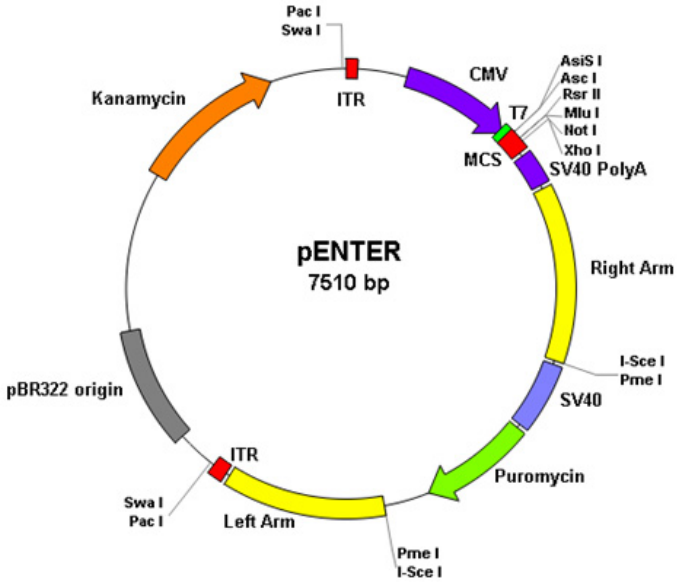


Figure 2.3: Vector map of Vigene ORF of cyclin A2 (CCNA2) or cyclin E1 (CCNE1) in pENTER.

Table 2.1: Cell lines used in this study.

The designation used throughout the study for each cell line is in bold. All cell lines used are of human origin.

Cell Line[8]	Obtained from
Calu-6	ATCC[9] #HTB-56
H1299	ATCC #CRL-5803
H1975	ATCC #CRL-5908
H1975 cDNA CCNA2	This work
H1975 cDNA CCNE1	This work
H1975 shRNA CCNA2	This work
H1975 shRNA NT	This work
PC-9	[10]
PC-9 cDNA CCNA2	This work
PC-9 cDNA CCNE1	This work
PC-9 shRNA CCNA2	This work
PC-9 shRNA NT	This work
SO25	[11]
SO25 cDNA CCNA2	This work
SO25 cDNA CCNE1	This work
SO25 cDNA CCNA2 + CCNE1	This work
SO45	[3]
SO45 cDNA CCNA2	This work
SO45 cDNA CCNE1	This work
SO45 cDNA CCNA2 + CCNE1	This work
SO46	[3]

[8] Histology; PC-9, H1975 both lung adenocarcinoma; Calu-6, H1299 both lung carcinoma
[9] ATCC = American type culture collection (Manassas, VA, USA)
[10] Kindly provided by Dr. Kazuto Nishio, Kinki University, Osaka, Japan
[11] Kindly provided by Samantha Olyha (Anderson Ryan laboratory)

2.1.4 Cell counting and seeding

Cell density and viability were measured using the Countess® automated cell counter (Life Technologies). A 1:1 mixture of a cell suspension and 0.4% trypan blue solution (Life Technologies) were added to a Countess® cell counting chamber slide and inserted into the Countess® automated cell counter for standard counting. The desired number of cells were then seeded in fresh culture media prior to any experiments. SO25, SO45 and SO46 cell lines were always plated without the presence of AZD6738. 1 or 2 μM AZD6738 was added after approximately 25 h. shRNA or cDNA-transfected cell lines were always plated without the presence of puromycin.

2.1.5 Cryostorage and thawing of cells

For cryopreservation, cells were grown to 80-90% confluency and trypsinised as described in 2.1.1. The cells were pelleted by centrifugation (225 x g, 5 min), the supernatant was aspirated, and the cells were re-suspended in 5mL of complete culture medium with 10% (v/v) dimethyl sulfoxide (DMSO; VWR, Radnor, PA, USA). 500 μL aliquots were then transferred to cryogenic tubes (Corning Incorporated) and frozen at -80 ˚C overnight in an isopropanol Mr. Frosty™ Freezing Container (Thermo Scientific) before being transferred into the vapour phase of a liquid nitrogen tank for long term storage.

To thaw cells from liquid nitrogen storage, the cells were first rapidly thawed at 37 ˚C. These cells were diluted in 6 mL of 37 ˚C complete culture medium and pelleted by centrifugation (225 x g, 5min). The supernatant was then aspirated and the cell pellet was re-suspended in 12 mL of 37 ˚C complete culture medium and transferred to a 75 cm^2 flask. Culture medium was changed the next day.

2.2 Drug Treatments

Stock solutions of AZD6738, AZD7762 (AstraZeneca; Macclesfield, UK), MK1775, VE822 (Selleck Chemicals; Houston, TX, USA) and gemcitabine (LC Laboratories; Woburn, MA, USA) were prepared in 100% DMSO at a concentration of 10 mM. All stock solutions were

aliquoted and stored at -20 ˚C until use and dilutions of the drugs for treatment of cells were made using complete culture media.

2.3 Resazurin Cell Viability Assay

Resazurin-based cell viability assays were carried out to assess the impact of DNA damage response inhibitors and chemotherapeutic drugs on cell proliferation and viability (O'Brien et al, 2000). Cells were seeded in 100 µL complete culture medium in triplicate in 96-well plates (Costar®, flat bottom; Corning Incorporated) at a density of 500 cells/well and incubated overnight to allow for re-attachment. Drugs and inhibitors were then added in 100 µL complete culture medium at the required concentrations and dilutions and plates were incubated for three days. In the optimisation step of this study, doxycycline was used instead of the drug and once optimised, drugs were investigated in the presence of doxycycline. The doxycycline concentration chosen for this study was 75 ng/mL and the doxycycline incubation period pre-drug treatment was 3 days.

On the fourth day after treatment, 20 µL of resazurin solution (0.125 mg/mL in dH_2O; Sigma-Adlrich) per 200 µL media was added to each well, including media-only "blank" wells and plates were incubated for 2 hours. In metabolically active cells, resazurin is reduced to highly fluorescent resorufin and this fluorescent signal is proportional to the number of viable cells. Fluorescence intensity was measured with a POLARstar Omega plate reader (BMG Labtech GmbH; Ortenberg, Germany) with excitation at 544 nm, emission at 590 nm, and gain 1000. The average of the values of the triplicate "blank" wells were subtracted from all other wells and normalised to the average of the vehicle-treated wells.

2.4 PicoGreen Cell Proliferation Assay

The PicoGreen assay is a sensitive and specific assay for dsDNA. The PicoGreen cell proliferation assay was used to measure cell growth (determined by increased dsDNA content) over a period of eight days. Cells were seeded in 100 µL complete culture medium in triplicate in 96-well plates (Costar®, flat bottom; Corning Incorporated) at a density of 500 cells/well and incubated overnight to allow for re-attachment. The following day, the medium in the first

column for “day 1” was aspirated and 100 µL of DNA lysis buffer (Table 2.2) was added per well. AZD6738 or 0.01% DMSO (vehicle control) were added in 100 µL complete culture medium to the appropriate remaining wells to reach a final concentration of 1, 2, or 4 µM and the plates were maintained in the incubator. Every 24 hours for eight days, the medium was aspirated in the appropriate column corresponding to the day and 100 µL of DNA lysis buffer was added to each well. After DNA lysis buffer was added to the final wells, Quant-iT™ PicoGreen® dsDNA reagent (Life Technologies) was diluted 1:200 in sterile PBS (Lonza; Basel, Switzerland) in the hood with the light off. 100 µL of this PicoGreen® solution was then added to each well, and the plates were incubated for 20 minutes. Fluorescence intensity was measured with a POLARstar Omega plate reader (BMG Labtech GmbH) with excitation at 480 nm, emission at 520 nm, and gain 1000. The average of the values of the triplicate “blank” wells (solely DNA lysis buffer) were subtracted from all other wells and normalised to the average of the wells from “day 1”.

Table 2.2: DNA lysis buffer composition.

DNA lysis buffer solution was prepared in the tissue culture hood under sterile condiions and filter sterilised with a 0.45 nm filter (Sartorius Stedim Biotech; Goettingen, Germany). The solution was stored at 4 °C.

Component	Amount	Final Concentration
0.5 M EDTA. pH 8.0[12]	2.5 mL	25 mM
Triton X-100[13]	50 µL	0.1%
dH_2O	47.45 mL	

2.5 ZsGreen Fluorescence Intensity Assay

2.5.1 Quantitative fluorescence assay using POLARstar Omega plate reader (BMG Labtech GmbH)

ZsGreen fluorescence can be used as a measure of shRNA produced as this gene is under the same promoter. Using a broad dose range (0 to 2000 ng/mL) for 24 hours treatment, doses can be selected at different treatment times to investigate effects at different induction levels at

[12] AccuGENE, Lonza
[13] VWR International; Randor, PA, USA

different times. Cells were seeded in 100 µL complete culture medium in triplicate in 96-well plates (Costar®, flat bottom; Corning Incorporated) at a density of 500 cells/well and incubated overnight to allow for re-attachment. The following day, doxycycline or 0.01% DMSO (vehicle control) were added in 100 µL complete culture medium to the wells to reach a final concentration of 2000 ng/mL in the first column of wells and serially diluted across the columns. The plates were maintained in the incubator for 24 hours. Fluorescence intensity was measured with a POLARstar Omega plate reader (BMG Labtech GmbH) with excitation at 480 nm, emission at 520 nm, and gain 1000. The average of the values of the triplicate "blank" wells (solely DNA lysis buffer) were subtracted from all other wells and normalised to the average of the vehicle-treated wells.

2.5.2 Qualitative fluorescence assay using FLoid Cell Imaging Station (Life Technologies)

During the optimisation step of this study, bright-field and green fluorescence images were taken of the 6-well plates with a FLoid Cell Imaging Station (Life Technologies) at 460x magnification (20x objective).

2.6 Protein Detection by Western Blotting

2.6.1 Preparation of cell extracts, gel electrophoresis and transfer

Cells were seeded in 6-well plates (Corning Incorporated) and grown until they reached 70% confluency. They were treated for 24 hours before cell lysis. To lyse cells, cells were washed twice in ice-cold (4 ˚C) 1 x PBS (Sigma-Aldrich) on ice. When assessing cell cycle in synchronised cells (0, 1, 2, 4, 8, 16 and 24 h), floating/dying cells were collected by collecting the media and PBS in falcon tubes that were centrifuged for 5 mins at 1800 rpm. The resulting pellet was resuspended in 150 µL 1 x PBS (Sigma-Aldrich) and transferred into Microcentrifuge tubes (Sigma-Aldrich) and centrifuged again for 5 mins at 2000 rpm. 40-100 µL lysis buffer (Table 2.3) supplemented with 1 mM sodium orthovanadate (Na_3VO_4; Sigma-Aldrich) and cOmplete™ protease inhibitor cocktail (Roche; Basel, Switzerland) was added to each plate on ice for 10 mins. Cells were then lysed by mechanical scraping and if collecting floating cells, the lysate was added to the cell pellet in the Microcentrifuge tube and vortexed together. The

cells were homogenised by sonication 3 x (10 secs on/5 secs off) (Bioruptor® Plus; Diagenode Inc.; Liege, Belgium) and centrifuged for 15 mins at 4 ˚C at 13,000 rpm.

Protein concentrations were determined using a NanoDrop 1000 spectrophotometer (Thermo Scientific) and diluted in lysis buffer stock and 2x Laemmli sample loading buffer (Sigma-Aldrich) to equal protein concentrations. The samples were then incubated at 95 ˚C for 10 mins in a dry heating block (AccuBlock™ Digital Dry Bath; Labnet International, Inc.; Edison, NJ, USA). 10 – 50 µg protein per lane was loaded onto a precast 4-15% or 4-20% gradient Mini-PROTEAN® TGX™ gel (BioRad; Hercules, CA, USA) alongside a Precision Plus Protein™ Dual Color ladder (BioRad). The gel was run at 250 V for approximately 20 mins with Trs/Glycine/SDS running buffer (BioRad). When assessing cDNA and shRNA transfection lysates, a Criterion™ TGX™ gel (BioRad) was used and run and 150 V for 1 h. Proteins were then transferred to nitrocellulose membranes (0.45 µm pore size Trans-Blot®; BioRad) in cold 1x Tris/Glycine buffer (BioRad) with 20% methanol (v/v; Sigma-Aldrich) for 35 mins at 150V (or 1 h at 90 V for larger gels) with an ice pack cooler and magnetic stirrer.

Table 2.3: Lysis buffer stock components for western blot cell extract collection.

Lysis buffer stock solution was aliquoted and stored at 4 ˚C.

Component	Amount	Final Concentration
1 M Tris-Hcl, pH 7.6[14]	1.25 mL	50 mM
NaCl[15]	200 mg	137 mM
(v/v) glycerol[7]	2.5 mL	10%
(v/v) Igepal[16]	25 µL	0.1%
10% (v/v) SDS[17]	250 µL	0.1%
2% sodium fluoride (NaF)[8]	2.626 mL	50 mM
dH_2O	16.1 mL	

2.6.2 Immunoblotting and Protein Detection using LI-COR

Following transfer, the nitrocellulose membranes were stained with Ponceau S solution (Sigma-Aldrich), cut where appropriate and washed twice with PBS-T or TBS-T (Table 2.4). Membranes were incubated in blocking buffer (1:1 solution of PBS or TBS and Odyssey® Blocking Buffer LI-COR) for 1 h at room temperature on a roller (Stuart® roller mixer SRT9D; Bibby Scientific; Staffordshire, UK) to block non-specific binding of antibodies to the membrane. The membranes were then incubated with buffer containing primary antibodies (Table 2.5), diluted to recommended concentrations in a 1:1 solution of PBS-T or TBS-T and Odyssey® Blocking Buffer, and incubated overnight at 4 ˚C on a roller, with the exception of pChk1 antibodies which were incubated for 48 h. Following primary antibody incubation, membranes were washed three times for 5 mins each in PBS-T or TBS-T and incubated with the appropriate fluorophore conjugated secondary antibodies (Table 2.6) for 1 hr at RT on a roller, diluted in 1:1 solution of PBS-T or TBS-T and Odyssey® Blocking Buffer. Membranes were then washed three times for 5 mins each in PBS-T or TBS-T, then once with PBS or TBS. Detection was carried out by infrared scanning densitometry (Odyssey Infrared Detection

[14] Promega; Madison, WI, USA
[15] VWR
[16] Sigma-Aldrich
[17] AppliChem GmbH; Darmstadt, Germany

System, LI-COR Biosciences) at wavelengths 680 nm and 800 nm. Membranes were stored in 1x PBS at 4 ˚C or dried at RT.

Further analysis was performed using Image Studio Lite Ver 5.2. On each membrane, the housekeeping genes (cyclophilin B) was used as loading control and in cases where quantification was needed for comparison of protein levels, band intensities were normalised to the corresponding loading control levels.

Table 2.4: Buffers and solutions used in immunoblotting.

Buffer	Composition
1x phosphate buffered saline (PBS)	5x PBS tablets[18] dissolved in 1 L dH_2O
PBS-T	1x PBS, 0.1% (v/v) Tween-20[10]
1x Tris-buffered saline (TBS)	1x pack OmniPur® TBS 20x Ready Pack Powder[19] dissolved in 20 L dH_2O
TBS-T	1x TBS, 0.1% (v/v) Tween-20

Table 2.5: Primary antibodies used for immunoblot analysis

Specification (Name)	Species/ clonality	Dilution (solution)	Manufacturer, catalogue number
Total ATM	Rabbit mAb	1:500 (PBS)	Abcam, #ab32420
Phospho-ATM Ser1981	Rabbit mAb	1:10,000 (PBS)	Epitomics Inc.[20], #2152-1
ATR	Goat pAb	1:500 (PBS)	Santa-Cruz Biotechnology[21], #sc-1887
Total CDC6	Rabbit mAb	1:1,000 (PBS)	Cell Signaling, #3387
phospho-CDC6 Ser54	Rabbit mAb	1:2,000 (PBS)	Abcam, #ab75809
phospho-CDK1/2/3/5 Tyr15	Rabbit mAb	1:2,000 (PBS)	Abcam. #ab133463
Total CHK1	Mouse mAb	1:1,000 (PBS)	Santa-Cruz Biotechnology, #sc-8408
phospho-CHK1 Ser317	Rabbit pAb	1:1,000 (TBS)	Cell Signaling, #2344
phospho-CHK1 Ser345	Rabbit pAb	1:500 (PBS)	Cell Signaling, #2341

[18] Sigma-Aldrich
[19] Calbiochem; Darmstadt, Germany
[20] Burlingame, CA, USA
[21] Dallas, TX, USA

phospho-CHK2 Thr68	Rabbit pAb	1:1,000 (PBS)	Cell Signaling, #2661
Cyclin A2	Mouse mAb	1:1,000 (PBS)	Abcam. #ab16726
Cyclin E1	Rabbit pAb	1:1,000 (PBS)	Santa-Cruz Biotechnology, #sc-481
FLAG® M2	Mouse mAb	1:2,000 (PBS)	Sigma-Aldrich #F1804
Geminin	Rabbit pAb	1:1,000 (PBS)	Thermo Scientific[22], #PA5-30612
phospho-H2AX Ser319	Mouse mAb	1:1,000 (PBS)	Merck Millipore[23], #05-636
phospho-histone H3 Ser10	Rabbit pAb	1:2,000 (PBS)	Merck Millipore, #06-570
total KAP1	Rabbit pAb	1:10,000 (PBS)	Bethyl Laboratories[24], #A300-274A
phospho-KAP1 Ser824	Rabbit pAb	1:2,000 (PBS)	Bethyl Laboratories, #A300-767A
PPIB (Cyclophilin B)	Rabbit pAb	1:2,000 (PBS)	Abcam, #ab16045
total RPA32	Mouse mAb	1:500 (PBS)	Abcam, #ab2175
phospho-RPA32 Ser4/Ser8	Rabbit pAb	1:2,000 (PBS)	Bethyl Laboratories #A300-245A

Table 2.6: Secondary antibodies used for two-colour detection with infrared fluorescence.

Specification (Name)	Species/clonality	Dilution	Manufacturer, catalogue number
IRDye® 800CW	goat polyclonal	1:5,000	LI-COR, #926-32211
IRDye® 680RD	goat polyclonal	1:5,000	LI-COR, #926-68070

2.7 Synchronisation of Cells

A variety of methods have been developed to synchronise cells at various stages of the cell cycle. A simple, effective method that produces synchronous cells in mitosis is the mitotic shake-off method first developed by Terasima and Tolmach in 1963. Many cell lines round up in mitosis and with some physical agitation, those in mitosis can be "shaken-off." When plated onto dishes, these cells move into G1 in a synchronised mode. However, a disadvantage to this method is the

[22] Waltham, MA, USA
[23] Billerica, MA, USA
[24] Montgomery, TX, USA

low yield of mitotic cells due to the small percentage of cells in mitosis at any one time. This low yield can be increased by the use of nocodazole, a mitotic inhibitor, as first described by Zieve et al in 1980.

In the morning of day 1, each cell line was seeded into two T150 flasks at a density of 10 x 10^6 cells/flask for 70% confluency in the late afternoon. Once cells were re-attached by late afternoon, the medium was aspirated and cells were washed once with 1x PBS. Complete culture medium was replaced and nocodazole (Sigma-Aldrich) was added to a final concentration of 50 ng/mL. On day 2, after a 16 h nocodazole treatment, mitotic cells were shaken off in the growth medium by firmly shaking the flasks against a hard surface ten times. The medium for each cell line was collected separately in 50 mL falcons. 5 mL PBS was added to each flask and the shake-off procedure was repeated and the PBS was transferred to the appropriate falcon tube. The mitotic cells in the falcon tubes were centrifuged at 1200 rpm for 5 mins, then the supernatant was aspirated, and the cells were washed twice in 10 mL fresh complete culture medium. Cells were then re-suspended in 9 mL complete culture medium. Mitotic cells were counted and seeded (see 2.1.4) into 6-well plates at a density of 10 x 10^5 cells/well and treated with drug or vehicle immediately. Cells were lysed at appropriate times and prepared for western blot analysis as outlined in section 2.6.

2.8 Live Cell Imaging

Synchronised and unsynchronised cells (see 2.7 for protocol used for synchronisation) were seeded in 100 µL complete culture medium in 96-well plates (Costar®, flat bottom; Corning Incorporated) at a density of 4,000 cells/well (PC9) or 8,000 cells (H1975). Cells were then incubated overnight at 37 °C before imaging. Approximately 30 mins before taking the plate to the microscope, AZD6738 or the vehicle (DMSO) was added to the cells to a final concentration of 0.5, 1, or 2 µM. CellTox™ Green (Promega; Madison, WI, USA) was finally added to the cells to a concentration of 1:1,000. Cells were imaged on Eclipse Ti-E Nikon microscope (Nikon UK Limited, Kingston Upon Thames, UK) that provided a humidified atmosphere at 37 °C and 5% CO_2 within an environmental chamber (Solent Scientific Ltd; Segensworth, UK. Images

were taken at a 100x magnification (10x objective) using the NIS-Elements Advanced Research Software 3.2 (Nikon UK Limited). The well positions were set and images were taken of the cells treated with AZD6738 or DMSO with bright field illumination and with fluorescence using the GFP filter cube over 24 h, with 1 image being taken every 15 mins. Nine images were taken for each well that were stitched up to give a wider view of the well.

In order to count the number of cells per time frame over 24 h for every condition, images taken at every hourly timepoint were printed and a set template was used. The template consisted of a gridline with 36 squares, 6 by 6, each small square's side measuring 1 cm. For each timepoint, one small square was chosen (centre) in which to count the number of cells. This count was multiplied by 36 to give the total number of cells per time-point. In the analysis of the data, binned groups were used. Three hourly timepoints were used per binned group, with the exception of the first group using two timepoints (0 and 1 h). The total number of cells per hourly timepoint was normalised to average of the total number of cells from the first binned group and averages were taken per binned group. Graphs were generated using Microsoft Excel and fit with a line of best fit (polynomial with order of 3). Doubling time was calculated using the equation of polynomial trendline from the raw data. ANOVA 2 factor with replication was performed without the first binned group.

To detect fluorescent cells, ImageJ was used. The function "find maxima" was used.

2.9 Flow Cytometry: DNA Content Analysis/Cell Cycle Analysis

In order to analyse DNA content by flow cytometry, cells were first seeded in 10cm dishes and grown until they were approximately 65% confluent. Cells were then treated with either 2 μM AZD6738 or 0.01% DMSO (vehicle control) for 24 h. Floating/detached cells were retained while attached cells were trypsinised. Both floating and attached cells were then combined and collected by centrifugation (225 x g, 4 mins). The supernatant was discarded and the cell pellets were fixed by the dropwise addition of 1.5 mL ice-cold 70% ethanol (Sigma-Aldrich) while vortexing. Pellets were then stored at -20 °C until preparation to run the samples. At this point, pellets were washed with 2 mL 1x PBS, resuspended and rehydrated for 2 mins. Cells were then

centrifuged at 225 x g for 5 mins and resuspended in 1 x PBS. Propidium iodide (PI; Calbiochem) was added to a final concentration of 20 µg/mL. PI stains DNA stoichiometrically and so the amount of fluorescent signal is directly proportional to the DNA content. The DNA content of cells was measured using a FACSort™ Flow Cytometer (BD Biosciences; San Jose, CA, USA) and BD CellQuest™ Pro Software. ModFit LT software (Verity Software House; Topsham, ME, USA) was utilised to determine the proportion of cells in G1, S or G2/M cell cycle phases, using the gating parameters shown in Figure 2.4.

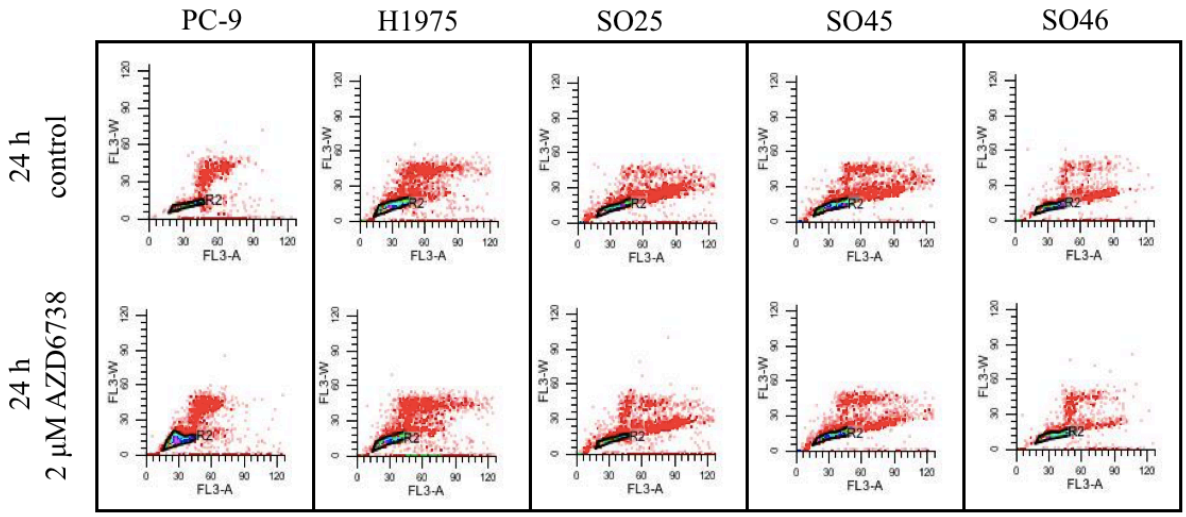


Figure 2.4: Parameters used in gating populations.

Pulse area (FL3-A) vs. pulse width (FL-W), with aneuploid cells to the right of the gated population.

2.10 DNA Purification from Mammalian Cell Culture (MasterPure kit)

PC9, SO25, SO45 and SO46 cells were each plated in 10 cm dishes until 85% confluent. Cells were trypsinised and pelleted and DNA was purified using the MasterPure™ DNA Purification Kit (Epicentre, Madison, WI, USA), following the manufacturer's instructions. Samples were stored at -20 °C until whole-exome DNA sequencing was carried out by a commercial provider (Source Bioscience, Nottingham, UK) using the HiSeq 2000 platform (Illumina).

2.11 Data Analysis and Statistics

GraphPad Prism® 7 (GraphPad Software, Inc.; La Jolla, CA, USA) was used for all statistical analysis and all values are expressed as the mean ±standard error of the mean (SEM) of at least three independent experiments unless otherwise stated. For data comparisons between two groups, such as inhibitor treated vs. vehicle control treated, two-sided Student's t-test was used. Survival response of inhibitor or vehicle control treated cells over 8 days were compared by analysis of variance (ANOVA) with cell line and treatment as factors, in order to detect statistically significant differences between parental and cDNA or shRNA-transfected cell lines. Differences with p values < 0.05 were considered significant.

CHAPTER 3

3 Characterization of Parental and Resistant Cell Lines

3.1 Sensitivity of cell lines to DNA damage response modulators

PC-9 cells were used as one of the cell lines to represent the response of a sensitive cell line to ATR inhibition, as previous work in the lab had established that these p53 mutant cells were relatively sensitive to ATR inhibition with an AZD6738 mean IC_{50} value of 0.5 μM ± 0.5 – 0.52 (data from Weber, 2015) (Table 3.1). H1975 NSCLC cells were used as the other cell line to represent the response of a more resistant cell line to ATR inhibition, with an AZD6738 mean IC_{50} value of 2.2 μM ± 2.1 – 2.4 (data from Weber, 2015). Both PC-9 and H1975 cell lines are EGFR mutants.

To determine the effects of replication stress on sensitivity to ATR inhibitors, I investigated a number of lung-derived human cell lines with a range of known IC_{50} values for AZD6738, with PC-9 the most sensitive and H1975 as the least sensitive (Table 3.1).

Table 3.1: Sensitivity of various human lung cancer cell lines to AZD6738.
Data taken from Weber, 2015.

Cell Line	Histological subtype	p53 expression status	AZD6738 IC_{50} [μM] (Mean ± SEM, range)
H1975	Adenocarcinoma	Homozygous mutant	2.2 (2.1-2.4)
H1299	Large cell carcinoma	Homozygous mutant	2.2 (1.9-2.4)
Calu-6	Anaplastic carcinoma	Null	0.7 (0.64-0.72)
PC-9	Adenocarcinoma	Homozygous mutant	0.5 (0.5-0.52)

These cell lines were treated with different classes of DNA damage response (DDR) modulators. Notably, the H1299 cell lines had relatively increased cell viability at intermediate concentrations (0.001 – 0.01 μM) of all four DDR modulators (Figure 3.1). The highest relative cell viability was apparent for H1299 in the presence of 0.01 μM MK1775 with an increased

cell viability of 237.30%. On the other hand, at the same concentration of MK1775, the more sensitive cell line Calu-6 exhibited a relative cell viability of 105.60%. MK1775 is a selective inhibitor of WEE1, which plays an important role in the G2/M checkpoint by inhibiting CDK1 and also plays a role in regulating firing of DNA replication origins (Dominguez-Kelly et al, 2011). Dose response curves for AZD6738 and VE822 have a similar profile for all four cell lines, which is as expected as they are both inhibitors of ATR. However, VE822 is a more potent inhibitor, as is put into evidence by the left-shift of the curves.

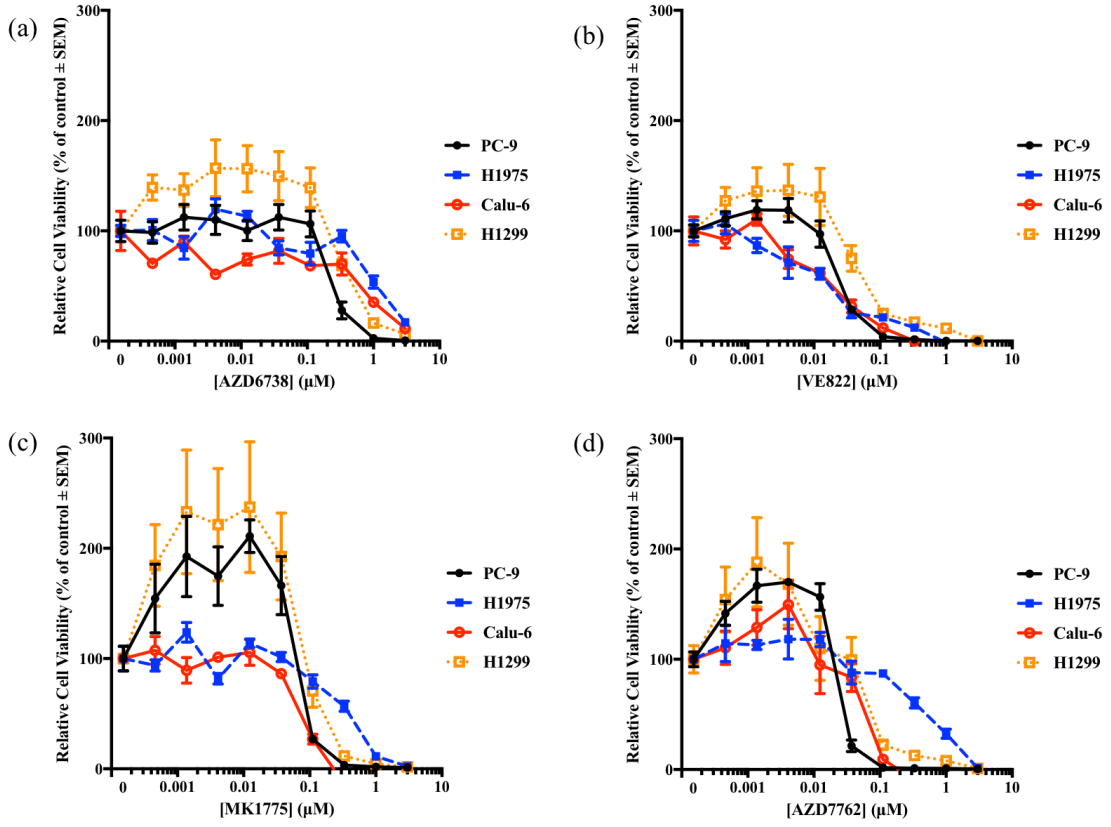


Figure 3.1: Responses of NSCLC cell lines to different classes of DNA damage response modulators.

Cells were incubated for 3 days with (a) AZD6738 (ATR inhibitor), (b) VE822 (ATR inhibitor), (c) MK1775 (WEE1 inhibitor), and (d) AZD7762 (CHK1/2 inhibitor). Relative cell viability was assessed using the resazurin proliferation assay and normalized to DMSO treated controls. Each point represents the mean of three independent experiments, each performed in triplicate with error bars = SEM.

3.2 Growth inhibition in synchronised and unsynchronised parental cells

To assess the growth rate of sensitive PC-9 cells and the more resistant H1975 cells in the presence and absence of AZD6738, unsynchronised and synchronised (mitotic shake-off) cells were imaged for up to 23 hrs in high and intermediate concentrations of ATR inhibitor, and untreated as control. Different concentrations of AZD6738 were used for PC-9 and H1975 cells due to their differing sensitivities to the ATR inhibitor (Table 3.1). In the absence of AZD6738, PC-9 cells had a faster growth rate (22 hrs for synchronised PC-9 cells) than H1975 cells (25 hrs for synchronised H1975 cells) (Table 3.2). In the presence of intermediate concentrations of AZD6738, both synchronised cell lines had decreased growth rates and doubling times that increased at a similar level (1.36 relative increase for PC-9 and 1.32 relative increase for H1975). At high AZD6738 concentrations however, synchronised H1975 cells maintained a similarly reduced growth rate as at intermediate concentrations with the same doubling time, whereas PC-9 cells exhibited a slower growth rate with a doubling time that increased 1.73 times relative to the control. Interestingly, when ATR inhibitor was added to synchronised H1975 cells, cells grew faster compared to control for up to 10 hrs (Figure 3.2). This observation that AZD6738 may increase growth rate in the acute response of H1975 cells, but not PC-9 cells, may be explained in part by its relatively slower growth rate.

Notably, despite the faster growth rate of PC-9 cells, in the presence of 1 μM AZD6738, synchronised PC-9 cells had a longer doubling time of 38 hrs compared to H1975 cells that had a doubling of 33 hrs. This highlights the relatively high sensitivity of PC-9 cells to AZD6738 in comparison to H1975 cells.

Table 3.2: Effect of AZD6738 treatment on doubling time of unsynchronised and synchronised PC-9 and H1975 cells.

N. C.* = not calculable.

AZD6738 treatment		Doubling time (hrs)
Unsynchronised		
	PC-9	
	Control	17
	0.5 μM	23
	1 μM	N. C.*
	H1975	
	Control	21
	1 μM	26
	2 μM	45
Synchronised		
	PC-9	
	Control	22
	0.5 μM	30
	1 μM	38
	H1975	
	Control	25
	1 μM	33
	2 μM	33

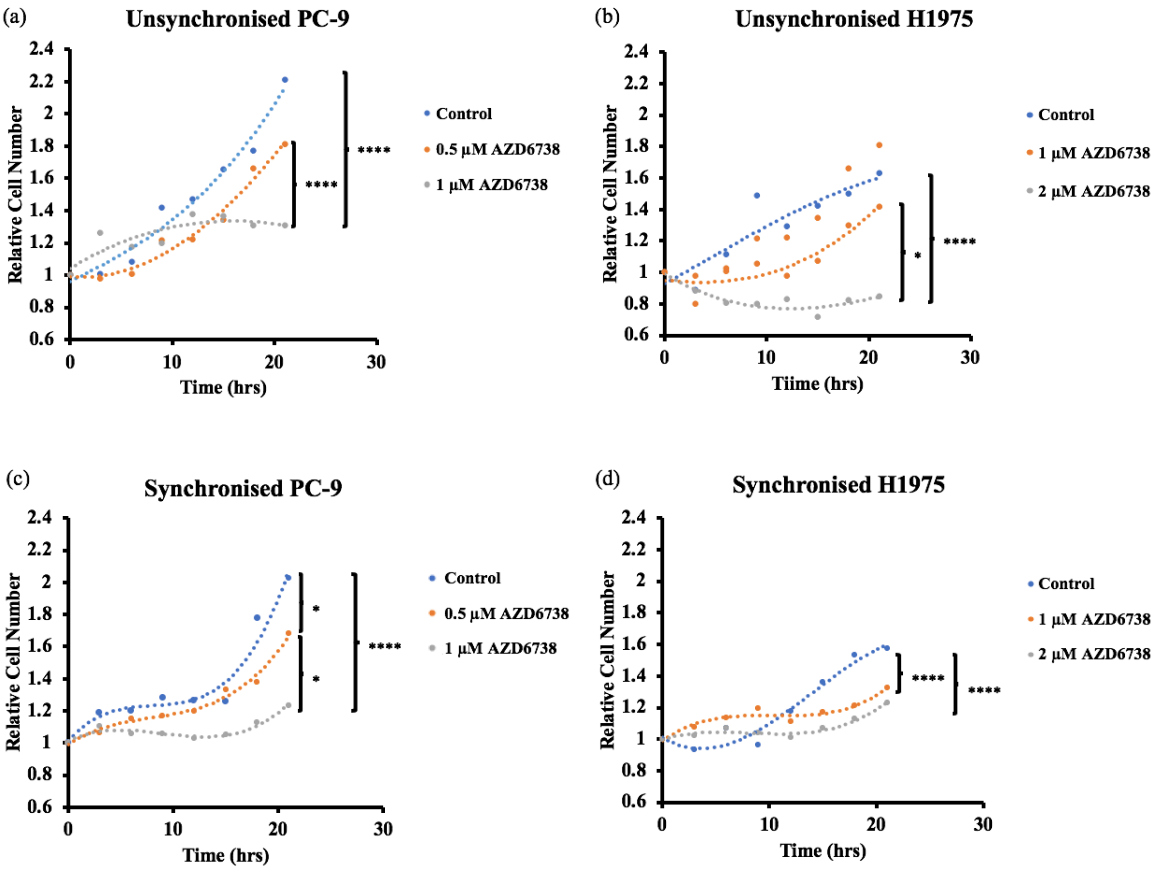


Figure 3.2: Relative cell growth of PC-9 and H1975 cells.

(a) Unsynchronised PC-9, (b) unsynchronised H1975, (c) synchronised PC-9, and (d) synchronised H1975 cells were treated with AZD6738 or DMSO control and changes in number of cells assessed for up to 23 hours. Images of cells were taken every 15 minutes using live-cell microscopy, cell numbers recorded every hour, and samples were normalized relative to values at 0 hrs. Data was analysed using ANOVA (2 factor with replication). **** = $p<0.0001$ and * = $p<0.05$.

3.3 Signalling response

To further investigate the response of PC-9 cells to ATR inhibitor treatment, western blot analyses were carried out. Both the ATM and ATR signalling pathways were investigated as it is known that there is significant overlap between the two pathways.

As a positive control, PC-9 cells were treated with 1 µM gemcitabine for up to 24 hrs in order to induce replication stress and early S-phase arrest (Figure 3.3). There was activation of pCHK1 S317 as expected. Following treatment with AZD6738 and gemcitabine, there was a clear decrease in pCHK1 S317 in the treated cells, indicating that AZD6738 was inhibiting ATR

kinase activity in these cells. On the other hand, pCHK1 S345 was detected in untreated cells, suggesting possible replication stress intrinsic to the cell line. With combination treatment, there was slight activation of ATR indicated by the detection of pCHK1 S317 at 2 hrs, suggesting that the concentration of AZD6738 was not sufficient to suppress ATR kinase activity. pRPA32 S4/S8 were detected at high levels when PC-9 cells were treated with gemcitabine for 4 and 24 hrs. Earlier studies have shown that these sites are phosphorylated by DSB-responsive DNA-PKs, which suggests that incubation with gemcitabine for an extended period of time can cause DNA replication forks to collapse, generating DSBs and RPA2 hyperphosphorylation (Zernik-Kobak et al, 1997; Anantha et al, 2007). The inhibitory Y15 phosphorylation site on CDK1/2 is phosphorylated by WEE1 kinase in response to ATR activation and is reduced to background levels (untreated) when ATR is inhibited. High levels are detected with 24 hr gemcitabine treatment at which point PC-9 cells are undergoing large amounts of replication stress, and are ATR is activated to induce cell cycle arrest.

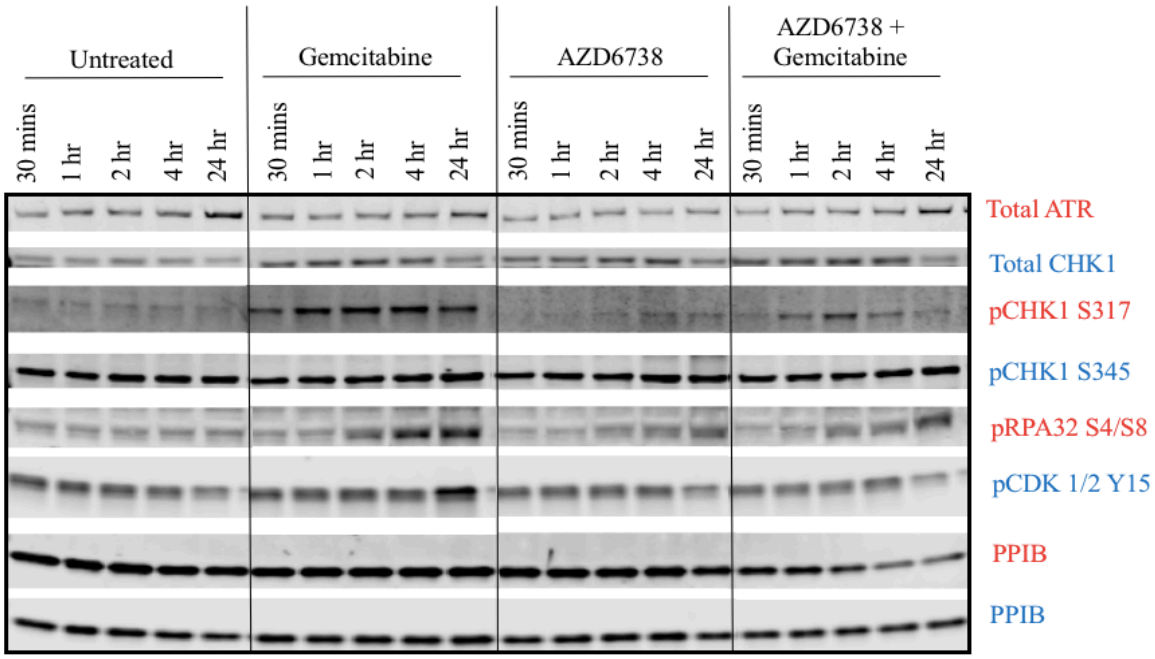


Figure 3.3: ATR signalling in PC-9 cells.

PC-9 cells were treated with either 0.01% DMSO, 1 µM gemcitabine, 1 µM AZD6738 or both 1 µM gemcitabine and 1 µM AZD6738 for up to 24 hours at which point lysates were collected. PC-9 treated with 1 µM gemcitabine served as a positive control for induced replication stress. Protein levels were assessed by western blot analysis. PPIB expression as a loading control for each gel (red, blue) are shown. Each gel represents two independent experiments.

Treatment of PC-9 cells with 1 μM gemcitabine activated ATM downstream signalling (Figure 3.4). Notably, ATM signalling (pATM, pKAP1, pCHK2) was strongly activated in PC-9 cells treated with 1 μM AZD6738 for 24 hrs. This activation of the ATM pathway upon treatment with ATR inhibitor suggests that PC-9 is responding to prolonged DNA replication stress through ATM signalling, and the activation of downstream pCHK2 is consistent with the S-phase arrest through CDK2. Combination treatment induced a similar response to the gemcitabine-induced response in the ATM signalling pathway. Compared to only AZD6738-treated cells, an earlier activation of the ATM signalling pathway was noticed when treated in combination, with pKAP1 being detected from 1 hr post treatment.

Furthermore, proteins involved in the regulation of the cell cycle were investigated. Decreases in phospho-histone H3 (pHH3, a marker of mitosis) were observed in cells treated with gemcitabine as expected as DNA synthesis is inhibited. In comparison, control cells showed high levels of mitosis at 1 and 24 hrs, consistent with the doubling time of 22 hrs observed for synchronised PC-9 cells in Table 3.1. There were no clear changes in levels of S phase cyclins, although levels of cyclin A2 was higher with 24 hr gemcitabine treatment, possibly indicating accumulation of cells in S-phase with high levels of replication stress.

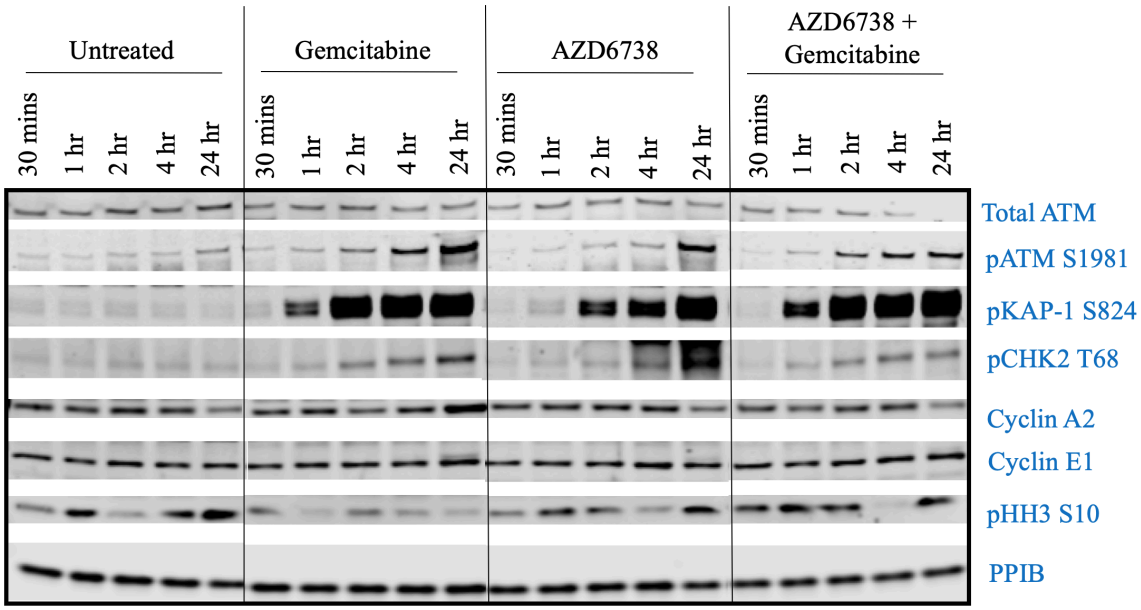


Figure 3.4: ATM signalling in PC-9 cells and cyclin levels.

PC-9 cells were treated with either 0.01% DMSO, 1 μM gemcitabine, 1 μM AZD6738 or both 1 μM gemcitabine and 1 μM AZD6738 for up to 24 hours at which point lysates were collected. PC-9 treated with 1 μM gemcitabine served as a positive control for induced replication stress. Protein levels were assessed by western blot analysis. PPIB expression as a loading control is shown. The gel represents two independent experiments.

3.4 Proliferation of ATR inhibitor resistant clones

Resistance has previously been reported for many anti-cancer therapies, in particular for kinase inhibitors (O'Hare et al, 2007; Wheeler et al, 2010; Barouch-bentov, 2012; Lovly & Pao, 2012; Hartsough et al, 2014). As such, it is likely that resistance will emerge in patients from the use of AZD6738, which is currently undergoing phase I/II clinical trials, and thus it would be useful to understand potential resistance mechanisms to counteract this problem. In order to identify potential mechanisms of resistance to ATR inhibitors, previous work in the lab established 3 cell lines resistant to AZD6738 using an in vitro assay system. PC-9 human non-small cell lung cancer cells were treated with 1 μM AZD6738. Six weeks later, distinct resistant clones emerged, and these were isolated and expanded in the presence of AZD6738 (1 μM for SO25 and SO46, or 2 μM for SO45). Throughout this study, the SO25 and SO45 cell lines were used for overexpression of cyclins as they displayed differing levels of resistance to AZD6738. PC-9 NSCLC cells were used to generate the resistant clones as earlier work in the lab had shown that

these p53 mutant cells were sensitive to ATR inhibition, with an AZD6738 mean IC_{50} value of 0.5 μM ± 0.5 – 0.52 (data from Weber, 2015).

To assess the growth rate of ATR-inhibitor resistant clones and parental PC-9 cells in the presence and absence of 0.5 μM AZD6738, a PicoGreen cell proliferation assay (measuring dsDNA as a surrogate of cell number) was performed over 8 days. In the absence of AZD6738, PC-9 cells had the fastest growth rate, while in the presence of AZD6738, cell growth did not increase beyond day 3 (Figure 3.5). In contrast, the ATR-inhibitor resistant clones continued to grow in the presence of 0.5 μM AZD6738, and by day 3 (SO25 and SO45) or day 4 (SO46), grew better in the presence of AZD6738 compared with controls, particularly the SO25 cell line. This characteristic of ATR-inhibitor resistant cells growing better in the presence of AZD6738 suggests a type of addiction to this inhibitor. This growth-accelerating effect from the addition of AZD6738, however, is still not sufficient to surpass the faster growth rate of the parental PC-9 cells growing in the absence of AZD6738.

H1975 cells display a similar response in their relative cell viability to PC-9 cells, which is as expected, as the concentrations used reflect their respective IC_{50} values and the cell line would be as sensitive in their response to the higher concentration of AZD6738 used.

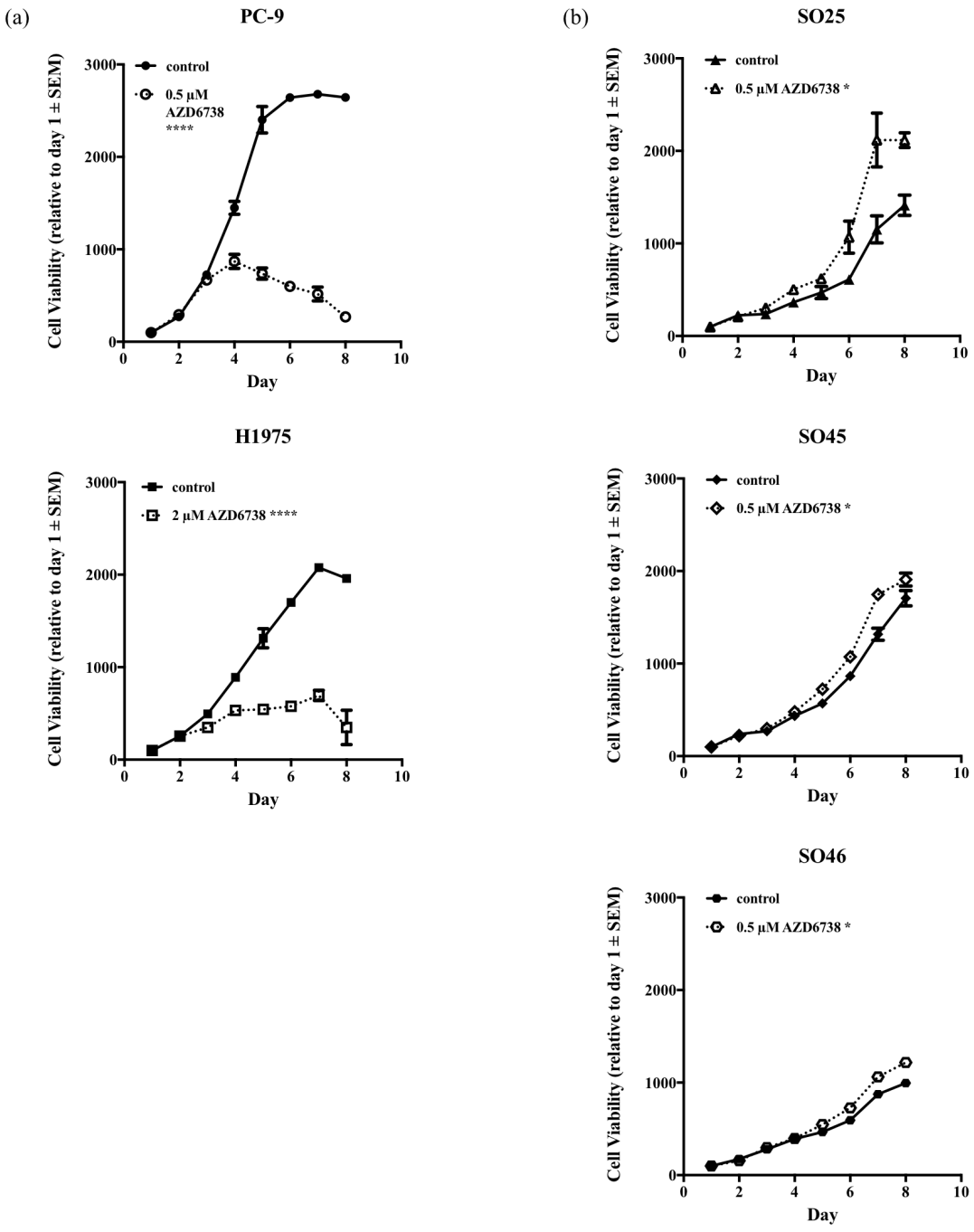


Figure 3.5: Cell viability of parental and resistant cells.

(a) PC-9 and H1975 cell lines, and (b) SO25, SO45 and SO46 resistant cells were treated with AZD6738 or DMSO control and changes in dsDNA content assessed for up to 8 days. DNA content was assessed by PicoGreen and samples were normalized relative to values from day 1. Graphs represent the mean of three independent experiments done in triplicate (± SEM). **** = $p<0.0001$ and * = $p<0.05$ (ANOVA).

3.5 Cell cycle analysis

As the growth rate of resistant cells differ from parental PC-9 cells in the presence of ATR inhibitor, their cell cycle profiles were compared in order to determine if the cell lines exhibit different cell cycle profiles. Cells were treated with 2 μM AZD6738 for 24 hrs before collecting for flow cytometry. An early S phase arrest was observed for PC-9 cells when treated with the ATR kinase inhibitor (Figure 3.6a), with treatment causing almost a two-fold increase of S phase cell population (Figure 3.6b). PC-9 cells have a homozygous p53 mutation and thus do not have a functioning G1 checkpoint. Potentially, as a result of this, a large proportion of the PC-9 cells aberrantly enter S phase from G1 and remain in S phase when ATR inhibitor is added. The G2/M checkpoint appears to be non-functional in AZD6738 treated PC-9 cells as cells empty from G2, implying low or no activation of ATM. This suggests a level of DNA damage too high to be repaired by the ATM pathway alone in the absence of ATR. The resistant cells had a larger G2 population when compared to parental PC-9 cells without treatment, and there were slight differences in cell cycle profiles between the different resistant clones (Figure 3.6b). Notably, the resistant cells do not exhibit an early S phase arrest when treated with AZD6738. In particular, SO25 cells become more similar to untreated parental PC-9 cells with lower G2/M and S cell populations compared to their untreated counterparts. H1975 cells exhibit a similar pattern to the resistant cell lines when treated with ATR inhibitor, with a lower S and G2 population when compared to control, becoming more similar to untreated parental PC-9 cells.

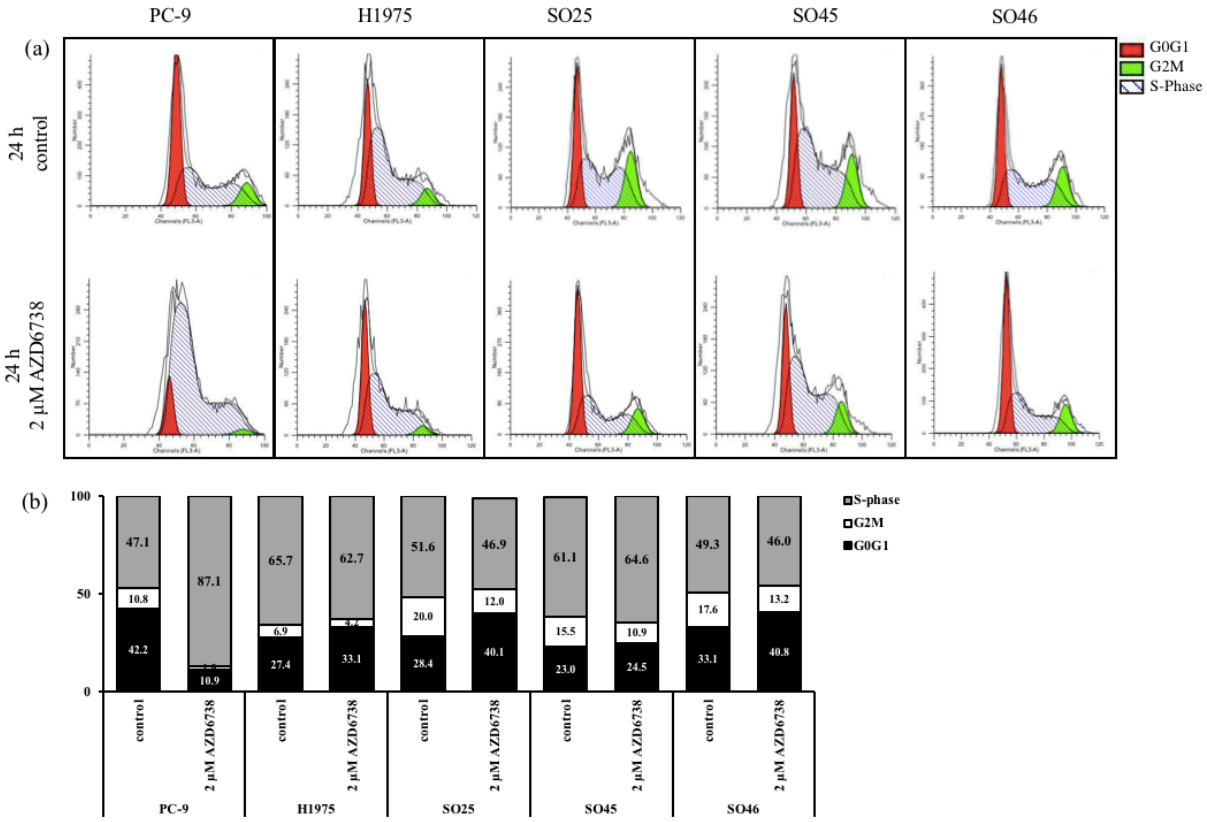


Figure 3.6: AZD6738 leads to early S-phase arrest in PC-9 cells.

PC-9, H1975, SO25, SO45 and SO46 cells were treated with AZD6738 for 24 hrs before harvested for assessment of cell cycle distribution by propidium iodide staining and FACS analysis. (a) shows representative images of n = 3 independent experiments. (b) shows quantification (percentages) of G0/G1, S and G2/M cell populations, calculated from the diploid cell population (with the exclusion of aneuploidy cells).

3.6 Key Findings

PC-9 cells were found to be more sensitive to ATR inhibitor AZD6738 and also to various inhibitors of the DDR pathway proteins in comparison to H1975 cells. PC-9 cells had a faster growth rate, and on the addition of AZD6738, displayed decreased proliferation. H1975 cells also had a stagnated growth rate in the presence of ATR inhibitor, but displayed resistance to the effects of ATR inhibition as its growth rate stayed the same beyond 1 µM AZD6738. The ATR inhibitor resistant cell lines, SO25, SO45 and SO46, generated from PC-9 cells, were more slowly growing than parental PC-9 cells. Notably, growth of resistant cells was stimulated by the presence of AZD6738, suggesting partial inhibitor dependence. FACS data revealed an accumulation of PC-9 cells in early S phase with the addition of AZD6738, proposing a

distinctive early S phase arrest in cells sensitive to ATR inhibition. On the other hand, resistant cell lines displayed a relatively unchanged cell cycle profile with AZD6738 treatment, as did H1975 cells, consistent with our hypothesis that resistance is cell cycle related.

CHAPTER 4

4 Overexpression of Cyclins in Parental and Resistant Cell Lines

4.1 Growth rate of cDNA-transfected parental cell lines

Previously in our laboratory, western blot analysis showed that S phase cyclins, cyclins A2 and E1, were downregulated in the ATR inhibitor-resistant cell lines (SO25, SO45 and SO46), and RNA-sequencing data revealed that resistant cell lines have lower transcript levels of these cyclins (Figure 1.3). It was likely that constitutively high expression of S phase cyclins will significantly affect cell proliferation, which would allow examination of the reverse effect of cyclin downregulation in resistant cells, thus cDNA ORFs were used to overexpress cyclin A2 (CCNA2) or cyclin E1 (CCNE1) in the core parental cell lines, PC-9 and H1975. Expression of the FLAG-tagged cyclin was confirmed by western blot (data not shown).

To assess the growth rate of cDNA transfected PC-9 and H1975 cells relative to their parental cell lines, a PicoGreen cell proliferation assay was performed over 8 days. Both parental cell lines grew at a steady rate (Figure 4.1). As expected, cDNA transfected cell lines had significantly higher growth rates compared to parental controls. PC-9 cDNA CCNE1 cells exhibited a significant 4.13-fold increase in cell growth at day 6 compared to parental PC-9 cells, whilst H1975 cDNA CCNA2 cells displayed 3.04-fold increase in relative cell growth at day 6. PC-9 cDNA CCNA2 cells exhibited a statistically significant ($p < 0.05$) difference in growth rate from day 3, whilst PC-9 cDNA CCNE1 cells showed a faster response from day 2. Similarly, H1975 cDNA CCNA2 cells displayed a significant increase in growth rate from day 2, whilst H1975 cDNA CCNE1 cells were delayed in their growth and exhibited a significantly increased growth rate post day 3. This data puts into evidence the significant role that cyclins play in driving forward cell cycle.

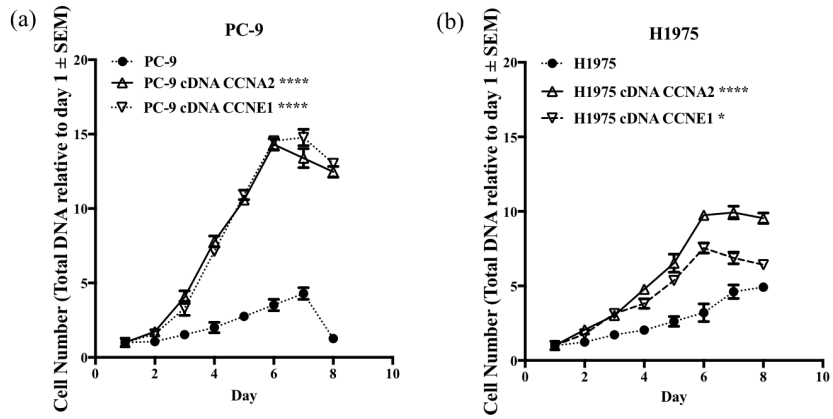


Figure 4.1: Cell viability of parental cells and cDNA transfected cells.

(a) PC-9 and (b) H1975 cell lines, and their respective cDNA-transfected cell lines were assessed for changes in dsDNA content for up to 8 days. DNA content was assessed by PicoGreen and samples were normalized relative to values from day 1. Graphs represent the mean of three independent experiments done in triplicate (± SEM). **** = $p<0.0001$ and * = $p<0.05$ (ANOVA).

4.2 Sensitivity of cDNA transfected parental cell lines to ATR inhibitor

As an increase in relative growth rate was observed for cDNA CCNA2 and cDNA CCNE1 transfected PC-9 and H1975 cells, I hypothesized whether cyclin overexpression increasing cell growth would affect sensitivity to ATR inhibitors. To investigate this, I carried out cell viability assays using resazurin. Parental PC-9 and H1975 cells exhibited the expected decrease in relative cell viability with increasing ATR inhibitor concentrations, with PC-9 cells displaying higher sensitivity. On the other hand, no increased sensitivity was observed for cDNA transfected parental cell lines and instead these cell lines unexpectedly had increased cell viability at intermediate concentrations (0.001 – 0.1 μM) of AZD6738 (Figure 4.2). Cells from the cDNA transfected cell lines showed similar responses to one another to increasing concentrations of AZD6738.

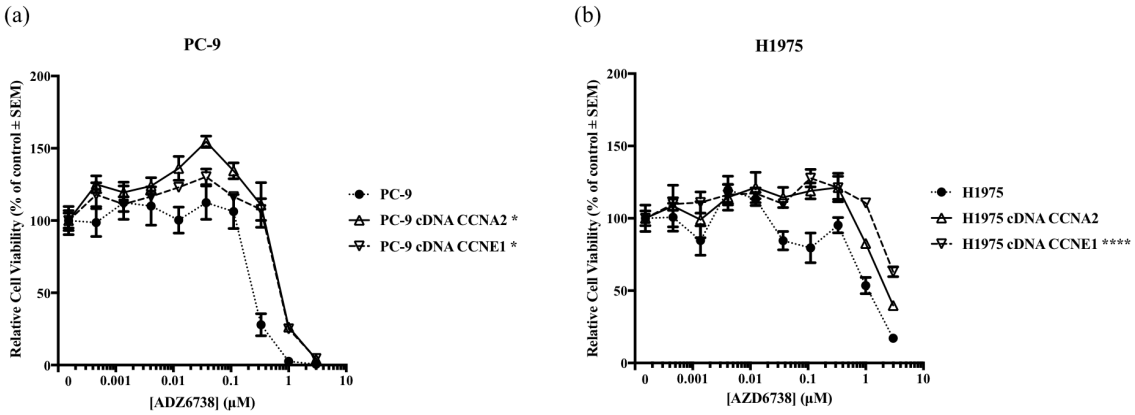


Figure 4.2: Responses of cDNA transfected parental cells to AZD6738.

(a) PC-9 and (b) H1975 core parental cell lines and their respective cDNA-transfected cell lines were incubated for 3 days with AZD6738. Relative cell viability was assessed using the resazurin proliferation assay and normalized to DMSO treated controls. Each point represents the mean of three independent experiments, each performed in triplicate with error bars = SEM. **** = $p<0.0001$ and * = $p<0.05$ (ANOVA).

Although dose-responses of cDNA transfected parental cells to increasing concentrations of AZD6738 indicated little evidence of sensitization, I hypothesized that the incubation time of 3 days was not sufficient for the cells to adapt and display their response, as resistance is cell-cycle related and cells need to go through several cell cycles. Data from Figure 4.1 had also indicated increased relative cell growth to be evident from day 2 or 3. Thus, it was decided to perform a cell survival assay in the presence of a constant concentration of AZD6738 over a longer period of time. A PicoGreen cell proliferation assay similar to the one carried out in 3.4 was performed over 8 days. Overall, all cell lines exhibited the expected decrease in cell growth with the addition of ATR inhibitor (Figure 4.3). Parental PC-9 cells experienced a 5.17-fold decrease in relative cell viability on day 7 with the addition of AZD6738, whereas PC-9 cDNA CCNE1 cells underwent a 13.01-fold reduction in relative cell viability, suggesting an extent of sensitization. Notably, for cDNA transfected H1975 cells, cell growth remained stagnant from day 2 in the presence of 2 μM AZD6738, whereas parental H1975 cell growth increased until day 7. For both cell lines, cyclin E1 appeared to have a bigger effect on inducing sensitivity to AZD6738, signifying the potential role of cyclin E1 in sensitization to ATR inhibition.

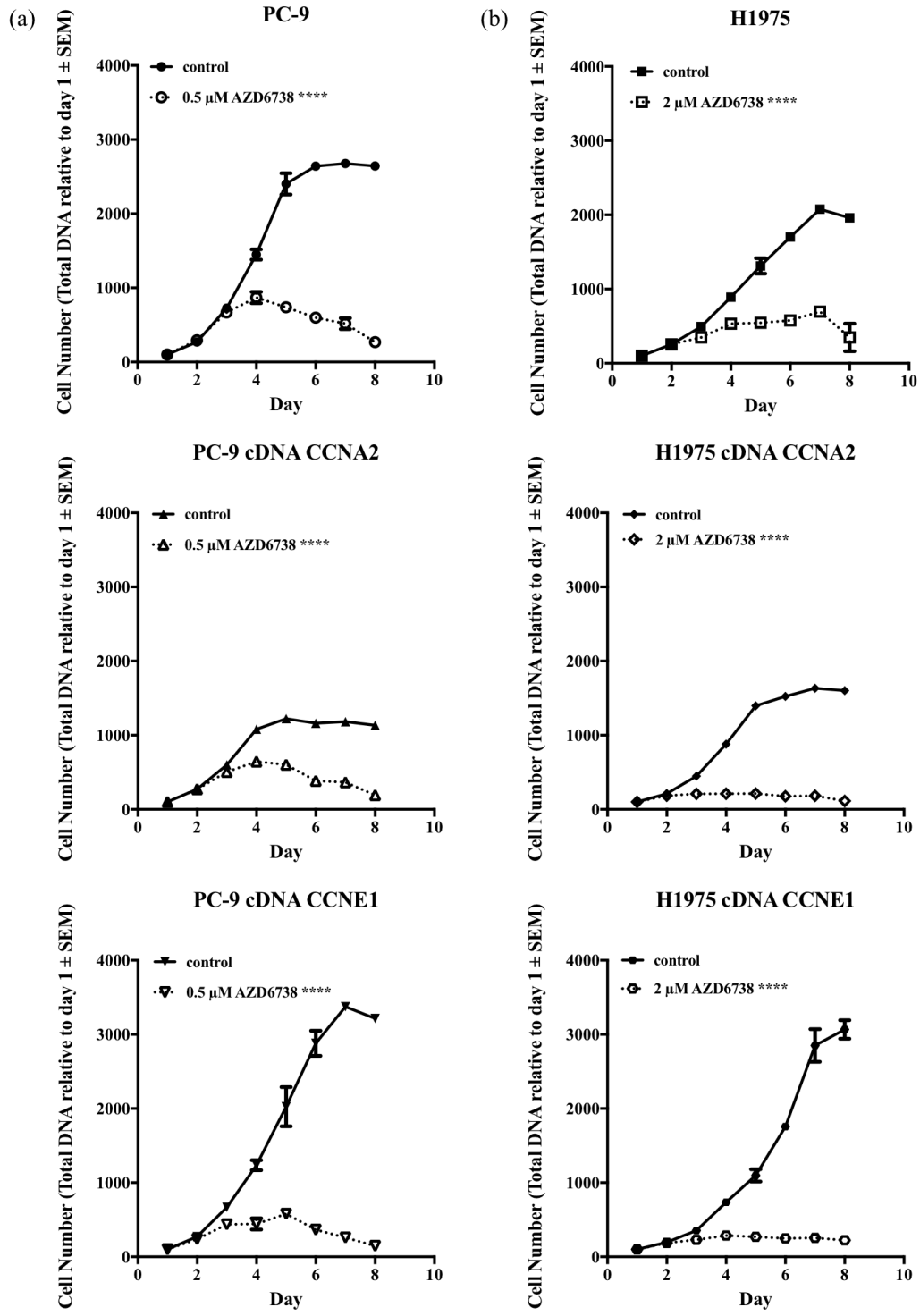


Figure 4.3: Cell viability of cDNA transfected parental cells in the presence of AZD6738.

(a) PC-9 and (b) H1975 cell lines, and their respective cDNA-transfected cell lines were treated with AZD6738 or DMSO control and changes in dsDNA content assessed for up to 8 days. DNA content was assessed by PicoGreen and samples were normalized relative to values from day 1. Graphs represent the mean of three independent experiments done in triplicate (± SEM). **** = $p<0.0001$.

4.3 Further cell cycle analysis of cDNA transfected parental cells

To further investigate the differential growth rates in parental PC-9 and cDNA transfected PC-9 cells, western blot analyses were carried out in synchronised (mitotic shake-off) cells. The cell cycle pathway was targeted as a result of the differences in growth rate.

Various differences were noted between parental PC-9 and cDNA-transfected cells in regard to cell cycle kinetics (Figure 4.4). In parental PC-9 cells, pHH3 S10 (a mitosis marker) was detected up to 4 hrs and at 24 hrs, consistent with its doubling time of 22 hrs (Table 3.2). In agreement with this, a double band of total RPA32 puts further evidence of mitosis happening up to 2 hrs. RPA32 is phosphorylated at the sites S23 and S29 by cyclin B/CDK1 in mitosis (Anantha & Borowiec, 2007). Notably, a second mitosis is apparent for parental PC-9 cells within the timespan of this study, indicated by RPA32 phosphorylation at 24 hrs and the increased pHH3 S10. On the other hand, PC-9 cDNA CCNA2 and PC-9 cDNA CCNE1 cells were more synchronised in their response, with the majority of the phosphorylated form of RPA32 being detected at 1 hr, suggesting a more tightly controlled cell cycle. PC-9 cDNA CCNA2 and PC-9 cDNA CCNE1 cells also seemed to have a delayed mitotic split, with no mitotic phosphorylated RPA32 being detected at 0 hr and pHH3 S10 being detected at higher levels at 1 hr than at 0 hr as was for parental PC-9 cells. pHH3 S10 levels were concentrated at this timepoint particularly for PC-9 cDNA CCNE1 cells. There was no clear effect of S phase cyclin overexpression on geminin, a DNA replication inhibitor.

Across all cell lines, pCDC6 S54 expression appeared to be correlated with the expression of both cyclins, suggesting phosphorylation may be activated by both cyclins A2 and E1. However, highest levels were detected with cyclin A2 expression at 16 hrs, implying cyclin A2 to be a stronger activator. This inhibitory phosphorylation, which is widely thought to be carried out by cyclin A/CDK2, relocalises pCDC6 S54 to the cytoplasm to allow firing of replication origins and progression through the cell cycle.

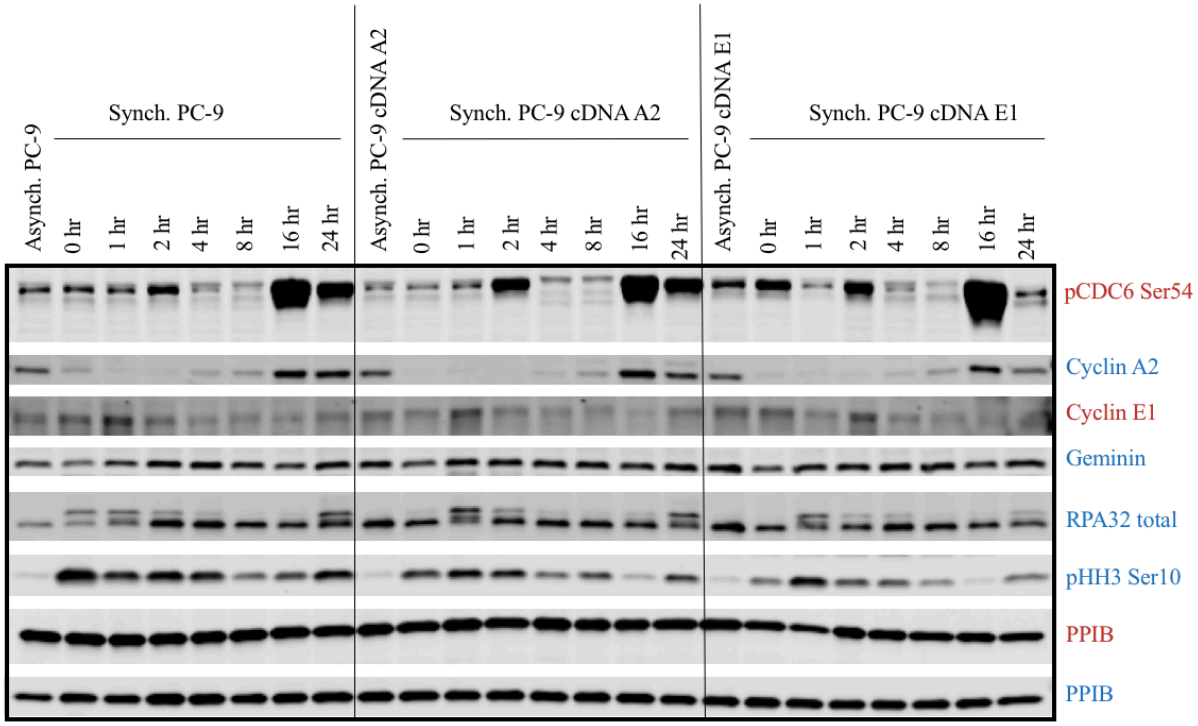


Figure 4.4: Cell cycle in cDNA transfected PC-9 cells.

PC-9 and cDNA-transfected PC-9 cells were synchronised using mitotic shake-off (post nocodazole treatment) before lysates were collected for up to 24 hrs. Floating cells were also collected. Asynchronous cells served as controls. Protein levels were assessed by western blot analysis. PPIB expression as a loading control for each gel (red, blue) are shown. Each gel represents one independent experiment.

4.4 Effect of overexpression of cyclins A2 and E1 in resistant cells

Previous work in the lab observed a downregulation of S-phase cyclins in the resistant cells compared to parental PC-9 cells, and thus it was hypothesised whether upregulation of these cyclins would reverse the resistant phenotype and re-sensitize the resistant cell lines to AZD6738. In two of the resistant cell lines, SO25 and SO45, cDNA ORFs were used to overexpress cyclin A2 (CCNA2) alone, cyclin E1 (CCNE1) alone, and both cyclins A2 and E1. Expression of the FLAG-tagged cyclin was confirmed by western blot (data not shown).

To investigate if transfection with cDNA of cyclin A2 and E1 re-sensitized resistant cell lines to ATR inhibitor, a PicoGreen cell proliferation assay similar to the one carried out in 3.4 was performed over 8 days. Overall, the resistant cell lines overexpressing cyclins did not present a statistically significant cell growth response compared to the controls (Figure 4.5). The cDNA-

transfected resistant cell lines still grew better in the presence of AZD6738 than in its absence. The exception to this case was SO25 cDNA CCNE1, which exhibited a significantly reduced growth rate compared to the control in the presence of AZD6738 from day 6. In the absence of ATR inhibitor, it exhibited an increased growth rate from day 6, growing 4-fold in 2 days. This, together with the observation of parental cells transfected with cyclin E1 cDNA exhibiting re-sensitization (Figure 4.3), may point to cyclin E1 playing an important role in inducing sensitivity to ATR inhibitors.

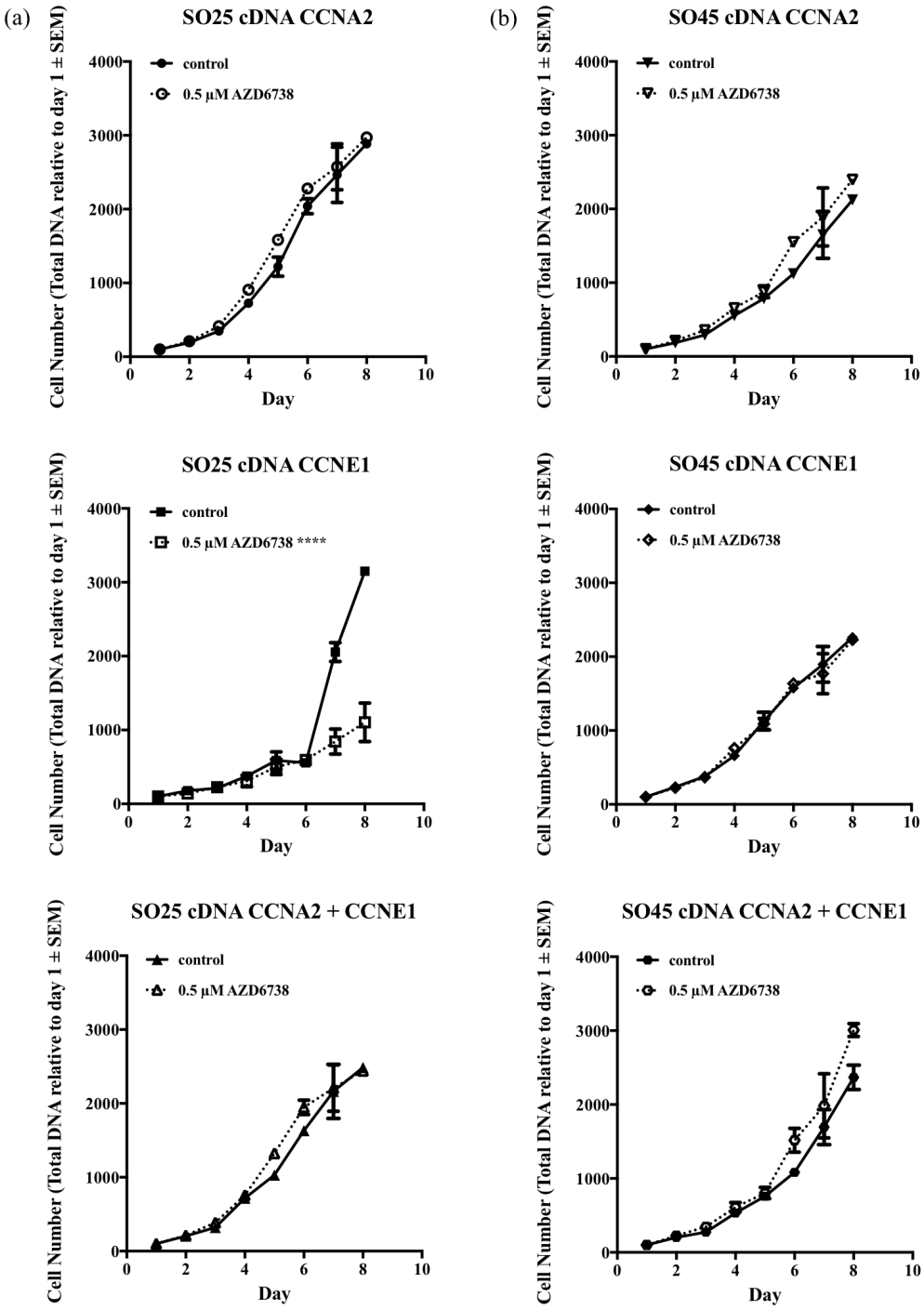


Figure 4.5: Cell viability of cDNA transfected resistant cells.

cDNA-transfected (a) SO25 and (b) SO45 cell lines were treated with AZD6738 or DMSO control and changes in dsDNA content assessed for up to 8 days. DNA content was assessed by PicoGreen and samples were normalized relative to values from day 1. Graphs represent the mean of three independent experiments done in triplicate (± SEM). **** = $p<0.0001$ (ANOVA).

4.5 Sensitivity to ATR inhibitors

To further investigate the differential responses to ATR inhibitor treatment in PC-9 and the resistant clones, cell viability assays were carried out using resazurin. Cells from two of the resistant clones showed a similar response to increasing concentrations of AZD6738 (Figure 4.6). Parental PC-9 cells exhibit the expected decrease in relative cell viability with increasing ATR inhibitor concentrations. On the other hand, the resistant clones have a distinct dose-response, maintaining stable cell viability at intermediate concentrations (0.1 – 1.0 μM) of AZD6738.

VE822 is a more potent ATR inhibitor, chemically unrelated to AZD6738. A dose-dependent decrease in relative cell viability was observed for PC-9 cells, while the AZD6738-resistant cells notably had increased viability at intermediate concentrations (0.01 – 0.1 μM) of VE822. The greatest relative resistance (209-fold) was apparent for VE822; 46.04% vs 0.22% relative cell viability at 1 μM in SO25 and PC-9 cells respectively. These data demonstrate that AZD6738-resistant SO25 and SO45 cell lines are cross-resistant to chemically unrelated ATR inhibitors. Furthermore, these resistant cells appear to grow better at intermediate concentrations of this ATR inhibitor.

The cDNA transfected SO25 cell lines (Figure 4.6b) and SO45 cell lines (Figure 4.6c) displayed a similar dose-response to their respective parental SO25 and SO45 cell lines, suggesting little evidence of re-sensitization to ATR inhibitors. This was found in line with cell viability data in Figure 4.5, where cell growth of cDNA transfected resistant cells was not impeded significantly with ATR inhibitor addition.

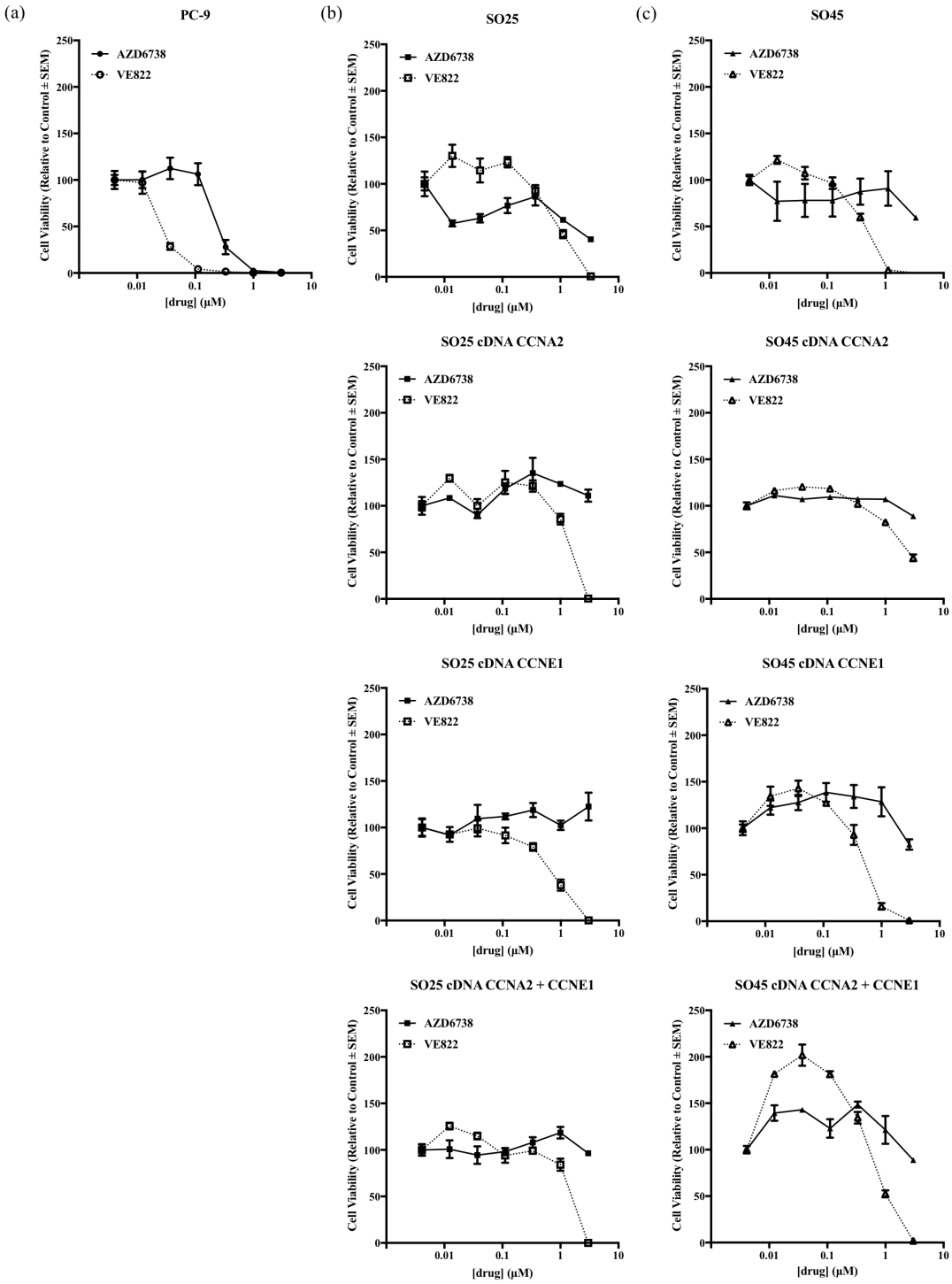


Figure 4.6: Responses of cDNA transfected resistant cell lines to ATRi's.

(a) PC-9, (b) SO25, cDNA-transfected SO25, (c) SO45, and cDNA-transfected SO45 cells were incubated for 3 days with AZD6738 or VE822. Relative cell viability was assessed using the resazurin proliferation assay and normalized to DMSO treated controls. Each point represents the mean of three independent experiments, each performed in triplicate with error bars = SEM.

4.6 Time-dependent dynamics

To further investigate the differential responses to ATR inhibitor treatment in parental PC-9 and resistant cells, western blot analyses were carried out in synchronised (mitotic shake-off) cells. The cell cycle pathway was targeted as a result of the differences in growth rate.

Several methods were used to synchronise cells, including a thymidine block. Adding excess thymidine to cells inhibits DNA replication, blocking cells in S phase (Whitefield et al, 2002). These cells are then released from S phase by washing in media, allowing them to move into the subsequent stages of the cell cycle. This method has commonly been used as a method of synchronisation as it allows for a constant rate of DNA synthesis to be maintained throughout S phase unlike other replication inhibitors (Adams, 1969). However, PC-9 cells did not recover well when incubated for long periods with thymidine, experiencing thymidine-induced cytotoxic effects. Thus, one of the most commonly used method of cell synchronisation, the mitotic shake-off method with nocodazole supplementation was settled on. This method, based on the morphological features of the cell, allows the enrichment of mitotic cells by the use of nocodazole, an inhibitor of microtubule formation (Grdina et al, 1984).

There were several similarities observed between PC-9 cells that were treated with ATR inhibitor and those that were left untreated (Figure 4.7a). Under both conditions, cyclin E1 expression was detected before cyclin A2 expression. This is as expected as cyclin E1 is expressed during G1 to early S phase, with levels peaking at the G1/S border, and cyclin A2 overtakes cyclin E1 as the main cyclin during S phase, with strongest expression during late S and early G2 phase. Surprisingly, early expression of cyclin E1 was detected under both conditions, from 0 hrs, during which time mitosis would be expected to occur. However, early S-phase cyclin expression may be a characteristic of this particular PC-9 cell line and may explain its relatively fast growth rate (Figure 3.2) and high sensitivity to ATR inhibitors (Table 3.1). PC-9 cells appeared to have accelerated from mitosis, past G1 and into S phase in just 4 hrs, shown by the weak double band of RPA32 at 0 hr, indicating mitotic phosphorylation of RPA32, and the detection of pCDC6 S54 at 4 hrs, indicating origin firing (Anantha & Borowiec, 2007). The inhibitory phosphorylation of CDC6 at S54 is thought to relocalise pCDC6 S54 from

pre-RC in the nucleus to the cytoplasm in order to allow firing of replication origins and S phase progression. pCDC6 S54 levels correlate with the cyclin A2 levels detected, which is as expected as cyclin A2 is thought to phosphorylate CDC6 at this site via its activation of CDK2 kinase. Levels of pHH3 S10 (a marker of mitosis) rightly corresponds to the doubling time of PC-9 cells, 22 hrs (Table 3.2). Geminin is known to function as a replication inhibitor by binding CDT1, and as such is absent during G1 phase and accumulates during S, G2 and M phases, at which point it is targeted for degradation by APC-dependent ubiquitination (McGarry & Kirschner, 1998). The weak band of geminin at 0 hr puts forward further evidence of mitosis occurring, and accumulation of geminin at 4, 8 and 16 hrs implies progression through S, G2 and M phases. CDT1 (a DNA replication licensing factor) is commonly used as a marker for S phase, but previous work in the lab established that levels of this protein were not significantly affected through the cell cycle in this cell line.

Various differences were observed for PC-9 cells treated with 1 μM AZD6738 in regard to cell cycle dynamics (Figure 4.7a). Notably, in treated cells, higher levels of pHH3 S10 were detected earlier from 16 hrs, indicating greater mitotic activity. The addition of ATR inhibitor seems to accelerate cells through the cell cycle, as the brake on DNA replication is no longer present. This is consistent with the observation during live-cell imaging where the addition of 1μM AZD6738 seemed to induce a faster growth rate during the first 10 hrs (Figure 3.2). It is important to note, however, that there is a disconnect between the pHH3 S10 levels detected and the S phase arrest that was observed in FACS analysis in response to ATR inhibitor treatment. Another key difference to note in Figure 4.7a is that cyclin E1 expression is more tightly controlled in AZD67378 treated cells compared to control. This would be in line with the concept of a faster cell cycle upon ATR inhibition.

Next, I investigated cell cycle kinetics of the resistant SO25 cell line when treated with 1 μM AZD6738 compared to untreated control (Figure 4.7b). Under both conditions, the SO25 cell line exhibited a much more delayed expression of S phase cyclins compared to parental PC-9 cells, mostly from 16 hrs post mitotic-shake off, as opposed to 0 hr in PC-9 cells. In contrast to the ATR inhibitor-sensitive PC-9 cells, delayed expression in SO25 cells suggests a more

controlled cell cycle, whereby the processes of replication initiation and origin firing (controlled by cyclin E1 and A2 respectively) are adapted to the slower growth rate of the resistant cells. Furthermore, cyclin E1 expression occurred for a shorter period of time coinciding with cyclin A2 expression, possibly indicating increased redundancy between cyclin E1 and A2 activity in resistant cells. pCDC6 S54, a marker of late G1/early S phase, was also detected at a later timepoint, coinciding with cyclin A2 expression. Surprisingly, total CDC6 (part of the pre-RC) was detected at high levels at mitosis (0 hr). Accumulation of geminin was evident at a later timepoint at 16 hrs in resistant cells, in contrast to 4 hrs in PC-9 cells, indicating a later onset of S phase in resistant cells. The addition of ATR inhibitor did not have any effects in the resistant cells as expected.

I additionally performed western blot analyses on cDNA CCNA2 transfected SO25 cells to further study differential control of the cell cycle (Figure 4.7c). In the absence of ATR inhibitor, cells more closely resembled cell cycle kinetics of resistant SO25 cells rather than PC-9 cells, with delayed cyclin E1 expression. However, cyclin E1 expression was not as delayed as in SO25 cells, with expression peaking at 8 hrs. Furthermore, cyclin A2 was detected earlier than in SO25 cells, from 4 hrs. In the presence of 1 μM AZD6738, SO25 cDNA CCNA2 cells appeared to accelerate through the cell cycle, shown by an earlier detection of pHH3 S10 in treated cells from 8 hrs. This is in fact similar to the response of parental PC-9 cells in the presence of ATR inhibitor, suggesting a potential restoration to parental characteristics in cDNA CCNA2 transfected resistant cells.

The key observation from the western blot analyses of Figure 4.7 is that PC-9 cells exhibit early S phase cyclin expression, whereas SO25 cells demonstrate a delayed expression of cyclin E1. The early timing of S phase cyclin expression in PC-9 cells could potentially explain its relatively high sensitivity to ATR inhibitor, as early cyclin E1 expression would lead to early priming and firing of replication origins, causing replication stress. The addition of ATR inhibitor would further increase replication stress levels in a cell line with intrinsically high replication stress, eventually inducing collapse of replication forks.

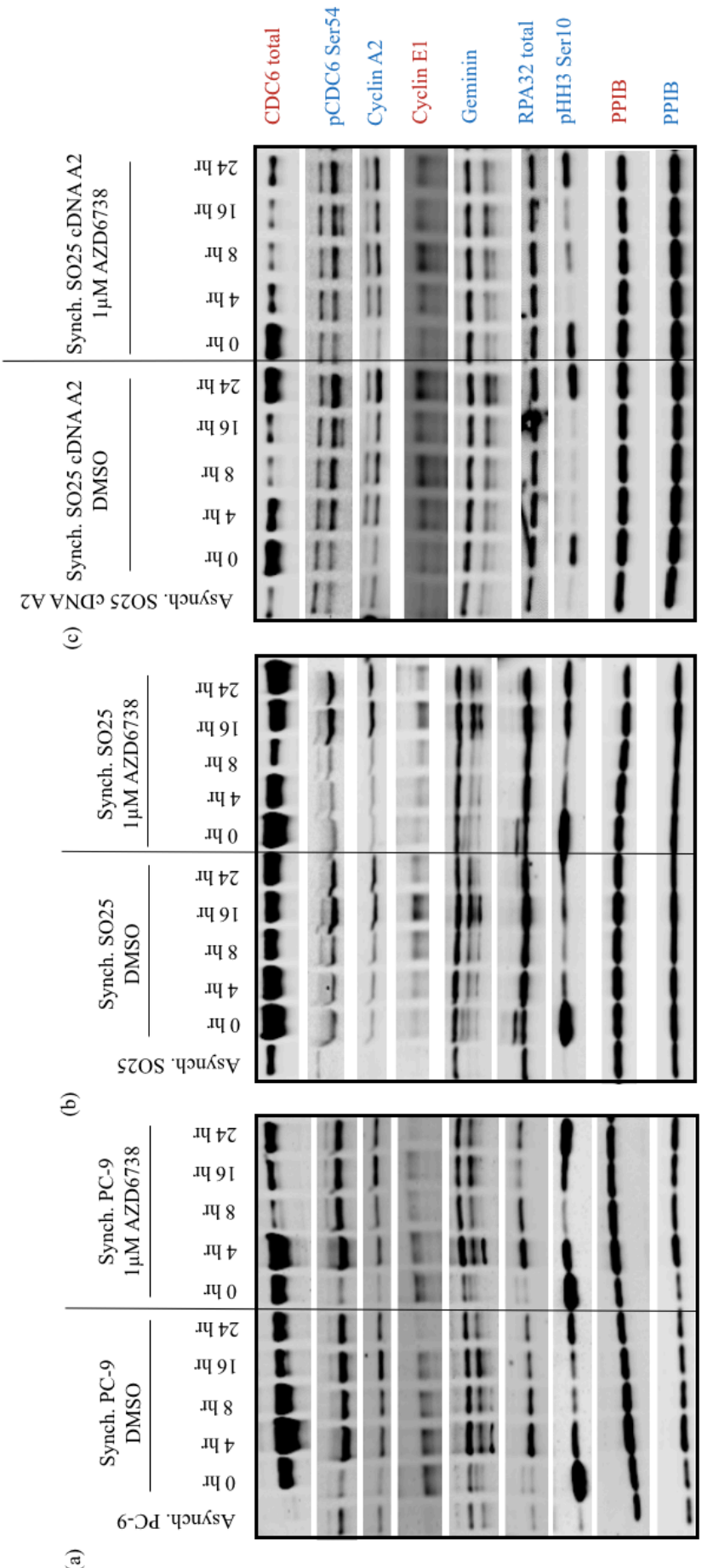


Figure 4.7: Cell cycle of synchronised cells.

(a) PC-9, (b) SO25, and (c) SO25 cDNA CCNA2 cells were synchronised using mitotic shake-off (post nocodazole treatment) and were treated with either 0.01% DMSO or 1 μM AZD6738 for up 24 hrs at which point lysates were collected. Asynchronous cells served as controls. Protein levels were assessed by western blot analysis. PPIB expression as a loading control for each gel (red, blue) are shown. Each gel represents one independent experiment.

CHAPTER 5

5 Knockdown of cyclin A2 in parental cells

5.1 Optimisation of knockdown cell lines

It was likely that sustained knockdown of S phase cyclins would markedly affect cell proliferation and survival, and therefore an inducible knockdown approach would be more amenable to experimental investigation. Previous work in the lab had shown cyclin A2 to be more prominent in its role in inducing resistance when knocked down using siRNA, thus cyclin A2 was chosen for knockdown in the two cell lines, PC-9 and H1975. Lentiviral-produced shRNA was used that is induced by the addition of doxycycline (a tetracycline-like antibiotic), and cells were also transfected with non-target shRNA, or untreated as controls. After a 3-day incubation with doxycycline (2 μg/mL), cyclin A2 protein levels were markedly reduced in PC-9 shRNA CCNA2 (0.16 relative to 0.71 normalised treated NT control), and in H1975 shRNA CCNA2 (0.23 relative to 0.77 normalised treated NT control) (Figure 5.1). Knockdown of cyclin A2 appeared to lead to lower levels of cyclin E1 protein in the PC-9 cell line (0.30 relative to 0.43 normalised untreated NT control), which may reflect underlying changes in cell cycle distribution following downregulation of cyclin A2.

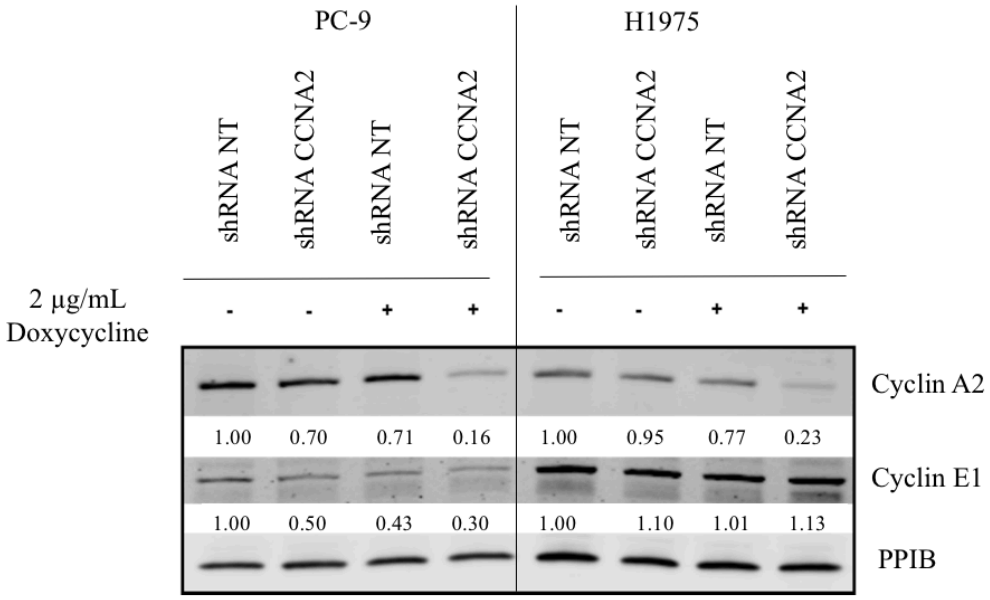


Figure 5.1: Cyclin levels in knockdown cells lines induced with 2 µg/mL doxycycline reveals 3-fold decrease compared to non-target (NT).

PC-9 and H1975 cells were transfected with shRNA against cyclin A2, produced using a lentiviral system. Control samples were treated with non-target shRNA. Doxycycline was added at the indicated concentration and lysates were collected 3 days post-induction. Protein levels were assessed by western blot analysis. Samples were quantified using Image Studio, with the sample relative densities scaled using the relative densities of the PPIB loading control.

A range of doxycycline concentrations and times were analysed (data shown in 2.2) to obtain an effective but non-toxic doxycycline concentration that successfully knocked down cyclin A2 expression. Resazurin and fluorescence assays were used covering a concentration range of 0 – 2000 ng/mL that started with the most commonly used concentration (2 µg/mL) for promoter activation. Decreased cell viability was found at concentrations > 1 µg/mL, suggesting a possible cytotoxic effect of doxycycline alone and/or in combination with induced GFP expression. Consequently, doxycycline concentrations lower than 1 µg/mL were evaluated, and an optimum concentration of 75 ng/mL was chosen, for an incubation period of 3 days. Using this optimum doxycycline concentration, a 1.6-fold knockdown (0.32 relative to 0.50 normalised treated NT control) is observed in PC-9 shRNA CCNA2 cells (Figure 5.2a). In H1975 shRNA CCNA2 cells, however, very low levels of cyclin A2 were detected by western blot analyses in the doxycycline-treated samples, indicating the toxic effect of doxycycline even

at this relatively low concentration (Figure 5.2b). Cyclin A2 knockdown in the PC-9 cells were similar to the downregulation observed for the ATR inhibitor resistant cell line, SO25. As shown previously in the lab, cyclin E1 protein levels were also downregulated in the resistant cells compared to parental PC-9 cells, at similar levels across the three resistant cell lines.

Unlike the cDNA transfected H1975 cell line that displayed overexpression of S phase cyclins (Figure 5.2b), the cDNA transfected PC-9 cell line appeared to express similar levels of cyclins A2 and E1 as the parental PC-9 cells (Figure 5.2a). This may be attributed to disparities in cell cycle distributions in different cell lines.

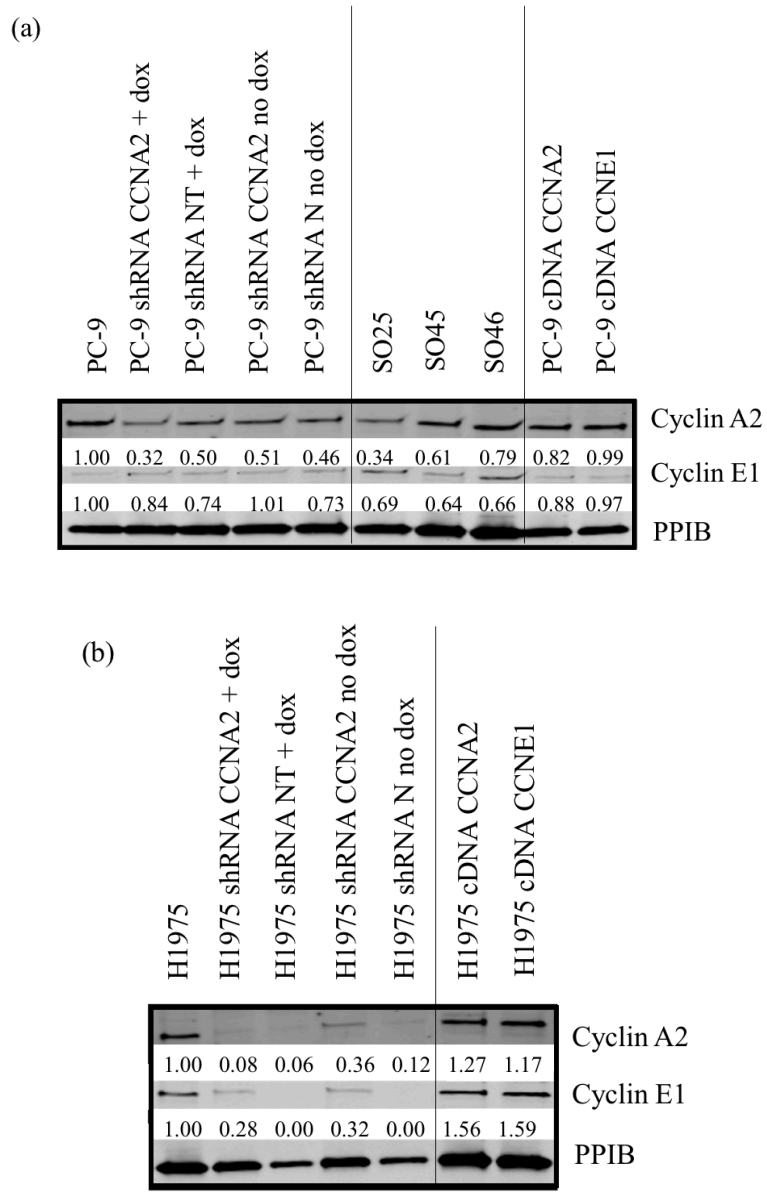


Figure 5.2: Cyclin levels in knockdown cell lines induced with optimum doxycycline concentration (75 ng/mL) reveals 2-fold decrease.

(a) PC-9 and **(b)** H1975 cells were transfected with shRNA against cyclin A2, produced using a lentiviral system. Control samples were treated with non-target shRNA. Optimum doxycycline concentration of 75 ng/mL was added to cells and lysates were collected 3 days post-induction. Resistant cell lines and cDNA-transfected parental cell lines were also collected as lysates to assess background cyclin levels relative to parental cell lines. Protein levels were assessed by western blot analysis. Samples were quantified using Image Studio, with the sample relative densities scaled using the relative densities of the PPIB loading control.

5.2 Sensitivity to DNA damage response modulators

To investigate if knockdown of cyclin A2 conferred resistance to ATR inhibitors, shRNA CCNA2 (shA2) cells were incubated with AZD6738 for 3 days, starting 3 days post doxycycline-addition. The control cells for each condition all exhibited the typical dose response seen previously with PC-9 cells in response to AZD6738 (Figure 4.6), while those with knockdown cyclin A2 were not as altered in their response as expected (Figure 5.3). However, PC-9 shA2 cells did have increased viability at intermediate concentrations (0.001 – 0.037 μM) of AZD7762 (Figure 5.3a), as was similarly observed for resistant cells in the presence of VE822 (Figure 4.6). The greatest relative resistance (1.74-fold) was apparent for AZD7762; 72.26% vs 41.40% relative cell viability at 0.1 μM in PC-9 shA2 cells and PC-9 shNT cells respectively. Interestingly, cyclin A2 knockdown H1975 cells showed a pattern of increased relative cell viability for all 4 DNA damage response modulators from a concentration of 1 μM compared to controls (Figure 5.3b). The greatest relative resistance was for AZD6738; 85.20% vs 45.78% cell viability in H1975 shA2 and H1975 shNT cells respectively.

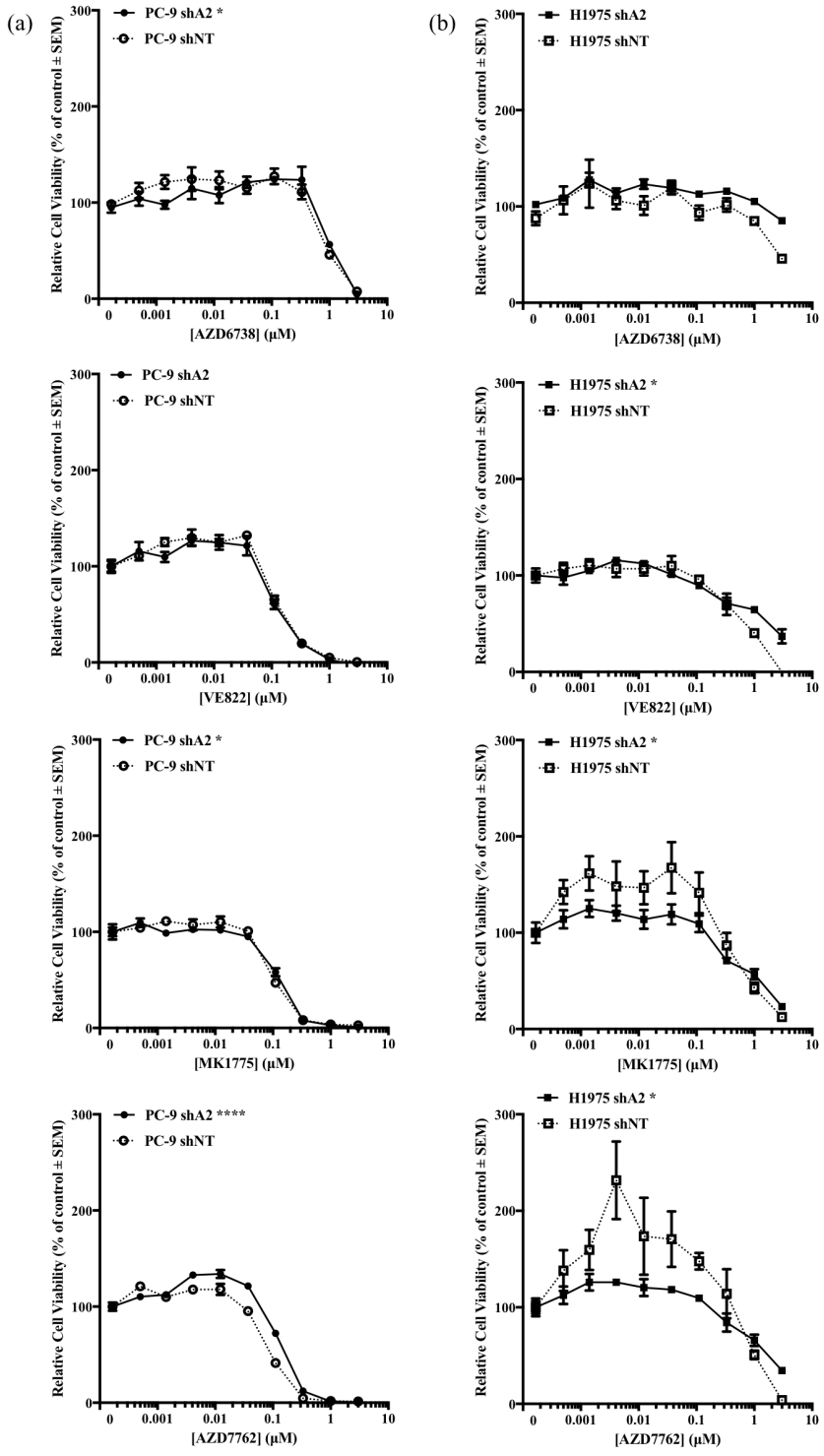


Figure 5.3: Response of knockdown cell lines to DNA damage response modulators.

Knockdown cell lines and their respective non-target (NT) control cell lines of (a) PC-9 and (b) H1975 were incubated with AZD6738, VE822, MK1775 or AZD7762 for 3 days, post a 3-day doxycycline treatment. Relative cell viability was assessed using the resazurin proliferation assay and normalized to DMSO treated controls. Each point represents the mean of three independent experiments, each performed in triplicate with error bars = SEM. **** = $p<0.0001$ and * = $p<0.05$ (ANOVA).

5.3 Proliferation of knockdown cells in the presence of AZD6738

As it was found that the effects of cyclin A2 knockdown were not very clear from a short-term dose-response experiment, it was thought there would be stronger outcomes from a more long-term assay, to allow cells to go through several cell cycles as resistance is cell-cycle related. Thus, I investigated the proliferation rates of cyclin A2 knockdown PC-9 and H1975 cells in the presence of AZD6738, using a resazurin assay over 8 days, post a 3-day doxycycline treatment.

In the absence of AZD6738, PC-9 shA2 and H1975 shA2 grew more slowly than their respective controls as expected (Figure 5.4), whilst in the presence of AZD6738, the knockdown cell lines grew better compared to their controls (from day 5 for PC-9 shA2 and day 2 for H1975 shA2). As the effects of cyclin A2 knockdown are only evident from day 2 post treatment with ATR inhibitor, this could possibly explain how knockdown cell lines did not exhibit as strong a dose-response as resistant cell lines in Figure 4.6. These data imply that downregulation of cyclin A2 does indeed increase relative cell viability in the presence of AZD6738, however this effect is only observable only over a long time period.

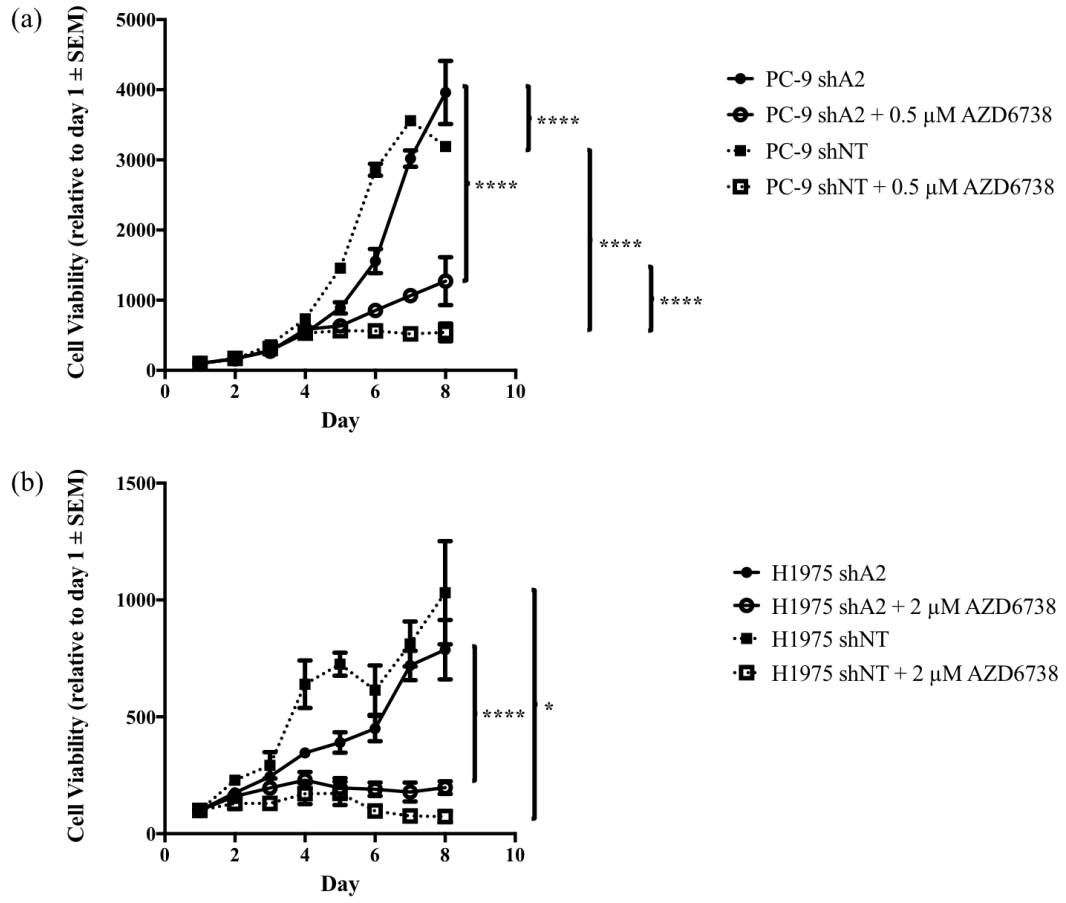


Figure 5.4: Cell viability of knockdown cells in the presence of AD6738.

Knockdown cell lines and their respective non-target (NT) control cell lines of (a) PC-9 and (b) H1975 were treated with AZD6738 or DMSO control, post a 3-day doxycycline treatment. Relative cell viability was assessed using the resazurin proliferation assay and normalized to DMSO treated controls. Each point represents the mean of three independent experiments, each performed in triplicate with error bars = SEM. **** = $p<0.0001$ and * = $p<0.05$ (ANOVA).

CHAPTER 6

6 Discussion

Resistance to chemotherapy is one of the main causes for failure of cancer therapeutics. It was estimated in the 1990s that up to 50% of cancer patients have resistant tumours (Pinedo & Giaccone, 1998). It is characterized by a lack of response to drug-induced growth inhibition and can either be intrinsic, due to heterogeneity within the tumour, or acquired, arising from drug exposure, for example via developing drug-detoxifying mechanisms (Gottesman; 2002; Luqmani, 2005; Lippert et al, 2011; Zahreddine & Borden, 2013). To combat this inevitable challenge, there remains a need for improved therapeutics approaches in order to delay or prevent progression of resistance.

ATR kinase inhibitors are in early clinical development and resistance mechanisms have not yet been described. Past efforts to identify mutations that may be determinants of ATR sensitivity include a genome-wide CRISPR-Cas9 screen carried out by Ruiz et al in mouse embryonic stem cells, which found lack of CDC25A protein to be a potential indicator of ATR inhibitor resistance. In human cancer cells, CDC25A levels correlated with response to ATR inhibitors. A deficiency in CDC25A protein led to failure to enter mitosis prematurely, thus such cells could tolerate high concentrations of ATR inhibitor. Following on from this, inhibition of WEE1 in these cells forced them into mitosis and re-sensitised them to ATR inhibitors (Ruiz et al, 2016).

Previous work in our laboratory had used the PC-9 NSCLC cell line to generate ATR inhibitor resistant cells, in which a downregulation of S phase cyclins was found. Compared to parental cells, these resistant cells exhibited significantly slower growth rates, with enhanced viability in the presence of ATR inhibitor (AZD6738), and with no S phase arrest with AZD6738 incubation. Subsequent work did not find a significant reduction in rates of DNA synthesis between parental and resistant lines, thus it was postulated that there may be a decrease in density of replication

origins and/or delayed firing of replicons to account for slower proliferation of resistant cells (Olyha, MRes thesis, 2016).

In this study, the hypothesis that expression of S phase cyclins affects sensitivity to ATR inhibitors was investigated using three approaches to alter cyclin expression in parental and resistant cell lines. Firstly, S phase cyclin levels were modulated in resistant lines to overexpress S phase cyclins, either each cyclin alone or in combination. Secondly, parental cell lines were modified by transfection with cyclin ORFs. Thirdly, an inducible shRNA system was used to knockdown cyclin levels in parental cell lines. From measuring cell proliferation, cell cycle distribution, responses to DDR modulators, DDR pathway protein levels and cell cycle kinetics, a model is now proposed that might at least in part explain a cell line's sensitivity to ATR inhibitors (Figure 6). In the ATR inhibitor-sensitive parental PC-9 cell line, cyclin E1 expression occurred in early G1 phase, whereas in the ATR inhibitor-resistant SO25 cell line, expression was restricted to early S phase. This suggests a more controlled cell cycle in the resistant cell line, with delayed priming and firing of replication origins. It could be inferred that sensitivity to ATR inhibition may be determined by aberrant S phase cyclin expression, specifically early cyclin E1 expression.

Firstly, I characterised responses to ATR inhibitor treatment in the parental cell lines and resistant cell lines, in order to have a reference with which to compare cyclin-modulated cell lines. The PC-9 cell line was identified as the more sensitive cell line in response to ATR inhibitor treatment in comparison to the more resistant H1975 cell line. I postulated that this sensitivity could stem from the difference in growth rates between the two cell lines. PC-9 cells have a faster growth rate, going through more cell cycles per time period, with more rounds of DNA replication, and thus, potentially more susceptible to DNA replication stress and ATR inhibition.

Western blot analysis showed that parental PC-9 cells treated with AZD6738 for up to 24 hrs activated ATM signalling, confirming a level of redundancy between the ATR and ATM signalling pathways. This response has also been reported by Murga et al, 2009, Dungrawala et al, 2015 and Kwok et al, 2016. pCHK1 S317, a marker of replication stress-induced ATR

activity, showed the highest levels in the control PC-9 cells treated with gemcitabine, an inhibitor of DNA replication known to induce S phase arrest. As expected, pCHK1 S317 levels decreased following treatment with AZD6738. On the other hand, levels of pCHK1 S345, another proposed ATR-specific marker, were detectable in untreated cells, suggesting potential intrinsic replication stress in the PC-9 cell line. In line with activation of the ATM signalling pathway being observed, it was evident that an extended period of treatment with gemcitabine induced DNA DSBs, indicated by high levels of pRPA32 S4/S8. These sites are thought to be DNA-PK specific in response to DSBs caused by replication fork collapse, as reported by Zernik-Kobak et al, 1997 and Anantha et al, 2007.

The ATR inhibitor resistant cells grew better and at a faster rate in the presence of the ATR inhibitor, AZD6738, than in its absence. A long-term cell growth assay showed that cell viability was enhanced at an intermediate concentration of 0.5 μM AZD6738. Incubation with increasing AZD6738 concentrations produced an unusual shape in their dose-response curves, and cross-resistance was exhibited when incubated with a chemically unrelated ATR inhibitor, VE822. Interestingly, at intermediate concentrations of a range of DNA damage response modulators, including AZD6738, the more resistant cell lines in the panel of NSCLC cell lines studied (H1299 and H1975) exhibited increased cell viability. An earlier study by Mak et al, 2014 had also reported increased cell growth for H1299 at lower concentrations of WEE1 (MK1775) or CHK1/2 (AZD7762) inhibitors. It is possible that using low doses of inhibitors, which induces limited inhibition of the ATR-CHK1-WEE1 pathway, disrupts cell cycle control, but does not result in mitotic catastrophe, and instead accelerates and shortens the cell cycle. Indeed, in our FACS data, the ATR inhibitor resistant cells had fewer cells in S and G2/M phase when treated with AZD6738 compared to without treatment, thus resembling the cell cycle profile of parental PC-9 cells. This suggests these AZD6738-treated ATR inhibitor resistant cells to have a cell cycle more similar to that of PC-9 cells, with a faster cell cycle progression. Consistent with the cell cycle profile, the long-term cell growth assay curves for resistant cells in the presence of ATR inhibitor resemble the curve of untreated PC-9 cells. Notably, the S phase arrest that was observed for the sensitive PC-9 cells was not apparent in the more resistant H1975 cells, with

the latter's cell cycle profile resembling that of the resistant cells, confirming that S phase arrest is a distinctive response to ATR inhibition in sensitive PC-9 cells.

The most informative data stemmed from comparing cell cycle kinetics in ATR inhibitor-resistant and parental PC-9 cells, that were synchronised following mitotic arrest. It was evident that the timing of the expression of S phase cyclins differed between the two cell lines, with delayed expression occurring in resistant cells. Notably, relatively early S phase cyclin expression was observed for PC-9 cells, indicating early priming (activated by cyclin E1) and firing (activated by cyclin A2) of replication origins. Consistent with cyclin A2 expression, activity of cyclin A2 was confirmed by expression of pCDC6 S54. Early S phase cyclin expression may explain the sensitivity of the PC-9 cell line in response to ATR inhibitors, as an early initiation of DNA replication could lead to high levels of replication stress. In comparison to PC-9 cells, the delayed and shorter expression of S phase cyclins, particularly cyclin E1, in ATR inhibitor resistant cells would lead to later origin priming and firing. These cells maintain a higher level of control over the cell cycle and can tolerate intermediate doses of ATR inhibitor well. This is reflected by their slower growth rate, with lower background levels of replication stress compared to parental PC-9 cells. Future work could identify a panel of cell lines with dysregulated S phase cyclin expression, potentially one similar to PC-9 cells with relatively early expression to determine whether this characteristic of early expression can potentially determine sensitivity to ATR inhibitors. By making use of a broader range of tumour and non-tumour cell lines than was used in this study, a pattern could be established to define correlation with ATR inhibitor sensitivity.

With the parental cells and resistant cells characterised in regard to their response to ATR inhibitor treatment, I generated cDNA transfected resistant cells. From a short-term dose-response study, there was modest re-sensitisation to ATR inhibitors. A possible explanation for this is that the cyclins were not expressed sufficiently as exogenous cyclins were degraded. Cellular levels of cyclins are under constant tight regulation, as reviewed by Bertoli et al, 2013 and Woo & Poon, 2003 (see section 1.6), and may be degraded in excess of a certain threshold. Although absolute levels of cyclins may have been strictly controlled in the cyclin cDNA

transfected resistant cells, our western blots suggest that the timing of cyclin expression may be differentially regulated in these cell lines compared to the resistant cells. A western blot of cDNA CCNA2 transfected resistant cells revealed cyclin E1 expression occurred earlier than in resistant cells. Furthermore, pHH3 S10 levels indicated that the cDNA CCNA2 transfected resistant cells went through the cell cycle at a similar rate to PC-9 cells, and when treated with ATR inhibitor, they appeared to accelerate through the cell cycle, comparable to parental PC-9. This could imply an extent of restoration to parental PC-9 phenotype of the cDNA CCNA2 resistant cells, although the extent was not sufficient to display significant re-sensitisation to ATR inhibitor.

A study by Macheret & Halazonetis, 2018 reported that CCNE1 oncogene activation could lead to replication stress. By mapping genome-wide DNA replication and transcription in cells, they found that oncogene-induced DNA replication stress involved a subset of novel, intragenic origins associated with a higher frequency of genomic rearrangements in cancer. They reported that with CCNE1 activation, G1 phase was shortened, and transcription was unable to inactivate all intragenic origins, leading to aberrant origin firing and DNA replication stress. In this study I overexpressed S phase cyclins in the core parental cell lines, PC-9 and H1975, as this would allow us to examine the reverse effect of cyclin downregulation, and to see if it was possible to further sensitise cells to ATR inhibitor treatment. It was apparent that each S phase cyclin equally played an important role in driving cell cycle, from the significantly increased cell growth rates of cyclin cDNA parental cells compared to parental cells. However, cyclin overexpression in the parental cells did not seem to increase relative sensitivity to AZD6738 during a short-term dose-response study, the possible explanation for this being the previously mentioned degradation of exogenously expressed cyclins.

Due to the differences in cell growth rates between cyclin cDNA expressing and parental cells being only observed from day three post-seeding, I investigated cell viability over a longer period. For both parental cell lines, in the presence of ATR inhibitor, significantly decreased growth rates were noted for cell lines with cyclin E1 overexpression, highlighting the potential importance of this S phase cyclin in inducing replication stress when overexpressed. CCNE1-

induced replication stress was reported by Macheret & Halazonetis, 2018, to cause a shortening of G1, and also by Resnitzky & Reed, 1995, where they found that G1 phase was shortened when cyclin E was coexpressed with cyclin D1. This shortening of G1 can be inferred from our western blot analyses of the cyclin cDNA PC-9 cells, in which the mitotic phosphorylated form of RPA32 is detected later compared to PC-9 cells, whilst the S-phase marker, pCDC6 S54, is detected at similar times. This could imply a shortening of G1 phase in cyclin cDNA PC-9 cells, possibly forcing a precocious S phase entry, inducing higher levels of replication stress, and subsequently decreasing cell viability when ATR is inhibited.

Prior to submitting the knockdown cell lines to ATR inhibitor treatment, it was essential to optimise the doxycycline-inducible system, one commonly used for regulating gene expression in vitro (Das et al, 2016). Previous studies by Fife et al, 1998 and Qin et al, 2015 on doxycycline use have reported higher doses may negatively affect proliferation, invasion and metastasis in different tumour types, thus an effective concentration that did not significantly affect cellular viability had to be determined. GFP has also been reported to affect a number of cellular functions, including the immune response and apoptosis (Ansari et al, 2016; Coumans et al, 2014; Liu et al, 1999). Consequently, to prevent any adverse effects from doxycycline or GFP, the lowest doxycycline concentration that was effective in inducing knockdown of cyclin A2 protein was chosen via fluorescence and cell viability assays.

Immunoblotting showed a two-fold decrease of cyclin A2 levels upon treatment with the optimum doxycycline concentration (75 ng/mL) of PC-9 shRNA CCNA2 cells. However, in H1975 shRNA CCNA2 cells, very low levels of cyclin A2 were detected in the doxycycline-treated sample. This may be explained by the differences that are intrinsic to the cell line but also by the variability of lentivirus transduction efficiency due to varying numbers of vector copies integrated into the target cell's genome or differences in the chromatin context of the inserted vector that may affect insert expression levels differently (Geraerts et al, 2006).

Knockdown cell lines did not exhibit a significant increase in cell viability in response to increasing concentrations of DNA damage response modulators (ATR, CHK1/2 and WEE1 inhibitors) using a short-term assay. However, when incubated for an extended period of time

of 8 days, knockdown cells displayed significantly increased cell growth in the presence of ATR inhibitor. By the end of 8-day assay, PC-9 shRNA CCNA2 cells had grown more than twice as much as NT (control) cells in the presence of AZD6738, and an increase in growth was also observed for H1975 shRNA CCNA2 cells. This suggests future studies should focus on longer term assays, as multiple time-dependent factors must be considered. Firstly, the time taken for RNA interference, secondly for the effect on the cell cycle to be exerted, and thirdly for the presence of the ATR inhibitor to take effect on the modulated cells. It would be worthwhile to investigate the long-term cell survival response of cyclin knockdown cell lines in the presence of other DDR modulators to observe whether they present cross-resistance similarly to resistant cells.

7 Conclusion and Hypothesis

In conclusion from this project, I propose a model where the timing of S phase cyclin expression contributes towards determining sensitivity to DDR modulators, specifically ATR inhibitors. Our cell cycle kinetics data showed that ATR inhibitor sensitive PC-9 cells expressed cyclin E1 early from mitosis, whereas ATR inhibitor resistant cells exhibited a more delayed cyclin E1 expression during G1/S phase. The mechanism by which early cyclin E1 expression induces ATR inhibitor sensitivity can be elucidated by the RNA-sequencing data (Figure 1.3), which revealed that compared to PC-9 cells there was an increase in Rb pathway activation and E2F inhibition in resistant cells. I interpret that in cells sensitive to ATR inhibition, early cyclin E1 expression causes premature S phase entry, via a faster hyperphosphorylation of pRb, resulting in a quicker activation of E2F and earlier transcription of S phase-promoting genes. I hypothesise that precocious entry into S phase is associated with firing of intragenic origins that fail to be inactivated by transcription due to G1 phase being shortened, and these give rise to replication forks that are prone to collapse (Macheret & Halazonetis, 2018). The earlier onset of S phase results in a lengthier S phase, and in order for cells to be viable under such conditions of high replication stress, ATR activity is critical for cell survival and may be activated for a longer period of time. Finally, as shown in our FACS data when PC-9 cells treated with AZD6738 resulted in an accumulation of cells in early S phase, ATRi-sensitive cells cannot

continue through the cell cycle without ATR activity, and when treated with ATR inhibitor they arrest in early S phase.

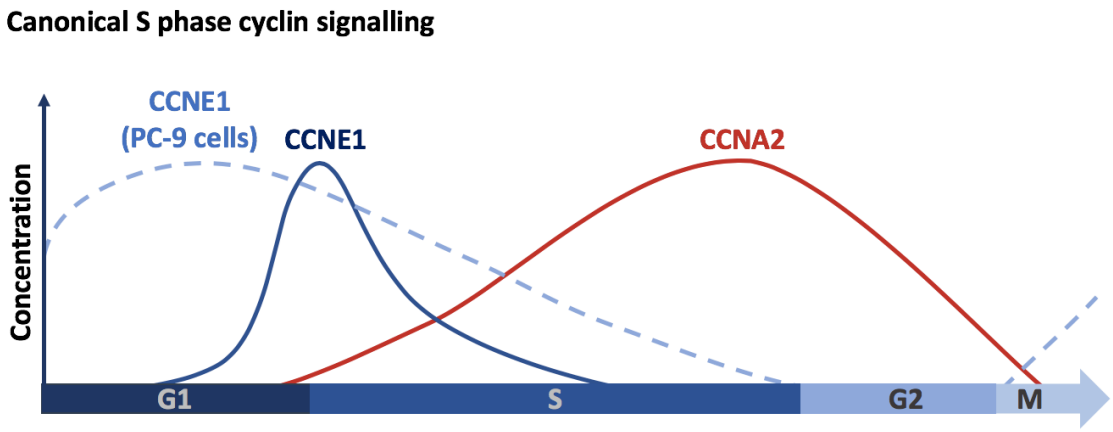


Figure 7: Model of S phase cyclin expression.

Cyclin expression levels vary over the cell cycle, and S phase cyclins, cyclin E1 and cyclin A2, play an important role in regulating entry and progression through S phase respectively. Cyclin E1 concentration rises sharply during mid G1 phase, peaks during G1/S transition and falls rapidly in mid S phase. Cyclin A2 level gradually increases shortly after cyclin E1 in late G1, peaks during S/G2 transition and decreases steadily in mitosis.

In PC-9 cells, a cell line sensitive to ATR inhibition, relatively early expression of cyclin E1 was observed, with expression spanning a larger proportion of the cell cycle compared to standard cycling cells. Cyclin E1 was detected during mitosis, through to G1, until end of S phase. Cyclin A2 levels were similar to standard cycling cells.

8 References

Adams, R. L. (1969). The effect of endogenous pools of thymidylate on the apparent rate of DNA synthesis. *Experimental Cell Research*, *56*(1), 55–8. Retrieved from http://www.ncbi.nlm.nih.gov/pubmed/5793055

American Association for the Advancement of Science. (n.d.). *Science of aging knowledge environment : SAGE KE.* American Association for the Advancement of Science. Retrieved from http://sageke.sciencemag.org/cgi/content/abstract/2001/9/or25

Anantha, R. W., Vassin, V. M., & Borowiec, J. A. (2007). Sequential and Synergistic Modification of Human RPA Stimulates Chromosomal DNA Repair. *Journal of Biological Chemistry*, *282*(49), 35910–35923. http://doi.org/10.1074/jbc.M704645200

Ansari, A. M., Ahmed, A. K., Matsangos, A. E., Lay, F., Born, L. J., Marti, G., … Sun, Z. (2016). Cellular GFP Toxicity and Immunogenicity: Potential Confounders in in Vivo Cell Tracking Experiments. *Stem Cell Reviews and Reports*, *12*(5), 553–559. http://doi.org/10.1007/s12015-016-9670-8

Arata, Y., Fujita, M., Ohtani, K., Kijima, S., & Kato, J. Y. (2000). Cdk2-dependent and -independent pathways in E2F-mediated S phase induction. *The Journal of Biological Chemistry*, *275*(9), 6337–45. Retrieved from http://www.ncbi.nlm.nih.gov/pubmed/10692433

Barouch-Bentov, R., & Sauer, K. (2011). Mechanisms of drug resistance in kinases. *Expert Opinion on Investigational Drugs*, *20*(2), 153–208. http://doi.org/10.1517/13543784.2011.546344

Bartek, J., & Lukas, J. (2003). Chk1 and Chk2 kinases in checkpoint control and cancer. *Cancer Cell*, *3*(5), 421–9. Retrieved from http://www.ncbi.nlm.nih.gov/pubmed/12781359

Bentley, N. J., Holtzman, D. A., Flaggs, G., Keegan, K. S., DeMaggio, A., Ford, J. C., … Carr, A. M. (1996). The Schizosaccharomyces pombe rad3 checkpoint gene. *The EMBO Journal*, *15*(23), 6641–51. Retrieved from http://www.ncbi.nlm.nih.gov/pubmed/8978690

Bertoli, C., Skotheim, J. M., & de Bruin, R. A. M. (2013). Control of cell cycle transcription during G1 and S phases. *Nature Reviews. Molecular Cell Biology*, *14*(8), 518–28. http://doi.org/10.1038/nrm3629

Blasina, A., Price, B. D., Turenne, G. A., & McGowan, C. H. (1999). Caffeine inhibits the checkpoint kinase ATM. *Current Biology : CB*, *9*(19), 1135–8. Retrieved from http://www.ncbi.nlm.nih.gov/pubmed/10531013

Brown, E. J., & Baltimore, D. (2000). ATR disruption leads to chromosomal fragmentation and early embryonic lethality. *Genes & Development*, *14*(4), 397–402. Retrieved from http://www.ncbi.nlm.nih.gov/pubmed/10691732

Cardoso, M. C., Leonhardt, H., & Nadal-Ginard, B. (1993). Reversal of terminal differentiation and control of DNA replication: cyclin A and Cdk2 specifically localize at subnuclear sites of DNA replication. *Cell*, *74*(6), 979–92. Retrieved from http://www.ncbi.nlm.nih.gov/pubmed/8402887

Casper, A. M., Nghiem, P., Arlt, M. F., & Glover, T. W. (2002). ATR regulates fragile site stability. *Cell*, *111*(6), 779–89. Retrieved from http://www.ncbi.nlm.nih.gov/pubmed/12526805

Charrier, J.-D., Durrant, S. J., Golec, J. M. C., Kay, D. P., Knegtel, R. M. A., MacCormick, S., … Pollard, J. R. (2011). Discovery of Potent and Selective Inhibitors of Ataxia Telangiectasia Mutated and Rad3 Related (ATR) Protein Kinase as Potential Anticancer Agents. *Journal of Medicinal Chemistry*, *54*(7), 2320–2330. http://doi.org/10.1021/jm101488z

Ciccia, A., & Elledge, S. J. (2010). The DNA Damage Response: Making It Safe to Play with Knives. *Molecular Cell*, *40*(2), 179–204. http://doi.org/10.1016/j.molcel.2010.09.019

Cimprich, K. A., & Cortez, D. (2008). ATR: an essential regulator of genome integrity. *Nature Reviews Molecular Cell Biology*, *9*(8), 616–627. http://doi.org/10.1038/nrm2450

Cliby, W. A., Roberts, C. J., Cimprich, K. A., Stringer, C. M., Lamb, J. R., Schreiber, S. L., & Friend, S. H. (1998). Overexpression of a kinase-inactive ATR protein causes sensitivity to DNA-damaging agents and defects in cell cycle checkpoints. *The EMBO Journal*, *17*(1), 159–169. http://doi.org/10.1093/emboj/17.1.159

Clurman, B. E., Sheaff, R. J., Thress, K., Groudine, M., & Roberts, J. M. (1996). Turnover of cyclin E by the ubiquitin-proteasome pathway is regulated by cdk2 binding and cyclin phosphorylation. *Genes & Development*, *10*(16), 1979–90. Retrieved from http://www.ncbi.nlm.nih.gov/pubmed/8769642

Connell-Crowley, L., Harper, J. W., & Goodrich, D. W. (1997). Cyclin D1/Cdk4 regulates retinoblastoma protein-mediated cell cycle arrest by site-specific phosphorylation. *Molecular Biology of the Cell*, *8*(2), 287–301. Retrieved from http://www.ncbi.nlm.nih.gov/pubmed/9190208

Cook, J. G., Park, C.-H., Burke, T. W., Leone, G., DeGregori, J., Engel, A., & Nevins, J. R. (2002). Analysis of Cdc6 function in the assembly of mammalian prereplication complexes. *Proceedings of the National Academy of Sciences*, *99*(3), 1347–1352. http://doi.org/10.1073/pnas.032677499

Coumans, J. V. F., Gau, D., Poljak, A., Wasinger, V., Roy, P., & Moens, P. (2014). Green fluorescent protein expression triggers proteome changes in breast cancer cells. *Experimental Cell Research*, *320*(1), 33–45. http://doi.org/10.1016/j.yexcr.2013.07.019

Coverley, D., Pelizon, C., Trewick, S., & Laskey, R. A. (2000). Chromatin-bound Cdc6 persists in S and G2 phases in human cells, while soluble Cdc6 is destroyed in a cyclin A-cdk2 dependent process. *Journal of Cell Science*, *113 (Pt 11)*, 1929–38. Retrieved from http://www.ncbi.nlm.nih.gov/pubmed/10806104

Coverley, D., Laman, H., & Laskey, R. A. (2002). Distinct roles for cyclins E and A during DNA replication complex assembly and activation. *Nature Cell Biology*, *4*(7), 523–528. http://doi.org/10.1038/ncb813

Dahmann, C., Diffley, J. F., & Nasmyth, K. A. (1995). S-phase-promoting cyclin-dependent kinases prevent re-replication by inhibiting the transition of replication origins to a pre-replicative state. *Current Biology : CB*, *5*(11), 1257–69. Retrieved from http://www.ncbi.nlm.nih.gov/pubmed/8574583

Dai, Y., & Grant, S. (2010). New Insights into Checkpoint Kinase 1 in the DNA Damage Response Signaling Network. *Clinical Cancer Research*, *16*(2), 376–383. http://doi.org/10.1158/1078-0432.CCR-09-1029

Das, A. T., Tenenbaum, L., & Berkhout, B. (2016). Tet-On Systems For Doxycycline-inducible Gene Expression. *Current Gene Therapy*, *16*(3), 156–67. http://doi.org/10.2174/1566523216666160524144041

De Bont, R., & van Larebeke, N. (2004). Endogenous DNA damage in humans: a review of quantitative data. *Mutagenesis*, *19*(3), 169–85. Retrieved from http://www.ncbi.nlm.nih.gov/pubmed/15123782

de Klein, A., Muijtjens, M., van Os, R., Verhoeven, Y., Smit, B., Carr, A. M., … Hoeijmakers, J. H. (2000). Targeted disruption of the cell-cycle checkpoint gene ATR leads to early embryonic lethality in mice. *Current Biology : CB*, *10*(8), 479–82. Retrieved from http://www.ncbi.nlm.nih.gov/pubmed/10801416

DeGregori, J., Leone, G., Ohtani, K., Miron, A., & Nevins, J. R. (1995). E2F-1 accumulation bypasses a G1 arrest resulting from the inhibition of G1 cyclin-dependent kinase activity. *Genes & Development*, *9*(23), 2873–87. Retrieved from http://www.ncbi.nlm.nih.gov/pubmed/7498785

Delacroix, S., Wagner, J. M., Kobayashi, M., Yamamoto, K. -i., & Karnitz, L. M. (2007). The Rad9-Hus1-Rad1 (9-1-1) clamp activates checkpoint signaling via TopBP1. *Genes & Development*, *21*(12), 1472–1477. http://doi.org/10.1101/gad.1547007

Domínguez-Kelly, R., Martín, Y., Koundrioukoff, S., Tanenbaum, M. E., Smits, V. A. J., Medema, R. H., … Freire, R. (2011). Wee1 controls genomic stability during replication by regulating the Mus81-Eme1 endonuclease. *The Journal of Cell Biology*, *194*(4), 567–579. http://doi.org/10.1083/jcb.201101047

Donzelli, M., & Draetta, G. F. (2003). Regulating mammalian checkpoints through Cdc25 inactivation. *EMBO Reports*, *4*(7), 671–677. http://doi.org/10.1038/sj.embor.embor887

Dungrawala, H., Rose, K. L., Bhat, K. P., Mohni, K. N., Glick, G. G., Couch, F. B., & Cortez, D. (2015). The Replication Checkpoint Prevents Two Types of Fork Collapse without Regulating Replisome Stability. *Molecular Cell*, *59*(6), 998–1010. http://doi.org/10.1016/j.molcel.2015.07.030

Dutta, A., & Stillman, B. (1992). cdc2 family kinases phosphorylate a human cell DNA replication factor, RPA, and activate DNA replication. *The EMBO Journal*, *11*(6), 2189–99. Retrieved from http://www.ncbi.nlm.nih.gov/pubmed/1318195

Ellison, V., & Stillman, B. (2003). Biochemical Characterization of DNA Damage Checkpoint Complexes: Clamp Loader and Clamp Complexes with Specificity for 5′ Recessed DNA. *PLoS Biology*, *1*(2), e33. http://doi.org/10.1371/journal.pbio.0000033

Errico, A., & Costanzo, V. (2012). Mechanisms of replication fork protection: a safeguard for genome stability. *Critical Reviews in Biochemistry and Molecular Biology*, *47*(3), 222–235. http://doi.org/10.3109/10409238.2012.655374

Fife, R. S., Sledge, G. W., Roth, B. J., & Proctor, C. (1998). Effects of doxycycline on human prostate cancer cells in vitro. *Cancer Letters*, *127*(1–2), 37–41. Retrieved from http://www.ncbi.nlm.nih.gov/pubmed/9619856

Flores-Rozas, H., Kelman, Z., Dean, F. B., Pan, Z. Q., Harper, J. W., Elledge, S. J., … Hurwitz, J. (1994). Cdk-interacting protein 1 directly binds with proliferating cell nuclear antigen and inhibits DNA replication catalyzed by the DNA polymerase delta holoenzyme. *Proceedings of the National Academy of Sciences of the United States of America*, *91*(18), 8655–9. http://doi.org/10.1073/pnas.91.18.8655

Fokas, E., Prevo, R., Pollard, J. R., Reaper, P. M., Charlton, P. A., Cornelissen, B., … Brunner, T. B. (2012). Targeting ATR in vivo using the novel inhibitor VE-822 results in selective sensitization of pancreatic tumors to radiation. *Cell Death & Disease*, *3*(12), e441. http://doi.org/10.1038/cddis.2012.181

Foote, K. M., Blades, K., Cronin, A., Fillery, S., Guichard, S. S., Hassall, L., … Wood, C. (2013). Discovery of 4-{4-[(3 *R*)-3-Methylmorpholin-4-yl]-6-[1-(methylsulfonyl)cyclopropyl]pyrimidin-2-yl}-1 *H* -indole (AZ20): A Potent and Selective Inhibitor of ATR Protein Kinase with Monotherapy in Vivo Antitumor Activity. *Journal of Medicinal Chemistry*, *56*(5), 2125–2138. http://doi.org/10.1021/jm301859s

Fotedar, R., & Roberts, J. M. (1991). Association of p34cdc2 with replicating DNA. *Cold Spring Harbor Symposia on Quantitative Biology*, *56*, 325–33. Retrieved from http://www.ncbi.nlm.nih.gov/pubmed/1668085

Gabrielli, B., Brooks, K., & Pavey, S. (2012). Defective cell cycle checkpoints as targets for anti-cancer therapies. *Frontiers in Pharmacology*, *3*, 9. http://doi.org/10.3389/fphar.2012.00009

Geng, Y., Eaton, E. N., Picón, M., Roberts, J. M., Lundberg, A. S., Gifford, A., … Weinberg, R. A. (1996). Regulation of cyclin E transcription by E2Fs and retinoblastoma protein. *Oncogene*, *12*(6), 1173–80. Retrieved from http://www.ncbi.nlm.nih.gov/pubmed/8649818

Geng, Y., Yu, Q., Sicinska, E., Das, M., Schneider, J. E., Bhattacharya, S., … Sicinski, P. (2003). Cyclin E ablation in the mouse. *Cell*, *114*(4), 431–43. Retrieved from http://www.ncbi.nlm.nih.gov/pubmed/12941272

Geraerts, M., Willems, S., Baekelandt, V., Debyser, Z., & Gijsbers, R. (2006). Comparison of lentiviral vector titration methods. *BMC Biotechnology*, *6*(1), 34. http://doi.org/10.1186/1472-6750-6-34

Gottesman, M. M., Fojo, T., & Bates, S. E. (2002). Multidrug resistance in cancer: role of ATP–dependent transporters. *Nature Reviews Cancer*, *2*(1), 48–58. http://doi.org/10.1038/nrc706

Gray, L. H., Conger, A. D., Ebert, M., Hornsey, S., & Scott, O. C. A. (1953). The Concentration of Oxygen Dissolved in Tissues at the Time of Irradiation as a Factor in Radiotherapy. *The British Journal of Radiology*, *26*(312), 638–648. http://doi.org/10.1259/0007-1285-26-312-638

Grdina, D. J., Meistrich, M. L., Meyn, R. E., Johnson, T. S., & White, R. A. (1984). Cell synchrony techniques. I. A comparison of methods. *Cell and Tissue Kinetics*, *17*(3), 223–36. Retrieved from http://www.ncbi.nlm.nih.gov/pubmed/6538812

Griffith, E., Walker, S., Martin, C.-A., Vagnarelli, P., Stiff, T., Vernay, B., … O'Driscoll, M. (2008). Mutations in pericentrin cause Seckel syndrome with defective ATR-dependent DNA damage signaling. *Nature Genetics*, *40*(2), 232–236. http://doi.org/10.1038/ng.2007.80

Guichard, S. M., Brown, E., Odedra, R., Hughes, A., Heathcote, D., Barnes, J., … Pass, M. (2013). Abstract 3343: The pre-clinical *in vitro* and *in vivo* activity of AZD6738: A potent and selective inhibitor of ATR kinase. *Cancer Research*, *73*(8 Supplement), 3343–3343. http://doi.org/10.1158/1538-7445.AM2013-3343

Hall, A. B., Newsome, D., Wang, Y., Boucher, D. M., Eustace, B., Gu, Y., … Pollard, J. R. (2014). Potentiation of tumor responses to DNA damaging therapy by the selective ATR inhibitor VX-970. *Oncotarget*, *5*(14), 5674–85. http://doi.org/10.18632/oncotarget.2158

Harbour, J. W., Luo, R. X., Dei Santi, A., Postigo, A. A., & Dean, D. C. (1999). Cdk phosphorylation triggers sequential intramolecular interactions that progressively block Rb functions as cells move through G1. *Cell*, *98*(6), 859–69. Retrieved from http://www.ncbi.nlm.nih.gov/pubmed/10499802

Hartsough, E., Shao, Y., & Aplin, A. E. (2014). Resistance to RAF inhibitors revisited. *The Journal of Investigative Dermatology*, *134*(2), 319–325. http://doi.org/10.1038/jid.2013.358

Hateboer, G., Wobst, A., Petersen, B. O., Le Cam, L., Vigo, E., Sardet, C., & Helin, K. (1998). Cell cycle-regulated expression of mammalian CDC6 is dependent on E2F. *Molecular and Cellular Biology*, *18*(11), 6679–97. Retrieved from http://www.ncbi.nlm.nih.gov/pubmed/9774682

Henricksen, L. A., & Wold, M. S. (1994). Replication protein A mutants lacking phosphorylation sites for p34cdc2 kinase support DNA replication. *The Journal of Biological Chemistry*, *269*(39), 24203–8. Retrieved from http://www.ncbi.nlm.nih.gov/pubmed/7929076

Herbig, U., Griffith, J. W., & Fanning, E. (2000). Mutation of cyclin/cdk phosphorylation sites in HsCdc6 disrupts a late step in initiation of DNA replication in human cells. *Molecular Biology of the Cell*, *11*(12), 4117–30. Retrieved from http://www.ncbi.nlm.nih.gov/pubmed/11102512

Hoeijmakers, J. H. J. (2009). DNA Damage, Aging, and Cancer. *New England Journal of Medicine*, *361*(15), 1475–1485. http://doi.org/10.1056/NEJMra0804615

Honda, R., Lowe, E. D., Dubinina, E., Skamnaki, V., Cook, A., Brown, N. R., & Johnson, L. N. (2005). The structure of cyclin E1/CDK2: implications for CDK2 activation and CDK2-independent roles. *The EMBO Journal*, *24*(3), 452–63. http://doi.org/10.1038/sj.emboj.7600554

Hutter, G., Nickenig, C., Garritsen, H., Hellenkamp, F., Hoerning, A., Hiddemann W., & Dreyling, M. (2004). Use of polymorphisms in the noncoding region of the human mitochondrial genome to identify potential contamination of human leukemia- lymphoma cell lines. *Hematol J*, 5(1): 61-68. http://doi.org/10.1038/sj.thj.6200317

Ishimi, Y., Komamura-Kohno, Y., You, Z., Omori, A., & Kitagawa, M. (2000). Inhibition of Mcm4,6,7 helicase activity by phosphorylation with cyclin A/Cdk2. *The Journal of Biological Chemistry*, *275*(21), 16235–41. http://doi.org/10.1074/jbc.M909040199

Jackson, P. K., Chevalier, S., Philippe, M., & Kirschner, M. W. (1995). Early events in DNA replication require cyclin E and are blocked by p21CIP1. *The Journal of Cell Biology*, *130*(4), 755–69. Retrieved from http://www.ncbi.nlm.nih.gov/pubmed/7642695

Jacq, X., Smith, L., Brown, E., Hughes, A., Odedra, R., Heathcote, D., … Guichard, S. M. (2012). Abstract 1823: AZ20, a novel potent and selective inhibitor of ATR kinase with in vivo antitumour activity. *Cancer Research*, *72*(8 Supplement), 1823–1823. http://doi.org/10.1158/1538-7445.AM2012-1823

Jardim, M. J., Wang, Q., Furumai, R., Wakeman, T., Goodman, B. K., & Wang, X.-F. (2009). Reduced ATR or Chk1 expression leads to chromosome instability and chemosensitization of mismatch repair-deficient colorectal cancer cells. *Molecular Biology of the Cell*, *20*(17), 3801–9. http://doi.org/10.1091/mbc.E09-04-0303

Jares, P., & Blow, J. J. (2000). Xenopus cdc7 function is dependent on licensing but not on XORC, XCdc6, or CDK activity and is required for XCdc45 loading. *Genes & Development*, *14*(12), 1528–40. Retrieved from http://www.ncbi.nlm.nih.gov/pubmed/10859170

Jeong, S.-Y., Kumagai, A., Lee, J., & Dunphy, W. G. (2003). Phosphorylated Claspin Interacts with a Phosphate-binding Site in the Kinase Domain of Chk1 during ATR-mediated Activation. *Journal of Biological Chemistry*, *278*(47), 46782–46788. http://doi.org/10.1074/jbc.M304551200

Jiang, W., McDonald, D., Hope, T. J., & Hunter, T. (1999). Mammalian Cdc7-Dbf4 protein kinase complex is essential for initiation of DNA replication. *The EMBO Journal*, *18*(20), 5703–13. http://doi.org/10.1093/emboj/18.20.5703

Jiang, W., Wells, N. J., & Hunter, T. (1999). Multistep regulation of DNA replication by Cdk phosphorylation of HsCdc6. *Proceedings of the National Academy of Sciences of the United States of America*, *96*(11), 6193–8. Retrieved from http://www.ncbi.nlm.nih.gov/pubmed/10339564

Jones, C. D., Blades, K., Foote, K. M., Guichard, S. M., Jewsbury, P. J., McGuire, T., … Yates, J. W. (2013). Abstract 2348: Discovery of AZD6738, a potent and selective inhibitor with the potential to test the clinical efficacy of ATR kinase inhibition in cancer patients. *Cancer Research*, *73*(8 Supplement), 2348–2348. http://doi.org/10.1158/1538-7445.AM2013-2348

Jones, R. M., Mortusewicz, O., Afzal, I., Lorvellec, M., García, P., Helleday, T., & Petermann, E. (2013). Increased replication initiation and conflicts with transcription underlie Cyclin E-induced replication stress. *Oncogene*, *32*(32), 3744–3753. http://doi.org/10.1038/onc.2012.387

Josse, R., Martin, S. E., Guha, R., Ormanoglu, P., Pfister, T. D., Reaper, P. M., … Pommier, Y. (2014). ATR Inhibitors VE-821 and VX-970 Sensitize Cancer Cells to Topoisomerase I Inhibitors by Disabling DNA Replication Initiation and Fork Elongation Responses. *Cancer Research*, *74*(23), 6968–6979. http://doi.org/10.1158/0008-5472.CAN-13-3369

Kaelin, W. G. (2005). The Concept of Synthetic Lethality in the Context of Anticancer Therapy. *Nature Reviews Cancer*, *5*(9), 689–698. http://doi.org/10.1038/nrc1691

Kastan, M. B., & Bartek, J. (2004). Cell-cycle checkpoints and cancer. *Nature*, *432*(7015), 316–323. http://doi.org/10.1038/nature03097

Kaufmann, S. H., Desnoyers, S., Ottaviano, Y., Davidson, N. E., & Poirier, G. G. (1993). Specific proteolytic cleavage of poly(ADP-ribose) polymerase: an early marker of chemotherapy-induced apoptosis. *Cancer Research*, *53*(17), 3976–85. Retrieved from http://www.ncbi.nlm.nih.gov/pubmed/8358726

Kemp, M. G., Akan, Z., Yilmaz, S., Grillo, M., Smith-Roe, S. L., Kang, T.-H., … Ünsal-Kaçmaz, K. (2010). Tipin-Replication Protein A Interaction Mediates Chk1 Phosphorylation by ATR in Response to Genotoxic Stress. *Journal of Biological Chemistry*, *285*(22), 16562–16571. http://doi.org/10.1074/jbc.M110.110304

Kim, S. T., Lim, D. S., Canman, C. E., & Kastan, M. B. (1999). Substrate specificities and identification of putative substrates of ATM kinase family members. *The Journal of Biological Chemistry*, *274*(53), 37538–43. Retrieved from http://www.ncbi.nlm.nih.gov/pubmed/10608806

Kitagawa, M., Higashi, H., Jung, H. K., Suzuki-Takahashi, I., Ikeda, M., Tamai, K., … Taya, Y. (1996). The consensus motif for phosphorylation by cyclin D1-Cdk4 is different from that for phosphorylation by cyclin A/E-Cdk2. *The EMBO Journal*, *15*(24), 7060–9. Retrieved from http://www.ncbi.nlm.nih.gov/pubmed/9003781

Knoblich, J. A., Sauer, K., Jones, L., Richardson, H., Saint, R., & Lehner, C. F. (1994). Cyclin E controls S phase progression and its down-regulation during Drosophila embryogenesis is required for the arrest of cell proliferation. *Cell*, *77*(1), 107–20. Retrieved from http://www.ncbi.nlm.nih.gov/pubmed/8156587

Knudsen, E. S., Buckmaster, C., Chen, T. T., Feramisco, J. R., & Wang, J. Y. (1998). Inhibition of DNA synthesis by RB: effects on G1/S transition and S-phase progression. *Genes & Development*, *12*(15), 2278–92. Retrieved from http://www.ncbi.nlm.nih.gov/pubmed/9694794

Kondo, T., Wakayama, T., Naiki, T., Matsumoto, K., & Sugimoto, K. (2001). Recruitment of Mec1 and Ddc1 checkpoint proteins to double-strand breaks through distinct mechanisms. *Science (New York, N.Y.)*, *294*(5543), 867–70. http://doi.org/10.1126/science.1063827

Konstantinidou, G., Bey, E. A., Rabellino, A., Schuster, K., Maira, M. S., Gazdar, A. F., … Scaglioni, P. P. (2009). Dual Phosphoinositide 3-Kinase/Mammalian Target of Rapamycin Blockade Is an Effective Radiosensitizing Strategy for the Treatment of Non-Small Cell Lung Cancer Harboring K-RAS Mutations. *Cancer Research*, *69*(19), 7644–7652. http://doi.org/10.1158/0008-5472.CAN-09-0823

Kumagai, A., & Dunphy, W. G. (2003). Repeated phosphopeptide motifs in Claspin mediate the regulated binding of Chk1. *Nature Cell Biology*, *5*(2), 161–165. http://doi.org/10.1038/ncb921

Kumagai, A., Kim, S.-M., & Dunphy, W. G. (2004). Claspin and the Activated Form of ATR-ATRIP Collaborate in the Activation of Chk1. *Journal of Biological Chemistry*, *279*(48), 49599–49608. http://doi.org/10.1074/jbc.M408353200

Kumagai, A., Lee, J., Yoo, H. Y., & Dunphy, W. G. (2006). TopBP1 activates the ATR-ATRIP complex. *Cell*, *124*(5), 943–55. http://doi.org/10.1016/j.cell.2005.12.041

Kumagai, A., Lee, J., Yoo, H. Y., & Dunphy, W. G. (2006). TopBP1 Activates the ATR-ATRIP Complex. *Cell*, *124*(5), 943–955. http://doi.org/10.1016/j.cell.2005.12.041

Kumagai, H., Sato, N., Yamada, M., Mahony, D., Seghezzi, W., Lees, E., … Masai, H. (1999). A novel growth- and cell cycle-regulated protein, ASK, activates human Cdc7-related kinase and is essential for G1/S transition in mammalian cells. *Molecular and Cellular Biology*, *19*(7), 5083–95. Retrieved from http://www.ncbi.nlm.nih.gov/pubmed/10373557

Kwok, M., Davies, N., Agathanggelou, A., Smith, E., Oldreive, C., Petermann, E., … Stankovic, T. (2016). ATR inhibition induces synthetic lethality and overcomes chemoresistance in TP53- or ATM-defective chronic lymphocytic leukemia cells. *Blood*, *127*(5), 582–595. http://doi.org/10.1182/blood-2015-05-644872

Lei, M., & Tye, B. K. (2001). Initiating DNA synthesis: from recruiting to activating the MCM complex. *Journal of Cell Science*, *114*(Pt 8), 1447–54. Retrieved from http://www.ncbi.nlm.nih.gov/pubmed/11282021

Leng, X., Connell-Crowley, L., Goodrich, D., & Harper, J. W. (1997). S-Phase entry upon ectopic expression of G1 cyclin-dependent kinases in the absence of retinoblastoma protein phosphorylation. *Current Biology : CB*, *7*(9), 709–12. Retrieved from http://www.ncbi.nlm.nih.gov/pubmed/9285720

Leone, G., DeGregori, J., Jakoi, L., Cook, J. G., & Nevins, J. R. (1999). Collaborative role of E2F transcriptional activity and G1 cyclindependent kinase activity in the induction of S phase. *Proceedings of the National Academy of Sciences of the United States of America*, *96*(12), 6626–31. Retrieved from http://www.ncbi.nlm.nih.gov/pubmed/10359762

Lindahl, T. (1993). Instability and decay of the primary structure of DNA. *Nature*, *362*(6422), 709–715. http://doi.org/10.1038/362709a0

Lippert, T. H., Ruoff, H.-J., & Volm, M. (2011). Current status of methods to assess cancer drug resistance. *International Journal of Medical Sciences*, *8*(3), 245–53. Retrieved from http://www.ncbi.nlm.nih.gov/pubmed/21487568

Liu, H.-S., Jan, M.-S., Chou, C.-K., Chen, P.-H., & Ke, N.-J. (1999). Is Green Fluorescent Protein Toxic to the Living Cells? *Biochemical and Biophysical Research Communications*, *260*(3), 712–717. http://doi.org/10.1006/bbrc.1999.0954

Liu, Q., Guntuku, S., Cui, X. S., Matsuoka, S., Cortez, D., Tamai, K., … Elledge, S. J. (2000). Chk1 is an essential kinase that is regulated by Atr and required for the G(2)/M DNA damage checkpoint. *Genes & Development*, *14*(12), 1448–59. Retrieved from http://www.ncbi.nlm.nih.gov/pubmed/10859164

López-Contreras, A. J., & Fernandez-Capetillo, O. (2010). The ATR barrier to replication-born DNA damage. *DNA Repair*, *9*(12), 1249–1255. http://doi.org/10.1016/j.dnarep.2010.09.012

Lovejoy, C. A., & Cortez, D. (2009). Common mechanisms of PIKK regulation. *DNA Repair*, *8*(9), 1004–1008. http://doi.org/10.1016/j.dnarep.2009.04.006

Lovly, C. M., & Pao, W. (2012). Escaping ALK Inhibition: Mechanisms of and Strategies to Overcome Resistance. *Science Translational Medicine*, *4*(120), 120ps2-120ps2. http://doi.org/10.1126/scitranslmed.3003728

Lukas, J., Herzinger, T., Hansen, K., Moroni, M. C., Resnitzky, D., Helin, K., … Bartek, J. (1997). Cyclin E-induced S phase without activation of the pRb/E2F pathway. *Genes & Development*, *11*(11), 1479–92. http://doi.org/10.1101/GAD.11.11.1479

Luqmani, Y. A. (2005). Mechanisms of Drug Resistance in Cancer Chemotherapy. *Medical Principles and Practice*, *14*(1), 35–48. http://doi.org/10.1159/000086183

Ma, T., Van Tine, B. A., Wei, Y., Garrett, M. D., Nelson, D., Adams, P. D., … Harper, J. W. (2000). Cell cycle-regulated phosphorylation of p220(NPAT) by cyclin E/Cdk2 in Cajal

bodies promotes histone gene transcription. *Genes & Development*, *14*(18), 2298–313. Retrieved from http://www.ncbi.nlm.nih.gov/pubmed/10995387

Macheret, M., & Halazonetis, T. D. (2018). Intragenic origins due to short G1 phases underlie oncogene-induced DNA replication stress. *Nature*, *555*(7694), 112–116. http://doi.org/10.1038/nature25507

Maira, S.-M., Stauffer, F., Brueggen, J., Furet, P., Schnell, C., Fritsch, C., … Garcia-Echeverria, C. (2008). Identification and characterization of NVP-BEZ235, a new orally available dual phosphatidylinositol 3-kinase/mammalian target of rapamycin inhibitor with potent in vivo antitumor activity. *Molecular Cancer Therapeutics*, *7*(7), 1851–1863. http://doi.org/10.1158/1535-7163.MCT-08-0017

Mak, J. P. Y., Man, W. Y., Ma, H. T., & Poon, R. Y. C. (2014). Pharmacological targeting the ATR–CHK1–WEE1 axis involves balancing cell growth stimulation and apoptosis. *Oncotarget*, *5*(21), 10546–57. http://doi.org/10.18632/oncotarget.2508

Masai, H., Matsui, E., You, Z., Ishimi, Y., Tamai, K., & Arai, K. (2000). Human Cdc7-related Kinase Complex. *Journal of Biological Chemistry*, *275*(37), 29042–29052. http://doi.org/10.1074/jbc.M002713200

McGarry, T. J., & Kirschner, M. W. (1998). Geminin, an inhibitor of DNA replication, is degraded during mitosis. *Cell*, *93*(6), 1043–53. Retrieved from http://www.ncbi.nlm.nih.gov/pubmed/9635433

Melo, J. A., Cohen, J., & Toczyski, D. P. (2001). Two checkpoint complexes are independently recruited to sites of DNA damage in vivo. *Genes & Development*, *15*(21), 2809–21. http://doi.org/10.1101/gad.903501

Méndez, J., & Stillman, B. (2000). Chromatin association of human origin recognition complex, cdc6, and minichromosome maintenance proteins during the cell cycle: assembly of prereplication complexes in late mitosis. *Molecular and Cellular Biology*, *20*(22), 8602–12. Retrieved from http://www.ncbi.nlm.nih.gov/pubmed/11046155

Mimura, S., & Takisawa, H. (1998). Xenopus Cdc45-dependent loading of DNA polymerase alpha onto chromatin under the control of S-phase Cdk. *The EMBO Journal*, *17*(19), 5699–707. http://doi.org/10.1093/emboj/17.19.5699

Mordes, D. A., & Cortez, D. (2008). Activation of ATR and related PIKKs. *Cell Cycle*, *7*(18), 2809–2812. http://doi.org/10.4161/cc.7.18.6689

Morgan, M. A., & Reuter, C. W. M. (2006). Molecularly targeted therapies in myelodysplastic syndromes and acute myeloid leukemias. *Annals of Hematology*, *85*(3), 139–163. http://doi.org/10.1007/s00277-005-0051-7

Murga, M., Bunting, S., Montaña, M. F., Soria, R., Mulero, F., Cañamero, M., … Fernandez-Capetillo, O. (2009). A mouse model of ATR-Seckel shows embryonic replicative stress and accelerated aging. *Nature Genetics*, *41*(8), 891–898. http://doi.org/10.1038/ng.420

Murray, A. W. (2004). Recycling the Cell Cycle: Cyclins Revisited. *Cell*, *116*(2), 221–234. http://doi.org/10.1016/S0092-8674(03)01080-8

Newton, R., Broughton, L. J., Lind, M. J., Morrison, P. J., Rogers, H. J., & Bradbrook, I. D. (1981). Plasma and salivary pharmacokinetics of caffeine in man. *European Journal of*

Clinical Pharmacology, *21*(1), 45–52. Retrieved from http://www.ncbi.nlm.nih.gov/pubmed/7333346

Nghiem, P., Park, P. K., Kim, Y., Vaziri, C., & Schreiber, S. L. (2001). ATR inhibition selectively sensitizes G1 checkpoint-deficient cells to lethal premature chromatin condensation. *Proceedings of the National Academy of Sciences of the United States of America*, *98*(16), 9092–7. http://doi.org/10.1073/pnas.161281798

Nghiem, P., Park, P. K., Kim, Y., Vaziri, C., & Schreiber, S. L. (2001). ATR inhibition selectively sensitizes G1 checkpoint-deficient cells to lethal premature chromatin condensation. *Proceedings of the National Academy of Sciences of the United States of America*, *98*(16), 9092–7. http://doi.org/10.1073/pnas.161281798

Nishida, H., Tatewaki, N., Nakajima, Y., Magara, T., Ko, K. M., Hamamori, Y., & Konishi, T. (2009). Inhibition of ATR protein kinase activity by schisandrin B in DNA damage response. *Nucleic Acids Research*, *37*(17), 5678–5689. http://doi.org/10.1093/nar/gkp593

Nurse, P. (1997). Checkpoint pathways come of age. *Cell*, *91*(7), 865–7. Retrieved from http://www.ncbi.nlm.nih.gov/pubmed/9428508

O'Brien, J., Wilson, I., Orton, T., & Pognan, F. (2000). Investigation of the Alamar Blue (resazurin) fluorescent dye for the assessment of mammalian cell cytotoxicity. *European Journal of Biochemistry*, *267*(17), 5421–6. Retrieved from http://www.ncbi.nlm.nih.gov/pubmed/10951200

O'Driscoll, M., Ruiz-Perez, V. L., Woods, C. G., Jeggo, P. A., & Goodship, J. A. (2003). A splicing mutation affecting expression of ataxia–telangiectasia and Rad3–related protein (ATR) results in Seckel syndrome. *Nature Genetics*, *33*(4), 497–501. http://doi.org/10.1038/ng1129

O'Hare, T., Eide, C. A., & Deininger, M. W. N. (2007). Bcr-Abl kinase domain mutations, drug resistance, and the road to a cure for chronic myeloid leukemia. *Blood*, *110*(7), 2242–2249. http://doi.org/10.1182/blood-2007-03-066936

O'Driscoll, M. (2009). Mouse models for ATR deficiency. *DNA Repair*, *8*(11), 1333–1337. http://doi.org/10.1016/j.dnarep.2009.09.001

Ohtani, K., DeGregori, J., & Nevins, J. R. (1995). Regulation of the cyclin E gene by transcription factor E2F1. *Proceedings of the National Academy of Sciences of the United States of America*, *92*(26), 12146–50. Retrieved from http://www.ncbi.nlm.nih.gov/pubmed/8618861

Ohtani, K., Tsujimoto, A., Ikeda, M., & Nakamura, M. (1998). Regulation of cell growth-dependent expression of mammalian CDC6 gene by the cell cycle transcription factor E2F. *Oncogene*, *17*(14), 1777–1785. http://doi.org/10.1038/sj.onc.1202105

Pan, Z. Q., Amin, A. A., Gibbs, E., Niu, H., & Hurwitz, J. (1994). Phosphorylation of the p34 subunit of human single-stranded-DNA-binding protein in cyclin A-activated G1 extracts is catalyzed by cdk-cyclin A complex and DNA-dependent protein kinase. *Proceedings of the National Academy of Sciences of the United States of America*, *91*(18), 8343–7. Retrieved from http://www.ncbi.nlm.nih.gov/pubmed/8078885

Pan, Z. Q., Park, C. H., Amin, A. A., Hurwitz, J., & Sancar, A. (1995). Phosphorylated and unphosphorylated forms of human single-stranded DNA-binding protein are equally active in simian virus 40 DNA replication and in nucleotide excision repair. *Proceedings of the*

National Academy of Sciences of the United States of America, *92*(10), 4636–40. Retrieved from http://www.ncbi.nlm.nih.gov/pubmed/7753855

Parisi, T., Beck, A. R., Rougier, N., McNeil, T., Lucian, L., Werb, Z., & Amati, B. (2003). Cyclins E1 and E2 are required for endoreplication in placental trophoblast giant cells. *The EMBO Journal*, *22*(18), 4794–803. http://doi.org/10.1093/emboj/cdg482

Peasland, A., Wang, L.-Z., Rowling, E., Kyle, S., Chen, T., Hopkins, A., … Curtin, N. J. (2011). Identification and evaluation of a potent novel ATR inhibitor, NU6027, in breast and ovarian cancer cell lines. *British Journal of Cancer*, *105*(3), 372–381. http://doi.org/10.1038/bjc.2011.243

Pelizon, C., Madine, M. A., Romanowski, P., & Laskey, R. A. (2000). Unphosphorylatable mutants of Cdc6 disrupt its nuclear export but still support DNA replication once per cell cycle. *Genes & Development*, *14*(19), 2526–33. Retrieved from http://www.ncbi.nlm.nih.gov/pubmed/11018019

Peng, C. Y., Graves, P. R., Thoma, R. S., Wu, Z., Shaw, A. S., & Piwnica-Worms, H. (1997). Mitotic and G2 checkpoint control: regulation of 14-3-3 protein binding by phosphorylation of Cdc25C on serine-216. *Science (New York, N.Y.)*, *277*(5331), 1501–5. Retrieved from http://www.ncbi.nlm.nih.gov/pubmed/9278512

Petersen, B. O., Lukas, J., Sørensen, C. S., Bartek, J., & Helin, K. (1999). Phosphorylation of mammalian CDC6 by cyclin A/CDK2 regulates its subcellular localization. *The EMBO Journal*, *18*(2), 396–410. http://doi.org/10.1093/emboj/18.2.396

Petersen, B. O., Wagener, C., Marinoni, F., Kramer, E. R., Melixetian, M., Lazzerini Denchi, E., … Helin, K. (2000). Cell cycle- and cell growth-regulated proteolysis of mammalian CDC6 is dependent on APC-CDH1. *Genes & Development*, *14*(18), 2330–43. http://doi.org/10.1101/GAD.832500

Pinedo, H. M., & Giaccone, G. (1998). *Drug resistance in the treatment of cancer*. Cambridge University Press. Retrieved from https://books.google.co.uk/books/about/Drug_Resistance_in_the_Treatment_of_Canc.html?id=maUHytrX9joC&redir_esc=y

Pires, I. M., Olcina, M. M., Anbalagan, S., Pollard, J. R., Reaper, P. M., Charlton, P. A., … Hammond, E. M. (2012). Targeting radiation-resistant hypoxic tumour cells through ATR inhibition. *British Journal of Cancer*, *107*(2), 291–299. http://doi.org/10.1038/bjc.2012.265

Powell, S. N., DeFrank, J. S., Connell, P., Eogan, M., Preffer, F., Dombkowski, D., … Friend, S. (1995). Differential sensitivity of p53(-) and p53(+) cells to caffeine-induced radiosensitization and override of G2 delay. *Cancer Research*, *55*(8), 1643–8. Retrieved from http://www.ncbi.nlm.nih.gov/pubmed/7712468

Powell, S. K., MacAlpine, H. K., Prinz, J. A., Li, Y., Belsky, J. A., & MacAlpine, D. M. (2015). Dynamic loading and redistribution of the Mcm2-7 helicase complex through the cell cycle. *The EMBO Journal*, *34*(4), 531–543. http://doi.org/10.15252/embj.201488307

Prevo, R., Fokas, E., Reaper, P. M., Charlton, P. A., Pollard, J. R., McKenna, W. G., … Brunner, T. B. (2012). The novel ATR inhibitor VE-821 increases sensitivity of pancreatic cancer cells to radiation and chemotherapy. *Cancer Biology & Therapy*, *13*(11), 1072–1081. http://doi.org/10.4161/cbt.21093

Prosperi, E., Scovassi, A. I., Stivala, L. A., & Bianchi, L. (1994). Proliferating Cell Nuclear Antigen Bound to DNA Synthesis Sites: Phosphorylation and Association with Cyclin D1 and Cyclin A. *Experimental Cell Research*, *215*(2), 257–262. http://doi.org/10.1006/excr.1994.1341

Qin, Y., Zhang, Q., Lee, S., Zhong, W.-L., Liu, Y.-R., Liu, H.-J., … Zhou, H.-G. (2015). Doxycycline reverses epithelial-to-mesenchymal transition and suppresses the proliferation and metastasis of lung cancer cells. *Oncotarget*, *6*(38), 40667–79. http://doi.org/10.18632/oncotarget.5842

Reaper, P. M., Griffiths, M. R., Long, J. M., Charrier, J.-D., MacCormick, S., Charlton, P. A., … Pollard, J. R. (2011). Selective killing of ATM- or p53-deficient cancer cells through inhibition of ATR. *Nature Chemical Biology*, *7*(7), 428–430. http://doi.org/10.1038/nchembio.573

Resnitzky, D., & Reed, S. I. (1995). Different roles for cyclins D1 and E in regulation of the G1-to-S transition. *Molecular and Cellular Biology*, *15*(7), 3463–9. Retrieved from http://www.ncbi.nlm.nih.gov/pubmed/7791752

Ruiz, S., Mayor-Ruiz, C., Lafarga, V., Murga, M., Vega-Sendino, M., Ortega, S., & Fernandez-Capetillo, O. (2016). A Genome-wide CRISPR Screen Identifies CDC25A as a Determinant of Sensitivity to ATR Inhibitors. *Molecular Cell*, *62*(2), 307–313. http://doi.org/10.1016/j.molcel.2016.03.006

Ruzankina, Y., Pinzon-Guzman, C., Asare, A., Ong, T., Pontano, L., Cotsarelis, G., … Brown, E. J. (2007). Deletion of the Developmentally Essential Gene ATR in Adult Mice Leads to Age-Related Phenotypes and Stem Cell Loss. *Cell Stem Cell*, *1*(1), 113–126. http://doi.org/10.1016/j.stem.2007.03.002

Ruzankina, Y., Schoppy, D. W., Asare, A., Clark, C. E., Vonderheide, R. H., & Brown, E. J. (2009). Tissue regenerative delays and synthetic lethality in adult mice after combined deletion of Atr and Trp53. *Nature Genetics*, *41*(10), 1144–9. http://doi.org/10.1038/ng.441

Saha, P., Chen, J., Thome, K. C., Lawlis, S. J., Hou, Z. H., Hendricks, M., … Dutta, A. (1998). Human CDC6/Cdc18 associates with Orc1 and cyclin-cdk and is selectively eliminated from the nucleus at the onset of S phase. *Molecular and Cellular Biology*, *18*(5), 2758–67. Retrieved from http://www.ncbi.nlm.nih.gov/pubmed/9566895

Sarkaria, J. N., Busby, E. C., Tibbetts, R. S., Roos, P., Taya, Y., Karnitz, L. M., & Abraham, R. T. (1999). Inhibition of ATM and ATR kinase activities by the radiosensitizing agent, caffeine. *Cancer Research*, *59*(17), 4375–82. Retrieved from http://www.ncbi.nlm.nih.gov/pubmed/10485486

Sasaki, T., Ramanathan, S., Okuno, Y., Kumagai, C., Shaikh, S. S., & Gilbert, D. M. (2006). The Chinese Hamster Dihydrofolate Reductase Replication Origin Decision Point Follows Activation of Transcription and Suppresses Initiation of Replication within Transcription Units. *Molecular and Cellular Biology*, *26*(3), 1051–1062. http://doi.org/10.1128/MCB.26.3.1051-1062.2006

Schulze, A., Zerfass, K., Spitkovsky, D., Middendorp, S., Bergès, J., Helin, K., … Henglein, B. (1995). Cell cycle regulation of the cyclin A gene promoter is mediated by a variant E2F site. *Proceedings of the National Academy of Sciences of the United States of America*, *92*(24), 11264–8. Retrieved from http://www.ncbi.nlm.nih.gov/pubmed/7479977

Smith, L., Liu, S. J., Goodrich, L., Jacobson, D., Degnin, C., Bentley, N., … Thayer, M. J. (1998). Duplication of ATR inhibits MyoD, induces aneuploidy and eliminates radiation-induced G1 arrest. *Nature Genetics*, *19*(1), 39–46. http://doi.org/10.1038/ng0598-39

Sobczak-Thepot, J., Harper, F., Florentin, Y., Zindy, F., Brechot, C., & Puvion, E. (1993). Localization of Cyclin A at the Sites of Cellular DNA Replication. *Experimental Cell Research*, *206*(1), 43–48. http://doi.org/10.1006/EXCR.1993.1118

Sørensen, C. S., Syljuåsen, R. G., Falck, J., Schroeder, T., Rönnstrand, L., Khanna, K. K., … Lukas, J. (2003). Chk1 regulates the S phase checkpoint by coupling the physiological turnover and ionizing radiation-induced accelerated proteolysis of Cdc25A. *Cancer Cell*, *3*(3), 247–58. Retrieved from http://www.ncbi.nlm.nih.gov/pubmed/12676583

Strausfeld, U. P., Howell, M., Rempel, R., Maller, J. L., Hunt, T., & Blow, J. J. (1994). Cip1 blocks the initiation of DNA replication in Xenopus extracts by inhibition of cyclin-dependent kinases. *Current Biology : CB*, *4*(10), 876–83. Retrieved from http://www.ncbi.nlm.nih.gov/pubmed/7850420

Strohmaier, H., Spruck, C. H., Kaiser, P., Won, K.-A., Sangfelt, O., & Reed, S. I. (2001). Human F-box protein hCdc4 targets cyclin E for proteolysis and is mutated in a breast cancer cell line. *Nature*, *413*(6853), 316–322. http://doi.org/10.1038/35095076

Su, T. T., & O'Farrell, P. H. (1998). Chromosome association of minichromosome maintenance proteins in Drosophila endoreplication cycles. *The Journal of Cell Biology*, *140*(3), 451–60. Retrieved from http://www.ncbi.nlm.nih.gov/pubmed/9456309

Sultana, R., Abdel-Fatah, T., Perry, C., Moseley, P., Albarakti, N., Mohan, V., … Madhusudan, S. (2013). Ataxia Telangiectasia Mutated and Rad3 Related (ATR) Protein Kinase Inhibition Is Synthetically Lethal in XRCC1 Deficient Ovarian Cancer Cells. *PLoS ONE*, *8*(2), e57098. http://doi.org/10.1371/journal.pone.0057098

Tanaka, T., & Nasmyth, K. (1998). Association of RPA with chromosomal replication origins requires an Mcm protein, and is regulated by Rad53, and cyclin- and Dbf4-dependent kinases. *The EMBO Journal*, *17*(17), 5182–5191. http://doi.org/10.1093/emboj/17.17.5182

Terasima, T., & Tolmach, L. J. (1963). Growth and nucleic acid synthesis in synchronously dividing populations of HeLa cells. *Experimental Cell Research*, *30*(2), 344–362. http://doi.org/10.1016/0014-4827(63)90306-9

Tewari, M., Quan, L. T., O'Rourke, K., Desnoyers, S., Zeng, Z., Beidler, D. R., … Dixit, V. M. (1995). Yama/CPP32 beta, a mammalian homolog of CED-3, is a CrmA-inhibitable protease that cleaves the death substrate poly(ADP-ribose) polymerase. *Cell*, *81*(5), 801–9. Retrieved from http://www.ncbi.nlm.nih.gov/pubmed/7774019

Treuner, K., Findeisen, M., Strausfeld, U., & Knippers, R. (1999). Phosphorylation of replication protein A middle subunit (RPA32) leads to a disassembly of the RPA heterotrimer. *The Journal of Biological Chemistry*, *274*(22), 15556–61. http://doi.org/10.1074/JBC.274.22.15556

Vendetti, F. P., Lau, A., Schamus, S., Conrads, T. P., O'Connor, M. J., & Bakkenist, C. J. (2015). The orally active and bioavailable ATR kinase inhibitor AZD6738 potentiates the anti-tumor effects of cisplatin to resolve ATM-deficient non-small cell lung cancer <i>in vivo</i> *Oncotarget*, *6*(42), 44289–305. http://doi.org/10.18632/oncotarget.6247

Voitenleitner, C., Rehfuess, C., Hilmes, M., O'Rear, L., Liao, P. C., Gage, D. A., … Fanning, E. (1999). Cell cycle-dependent regulation of human DNA polymerase alpha-primase activity by phosphorylation. *Molecular and Cellular Biology*, *19*(1), 646–56. Retrieved from http://www.ncbi.nlm.nih.gov/pubmed/9858588

Walter, J., & Newport, J. (2000). Initiation of eukaryotic DNA replication: origin unwinding and sequential chromatin association of Cdc45, RPA, and DNA polymerase alpha. *Molecular Cell*, *5*(4), 617–27. Retrieved from http://www.ncbi.nlm.nih.gov/pubmed/10882098

Weber, A. M., & Ryan, A. J. (2015). ATM and ATR as therapeutic targets in cancer. *Pharmacology & Therapeutics*, *149*, 124–138. http://doi.org/10.1016/j.pharmthera.2014.12.001

Weber, A. M., & Ryan, A. J. (2015). ATM and ATR as therapeutic targets in cancer. *Pharmacology & Therapeutics*, *149*, 124–138. http://doi.org/10.1016/J.PHARMTHERA.2014.12.001

Wheeler, D. L., Dunn, E. F., & Harari, P. M. (2010). Understanding resistance to EGFR inhibitors—impact on future treatment strategies. *Nature Reviews Clinical Oncology*, *7*(9), 493–507. http://doi.org/10.1038/nrclinonc.2010.97

Whitfield, M. L., Sherlock, G., Saldanha, A. J., Murray, J. I., Ball, C. A., Alexander, K. E., … Botstein, D. (2002). Identification of genes periodically expressed in the human cell cycle and their expression in tumors. *Molecular Biology of the Cell*, *13*(6), 1977–2000. http://doi.org/10.1091/mbc.02-02-0030.

Won, K. A., & Reed, S. I. (1996). Activation of cyclin E/CDK2 is coupled to site-specific autophosphorylation and ubiquitin-dependent degradation of cyclin E. *The EMBO Journal*, *15*(16), 4182–93. Retrieved from http://www.ncbi.nlm.nih.gov/pubmed/8861947

Woo, R. A., & Poon, R. Y. C. (2004). Activated oncogenes promote and cooperate with chromosomal instability for neoplastic transformation. *Genes & Development*, *18*(11), 1317–30. http://doi.org/10.1101/gad.1165204

Woo, R. A., & Poon, R. Y. C. (n.d.). Cyclin-dependent kinases and S phase control in mammalian cells. *Cell Cycle (Georgetown, Tex.)*, *2*(4), 316–24. Retrieved from http://www.ncbi.nlm.nih.gov/pubmed/12851482

Wouters, B. G., & Brown, J. M. (1997). Cells at intermediate oxygen levels can be more important than the "hypoxic fraction" in determining tumor response to fractionated radiotherapy. *Radiation Research*, *147*(5), 541–50. Retrieved from http://www.ncbi.nlm.nih.gov/pubmed/9146699

Xiao, Z., Chen, Z., Gunasekera, A. H., Sowin, T. J., Rosenberg, S. H., Fesik, S., & Zhang, H. (2003). Chk1 Mediates S and G $_2$ Arrests through Cdc25A Degradation in Response to DNA-damaging Agents. *Journal of Biological Chemistry*, *278*(24), 21767–21773. http://doi.org/10.1074/jbc.M300229200

Yam, C. H., Fung, T. K., & Poon, R. Y. C. (2002). Cyclin A in cell cycle control and cancer. *Cellular and Molecular Life Sciences : CMLS*, *59*(8), 1317–26. Retrieved from http://www.ncbi.nlm.nih.gov/pubmed/12363035

Zahreddine, H., & Borden, K. L. B. (2013). Mechanisms and insights into drug resistance in cancer. *Frontiers in Pharmacology*, *4*, 28. http://doi.org/10.3389/fphar.2013.00028

Zarkowska, T., & Mittnacht, S. (1997). Differential phosphorylation of the retinoblastoma protein by G1/S cyclin-dependent kinases. *The Journal of Biological Chemistry*, *272*(19), 12738–46. Retrieved from http://www.ncbi.nlm.nih.gov/pubmed/9139732

Zeng, X. R., Hao, H., Jiang, Y., & Lee, M. Y. (1994). Regulation of human DNA polymerase delta during the cell cycle. *The Journal of Biological Chemistry*, *269*(39), 24027–33. Retrieved from http://www.ncbi.nlm.nih.gov/pubmed/7929054

Zernik-Kobak, M., Vasunia, K., Connelly, M., Anderson, C. W., & Dixon, K. (1997). Sites of UV-induced phosphorylation of the p34 subunit of replication protein A from HeLa cells. *The Journal of Biological Chemistry*, *272*(38), 23896–904. Retrieved from http://www.ncbi.nlm.nih.gov/pubmed/9295339

Zhang, H. S., Gavin, M., Dahiya, A., Postigo, A. A., Ma, D., Luo, R. X., … Dean, D. C. (2000). Exit from G1 and S Phase of the Cell Cycle Is Regulated by Repressor Complexes Containing HDAC-Rb-hSWI/SNF and Rb-hSWI/SNF. *Cell*, *101*(1), 79–89. http://doi.org/10.1016/S0092-8674(00)80625-X

Zhao, H., Watkins, J. L., & Piwnica-Worms, H. (2002). Disruption of the checkpoint kinase 1/cell division cycle 25A pathway abrogates ionizing radiation-induced S and G2 checkpoints. *Proceedings of the National Academy of Sciences*, *99*(23), 14795–14800. http://doi.org/10.1073/pnas.182557299

Zhao, J., Kennedy, B. K., Lawrence, B. D., Barbie, D. A., Matera, A. G., Fletcher, J. A., & Harlow, E. (2000). NPAT links cyclin E-Cdk2 to the regulation of replication-dependent histone gene transcription. *Genes & Development*, *14*(18), 2283–97. Retrieved from http://www.ncbi.nlm.nih.gov/pubmed/10995386

Zieve, G. W., Turnbull, D., Mullins, J. M., & McIntosh, J. R. (1980). Production of large numbers of mitotic mammalian cells by use of the reversible microtubule inhibitor nocodazole. Nocodazole accumulated mitotic cells. *Experimental Cell Research*, *126*(2), 397–405. Retrieved from http://www.ncbi.nlm.nih.gov/pubmed/6153987

Zou, L., & Stillman, B. (2000). Assembly of a complex containing Cdc45p, replication protein A, and Mcm2p at replication origins controlled by S-phase cyclin-dependent kinases and Cdc7p-Dbf4p kinase. *Molecular and Cellular Biology*, *20*(9), 3086–96. Retrieved from http://www.ncbi.nlm.nih.gov/pubmed/10757793

Zou, L., & Elledge, S. J. (2003). Sensing DNA Damage Through ATRIP Recognition of RPA-ssDNA Complexes. *Science*, *300*(5625), 1542–1548. http://doi.org/10.1126/science.1083430